Parks Victoria Technical Series

Number 114

An enhanced Signs of Healthy Parks monitoring program for Victoria's Marine National Parks and Marine Sanctuaries: Point Addis Marine National Park

May 2020

Parks VICTORIA

Healthy Parks Healthy People®

VICTORIA State Government

First published 2020

Published by Parks Victoria

Level 10, 535 Bourke Street, Melbourne Victoria 3000

Authors

Daniel Ierodiaconou, Sam Wines, Paul Carnell, Paul Tinkler, Blake Allan, Mary Young - Deakin University

Jan Carey - University of Melbourne

Steffan Howe, Jacqui Pocklington - Parks Victoria

National Library of Australia

Cataloguing-in-publication data

Includes bibliography.

ISSN 1448-4935

Citation:

Ierodiaconou D, Wines S, Carnell P, Tinkler P, Allan B, Carey J, Young M, Howe S, Pocklington J. 2020. An enhanced Signs of Healthy Parks monitoring program for Victoria's Marine National Parks and Marine Sanctuaries: Point Addis Marine National Park. Parks Victoria Technical Series 114.

Front cover: Port Phillip Heads Marine National Park

Photo: Museum Victoria

Executive Summary

Parks Victoria has established extensive marine research and monitoring programs for its marine protected areas (MPAs) with the aim of addressing significant management challenges. These challenges focus on both improving baseline knowledge of the MPAs and addressing applied management questions. The Signs of Healthy Parks (SHP) monitoring program aims to ensure systematic, robust and integrated ecological monitoring across the MPA network. Building on Parks Victoria's Conservation Action Planning process, the SHP program aims to monitor the health of protected areas using a range of environmental indicators that in turn provide information about the natural values and ecological processes within the parks, as well as potential threats. The collection of data is based on focused monitoring questions, which address specific management needs. Parks Victoria has implemented subtidal and intertidal reef monitoring programs in a large number of the MPAs from as far back as 1998, however they only cover a small proportion of the key habitats in the parks. The monitoring program for Victoria's MPAs is now being expanded to address key management questions linked to draft Conservation Plans for the marine national parks (MNP) and sanctuaries. This updated SHP program does this by fostering partnerships and collaborative projects to design, implement and evaluate monitoring programs. Deakin University as part of the Research Partners Panel Program were engaged by Parks Victoria to trial a suite of monitoring approaches in Point Addis Marine National Park. The results from this study provide considerable new knowledge of the distribution and functioning of intertidal, subtidal and mesophotic habitats within Point Addis Marine National Park and a framework to expand monitoring across the MNP estate.

Contents

Index of figures

Index of tables

1. Introduction

Parks Victoria manages a system of 13 Marine National Parks and 11 Sanctuaries, making up approximately 5.3 % of Victoria's state waters. Established in 2002, the network of marine national parks and sanctuaries was designed to represent the diversity of Victoria's marine environment, its habitats, and associated flora and fauna (Victorian Environmental Assessment Council 2014). In order to reliably manage these areas, an understanding of the natural values that occur within the parks, sanctuaries and reserves is essential (Devillers et al. 2015). Parks Victoria has established extensive marine research and monitoring programs for its marine protected areas (MPAs), which address significant management challenges. Such challenges include focusing on both improving baseline knowledge of the MPAs, as well as addressing applied novel management questions. Parks Victoria's research program is guided by the research themes outlined in Parks Victoria's Environmental Research Strategy 2012-2025 and their monitoring program is guided by a draft state-wide marine monitoring framework based on priorities identified through the Conservation Planning process for the marine national parks and sanctuaries.

1.1 Previous Long-term Monitoring Programs

Parks Victoria's long-term Subtidal Reef Monitoring Program (SRMP) was designed using best scientific practices in the early 1990s and initiated in (what is now) the system of marine national parks and sanctuaries in 1998. These surveys are currently conducted in 13 marine national parks and sanctuaries across the state (Power & Boxshall 2007). This program used diver underwater visual census methods, which allow descriptions of macroalgae, fish and macroinvertebrate communities at each monitoring site, as well as indications of change through time. Furthermore, an Intertidal Reef Monitoring Program (IRMP) was first implemented in late 2002 with sampling at some sites beginning in the summer of 2002-2003 (Power & Boxshall 2007). This method involved the monitoring of invertebrates and macroalgae present in the intertidal zone on reefs within nine targeted MPAs as well as at nine matched reference sites outside the MPAs (see Hart and Edmunds (2005) for full methodological details).

1.2 New MPA Monitoring Framework

Parks Victoria has since adopted an Adaptive Management Framework and Conservation Planning process, resulting in more clearly defined goals and objectives for managing key natural assets and threats. A draft state-wide monitoring plan based on conservation, management and monitoring priorities identified for each park through the Conservation Planning process, has been developed and includes potential indicators for subtidal and intertidal reef communities, as well as other key habitats/ecosystems, and key threats to these priority natural assets. The process for identifying monitoring priorities at the state-wide level was endorsed by Parks Victoria and involved three consecutive assessments

including: 1) priority parks (i.e. representative, IUCN category II etc.), 2) priority Key Ecological Attributes (KEAs) in priority parks, and 3) priority threats to KEAs in priority parks.

The new monitoring program will focus on KEAs and threats in at least one of the large marine national parks within each bioregion, currently identified as Discovery Bay MNP (Otway bioregion), Point Addis MNP (Central Victoria bioregion), Port Phillip Heads MNP (Victorian Embayments bioregion), Wilsons Promontory MNP (Flinders bioregion) and Cape Howe MNP (Twofold Shelf bioregion). It will also address monitoring priorities identified for other parks using a range of delivery models as resources permit.

1.3 Point Addis Marine National Park

This study assessed the area within and adjacent to the no-take Point Addis Marine National Park by integrating historical data dating from 2003 and with new data collected as part of this project in 2017 and 2018. The site extends along 23 km of coastline from the iconic Bells Beach in the east to Aireys Inlet in the west. It covers an area of 4,416 ha (44.166 km^2), from the shoreline to Victorian state water limits (~5 km offshore) to depths of 60 m. Lower eulittoral reef in this area is largely dominated by *Durvillaea potatorum* and *Hormosira banksii*. Infralittoral reefs consist of large canopy-forming macroalgae (predominantly *Ecklonia radiata* and *Phyllospora comosa*) and a mixed red and green algal understorey. These reefs also provide refuge for commercially targeted species of invertebrates such as abalone (*Haliotis* spp.) and southern rock lobster (*Jasus edwardsii*) (Woods et al. 2014). The Point Addis Marine National Park and adjacent waters also contain large rhodolith beds (free-living coralline algae) in deep soft sediment areas within and adjacent the MNP (Holmes et al. 2008, Ierodiaconou et al. 2011). In the mesophotic zone, circalittoral reefs are dominated by sessile benthic invertebrates including ascidians, soft corals, sponges and gorgonian fans (Barton et al. 2012).

1.4 Monitoring Priorities of the Point Addis MNP

A number of monitoring priorities have been identified for Point Addis MNP. These priorities are outlined below.

1.4.1 Subtidal reefs (including shallow and deep reefs)

- Large mobile fish (including sharks and rays) especially those that are ‘site attached’, rather than transitory.
- Mobile macroinvertebrates, especially abalone and rock lobster as these are keystone species and illegal fishing has been identified as a major threat to these invertebrates in the park.
- Brown macroalgae dominated communities (*Ecklonia radiata*, *Durvillaea potatorum*, *Phyllospora comosa*, *Seirococcus axillaris*, *Acrocarpia paniculata*).

- *Macrocystis pyrifera* ecological community (where present).

1.4.2 Intertidal reefs

- Brown algae (*Hormosira banksii*) dominated communities (in low-mid littoral zone).
- Other algae and sessile invertebrate communities – algae (erect coralline algae, turf algae, e.g. *Capriola implexa*, green algae, i.e. *Ulva* spp. and *Cladophora* spp.) and sessile invertebrates (e.g. *Chthamalus antennatus*, *Xenostrobus pulex*, *Galeolaria caespitosa*).

1.5 Objectives

The overarching objective of this project was to develop a targeted monitoring program for the Point Addis Marine National Park based on the previously stated key conservation, management and monitoring objectives established for the park, and to use these as a pilot for an expanded state-wide MPA monitoring program. Particular objectives related to this overarching goal include:

- Compile seabed bathymetry data to develop full coverage maps of the Point Addis MNP and adjacent waters to assist in characterisation of the seabed.
- Implement Reef Life Survey methods at existing SRMP MPA and reference sites on shallow subtidal reefs to compare abundance and diversity of fish and invertebrate populations and canopy forming algae through time.
- Implement a Baited Remote Underwater Video survey (BRUVs) of demersal fish assemblages within and adjacent to the MPA to compare abundance and diversity of fish populations surveyed as part of this project with those observed during previous BRUV surveys in Point Addis MNP.
    - Initiate time-series monitoring of demersal fish assemblages across the entire depth range of the park.
    - Understand the effect of seafloor structure on abundance and diversity of fish using spatially-explicit distribution modelling techniques.
- Implement Unmanned Aerial Vehicle (UAV) surveys for intertidal reef platforms inside the park using the methods previously tested by Deakin University (Murfitt et al. 2017).
    - Develop an approach to capture intertidal reef extent imagery and extraction of platform wide *H. banksii* canopy cover.
    - Extend time-series IRMP monitoring of *H. banksii* canopy cover using virtual quadrats extracted from UAV data.

- Use image classification approaches to create estimates of *H. banksii* coverage and fragmentation statistics across the intertidal platform.
- Test environmental and structural metrics to evaluate *H. banksii* distribution and fragmentation.

- Use standardised fishery stock assessment methods to assess the effect of this MPA on the local population of Southern Rock Lobster, *Jasus edwardsii*.
  - Determine whether protection is associated with increased biomass or size of individuals.
  - Determine the effect of seafloor structure and distance from MPA on lobster count, biomass and sex ratios.
- Develop and implement robust survey designs for brown macroalgal dominated communities on deeper reefs (> 10 m depth) and KEAs in deeper soft sediment communities using oblique video and downward facing still images from towed video surveys, and draft standard operating procedures.
- Add data collected as part of this project to control charts developed for the Point Addis Marine National Park report card and new opportunities through BRUVs timeseries.

2. Method

2.1 Intertidal Reef Monitoring

2.1.1 Unmanned Aerial Vehicle surveys of intertidal reefs

In order to update previous visual census methods and take advantage of scientific advancements using Unmanned Aerial Vehicles (UAVs), this study implemented an updated methodology for monitoring tested by Deakin University (Murfitt et al. 2017). Deakin University is a Civil Aviation Safety Authority (CASA) certified commercial Remotely Piloted Aircraft (RPA) operator (CASA.ReOC.6496). Surveys were conducted using a small (< 2 kg) multi-rotor airframe (DJI Phantom 4 Pro) carrying a multispectral imaging sensor.

The Point Addis intertidal platform was surveyed on two different dates; April 21st 2018, and March 28th 2019. Flying height, overlap, speed, and flight time per battery were all set based on previous research of intertidal platforms, which concluded that higher altitude allows for faster speed and more area captured in each image, ultimately allowing for a larger area to be sampled (Figure 1). However, higher altitude is a compromise resulting in lower resolution imagery (Figure 2). For the proposed purpose of mapping *Hormosira banksii* extent, the UAV was flown at 20 m above the platform on east/west lines, capturing 70 % front overlap and 80 % side overlap between images and flying at 3 m/s, running through the autonomous software Pix4D Capture. All flights were planned for a maximum of 12 minutes of flight time. On both occasions Parks Victoria staff undertook Sea Search intertidal reef cover quadrat surveys (Brown et al., 2018). This provided ground truth data across the intertidal platform using a standard quadrat approach to obtain percentage canopy cover of *Hormosira banksii* for comparison with drone estimates (in 2018, very low shore samples were also undertaken looking for different algal species cover).

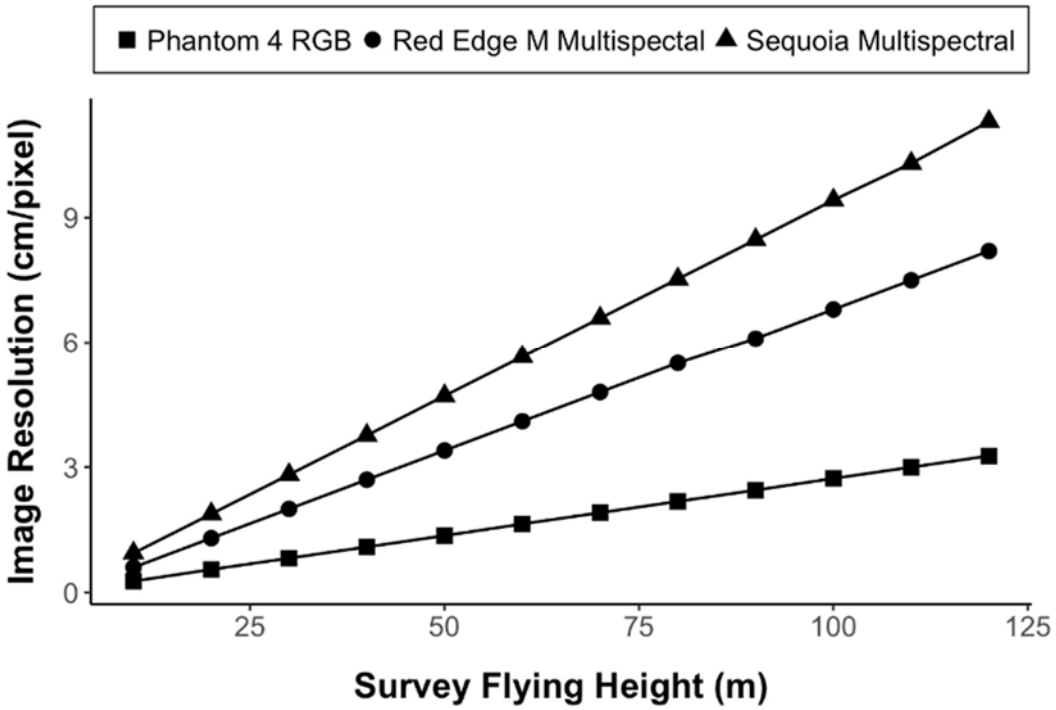

Figure 1. Resolution compared to survey height for each image sensor used in this study. Sensors used were DJI Phantom 4 on-board RGB camera (20 effective MP, FOV 94°, 20 mm of 35 mm format equivalent, f/2.8, focus at ∞), Parrot Sequoia multispectral camera (1.2 effective MP, 10 bit colour depth, 4.0 mm Focal Length, 4.8 mm x 3.6 mm Imager size, and 61.9° Horizontal FOV), and Micasense Red Edge M multispectral camera (1.2 effective MP, 16 bit colour depth, 5.4 mm Focal Length, 4.8 mm x 3.6 mm Imager size, and 47.9° Horizontal FOV). Flight heights are expressed in metres above ground level (AGL).

10 m

20 m

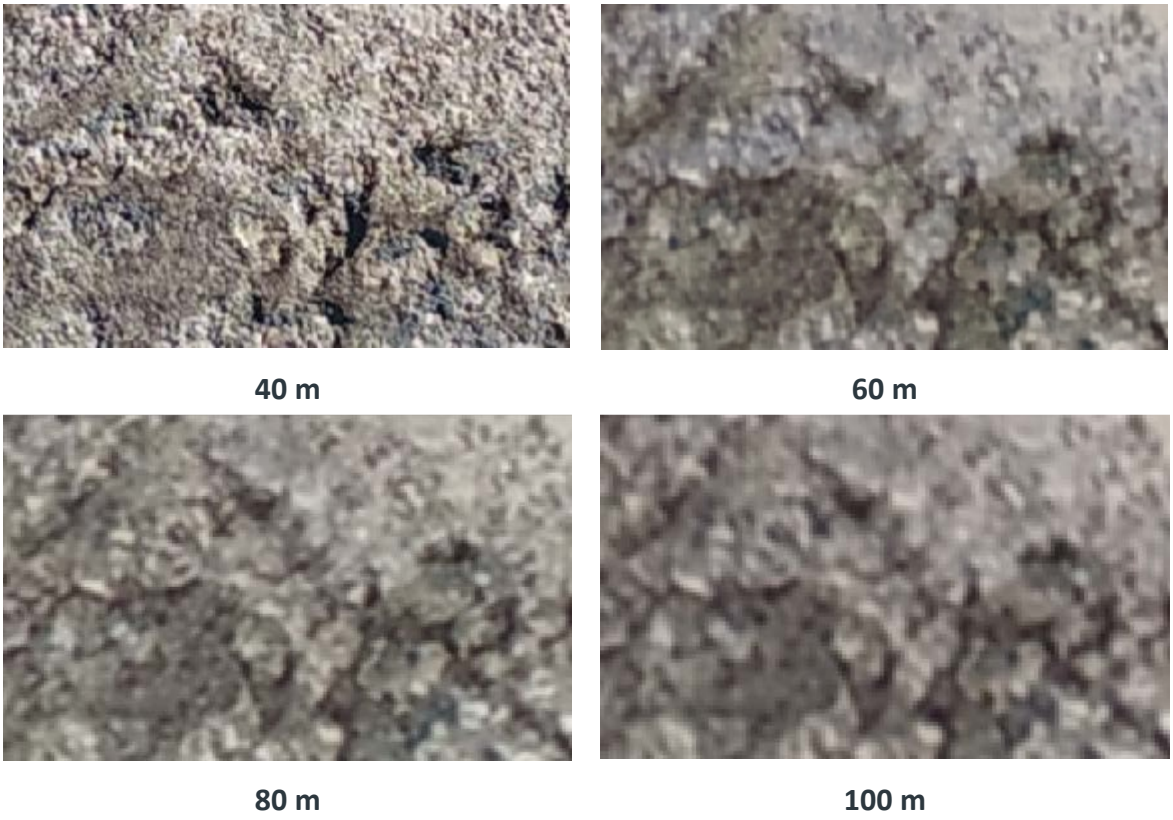

Figure 2. Comparative image resolution of processed images from DJI Phantom 4 onboard RGB camera (20 effective MP, FOV 94°, 20 mm of 35 mm format equivalent, f/2.8, focus at ∞) at survey heights from 10 m to 100 m with field of view approximately 4 m x 2 m. Superior image quality can be observed in the surveys at 10 m, 20 m and 40 m due to the lower flying altitude along with better ambient lighting conditions and absence of water on shore platform.

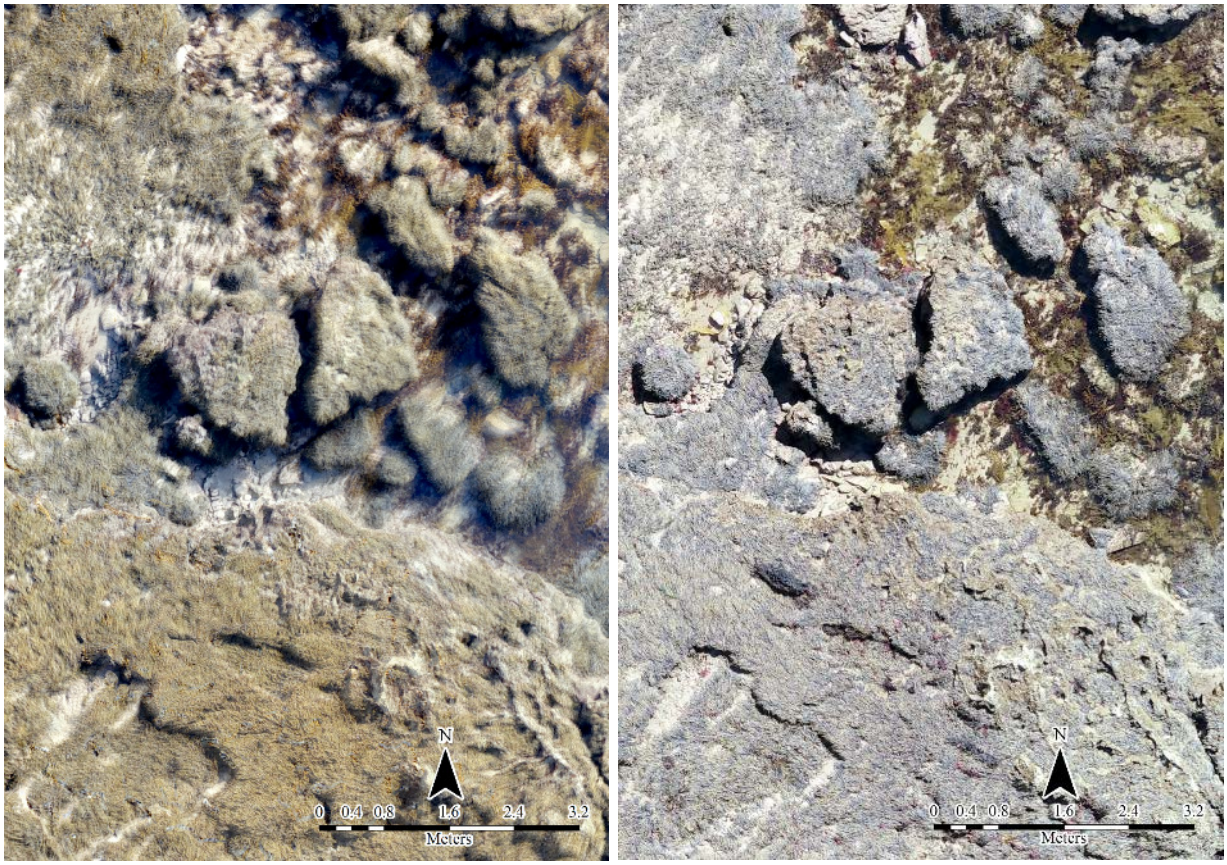

Figure 3. Comparison of image quality based on weather conditions and tide. Both images were captured at 20 m. The image on the left was captured on April 21st 2018, early in the morning and some standing water. The image on the right was captured on March 28th 2019, close to midday and with little standing water on the platform.

The weather on April 21st 2018 was a sunny day with a low tide of 0.21 m (mean sea level, Australian Height Datum, Geoscience Australia) and winds < 10 kts, however low tide was 0912h, so multispectral mapping was conducted earlier than recommended (recommended flight time is within 2.5 hours of solar noon). The lower light conditions can increase blur in both the RGB and multispectral imagery (Figure 3) but requirements for data capture on a very low tide meant that mapping proceeded. The weather on March 28th 2019 was a sunny day with a low tide of 0.23 m and winds < 10 kts, and low tide was 1151h, so multispectral mapping was conducted within 2.5 hours of solar noon.

In 2018, the flights were conducted with the DJI Phantom 4 Advanced UAV with in-built 20 MP camera, and carrying a Parrot Sequoia multispectral camera (1280 x 960 resolution, 10 bit colour depth, 4.0 mm Focal Length, 4.8 mm x 3.6 mm Imager size, and 61.9° Horizontal FOV) provided by Parks Victoria. The Parrot Sequoia multispectral camera required much more data processing than anticipated to generate useable results. As such the 2019 flights were with the same UAV (DJI Phantom 4 Advanced with in-built 20 MP camera), but carrying a Red Edge M multispectral camera purchased by Deakin University (1280 x 960

resolution, 16 bit colour depth, 5.4 mm Focal Length, 4.8 mm x 3.6 mm Imager size, and 47.9° Horizontal FOV).

The total area captured was approximately 40,800 m^2 at 20 m, requiring 7 flights. Ground Control Points (GCPs) were placed within the mapping area and marked with a Real Time Kinematic (RTK) GPS. In 2018, twenty Ground Control Points (GCPs) were placed within the mapping area and the average error of the marked points was 6.59 (± 0.28) mm horizontal and 7.58 (± 1.83) mm vertical error. In 2019, fifteen GCPs were placed within the mapping area and either marked with a RTK GPS, or using Propeller AeroPoints. The average error of the marked points was 2.74 (± 0.68) mm horizontal and 9.1 (± 1.4) mm vertical error. The accuracy of the final models were within 5 cm horizontal and 10 cm vertical indicating a good model fit comparable with survey grade expectations.

The data was processed in Pix4D version 4.3.33 (© 2020 Pix4D SA). The outputs generated from the RGB imagery were an RGB Orthomosaic and a Digital Surface Model (DSM) of the entire platform. The outputs generated from the multispectral imagery included individual spectral reflectance layers for each spectral band captured and a Normalised Difference Vegetation Index (NDVI) calculated from the reflectance bands. The resolution of each output is recorded in Table 2.

Table 1. A list of the outputs generated from the UAV aerial imagery in Pix4D for 2018 and 2019, and their respective resolutions.

2018		
Output	**Camera**	**Resolution**
RGB Orthomosaic	DJI 20 MP camera with 1-inch CMOS sensor	0.54 cm/pixel
DSM	DJI 20 MP camera with 1-inch CMOS sensor	0.54 cm/pixel
Individual Spectra (Green, Red, Red-Edge, Near-Infrared)	Parrot Sequoia	2.10 cm/pixel
NDVI	Parrot Sequoia	2.10 cm/pixel

2019		
Output	**Camera**	**Resolution**
RGB Orthomosaic	DJI 20 MP camera with 1-inch CMOS sensor	0.50 cm/pixel
DSM	DJI 20 MP camera with 1-inch CMOS sensor	0.50 cm/pixel
Individual Spectra (Blue Green, Red, Red-Edge, Near-Infrared)	Micasense Red Edge M	1.29 cm/pixel
NDVI	Micasense Red Edge M	1.29 cm/pixel

NDVI output values between 0.68-0.92 represented the majority of the vegetation within the imagery, and was extracted as a general vegetation layer. However, this value range also included many of the sections of the platform which were in shadow, irrespective of whether or not they had vegetation. This was more apparent in the 2019 dataset than the 2018 dataset. The RGB Orthomosaic was used to remove the areas of shadow from the vegetation layer. An ISO Unsupervised Classification was conducted on the RGB Orthomosaic, allocating each pixel in the orthomosaic to one of 30 classes based on the colour of the pixel. Each of the 30 classes was manually assessed for what it represented on the platform, and the classes representing non- *H. banksii* vegetation and shadows were used to erase those sections from the vegetation layer. This process was conducted separately for the 2018 and 2019 datasets, as the lighting varied between years, affecting the class allocation processing on the platform. The DSM was used to generate a data layer representing all sections inundated with water, which was also removed from the vegetation layer. The resulting layers were representative of *H. banksii* coverage on the Point Addis intertidal platform for 2018 and 2019. After running classifications, we visually determined that isolated polygons below 20 cm^2 were unlikely to be *H. banksii* and artefacts of the classification process, and thus removed those polygons from the coverage maps. Finally, the *H. banksii* cover for the Point Addis intertidal platform was calculated for 2018 and 2019.

Virtual Quadrats were then generated which corresponded to the On-Ground Quadrats scored for *H. banksii* percentage cover during the UAV operations. Twenty On-Ground Quadrats were scored in 2018, and all were included in the comparative study. Twenty-five On-Ground Quadrats were scored in 2019, however 7 of the quadrats were not marked with RTK precision due to network loss to the RTK GPS, and 1 Quadrat was outside of the main platform, resulting in 17 quadrats included in the comparative study for 2019. On-Ground Quadrats were measured using a 50 cm x 50 cm quadrat with the outside corners marked with the RTK GPS, resulting in virtual quadrats measuring an average of 58 cm x 58 cm, 34 % larger than the On-Ground Quadrats. Due to this, percentage cover within the quadrat was used instead of area, to scale for the difference.

Nine patch analysis windows measuring 25 m x 25 m were allocated across the Point Addis intertidal platform, and visually broken into three broad densities: low *H. banksii* coverage (3 windows), moderate *H. banksii* coverage (3 windows), and dense *H. banksii* coverage (3 windows). The percentage of *H. banksii* cover within the patch analysis windows was calculated for 2018 and 2019. The *H. banksii* coverage present in each of the patch analysis windows were quantified against landscape pattern indices (*H. banksii* Cover (%), Number of Patches, Maximum Patch Area (m^2), Mean Patch Area (m^2), Total Perimeter (m), Mean Patch Perimeter (m), and Edge Density). The percentage cover of *H. banksii* and the number of patches provide a general index of spatial heterogeneity across an entire landscape. The maximum patch area indicates whether the window was dominated by a single patch. Minimum patch size was not included as it was always at the single pixel scale from clipping

the window edge. The mean patch size provides an indication of coverage, while the standard deviation is a measure of absolute variation that is a function of the mean patch size and the difference in patch size among patches. The perimeter measures provide an indication of connectivity, while edge distance standardizes patch edges to a per unit area basis. The patch analysis windows create false patch edges on the perimeter of the windows, but this was uniform across all windows, and minimal compared to total edge length, so was included in the analysis.

2.2 Subtidal monitoring

2.2.1 Bathymetric variables for subtidal survey design

As a foundation for sampling design, a 5 m horizontal resolution bathymetric grid of approximately 100 km^2 was generated for the Point Addis MNP and adjacent waters using a combination of multibeam sonar and LiDAR data. Multibeam bathymetry was acquired as part of the Victorian Marine Habitat Mapping Project (Ierodiaconou et al. 2007; Holmes et al. 2008). Data were obtained from two surveys in November–December 2006 and November–December 2007, using a Reson Seabat 8101 multibeam echosounder operating at a frequency of 240 kHz and 150° angular sector coverage. Data logging, *in situ* quality control, display, navigation, and post-processing were all carried out using the Starfix Suite 7.1 (Fugro proprietary software). LiDAR data were commissioned by the Victorian State Government's Department of Environment and Primary Industries to assess the impacts of climate change on the coastal zone. Bathymetric LiDAR data were collected in 2007 using a LADS Mk II system coupled with a GEC-Marconi FIN3110 inertial motion sensing system and a dual frequency kinematic geographic positioning system (kGPS), mounted aboard a DeHavilland Dash-8 aircraft. Flight lines for the mapping survey were spaced at approximately 220 m, with a swath width of 240 m, leading to a line overlap of 10 m (Zavalas et al. 2014, Young et al. 2015). This dataset included seamless mosaics from +10 m elevation to −25 m depth along the entire coastal extent of the study site (Quadros & Rigby 2010). To create a seamless transition between the two data products, multibeam data was transformed from LAT to AHD using the Auscoast VDT transformation tool (Keysers et al. 2013). Following this, the *Mosaic Raster to New Dataset* tool within ArcGIS 10.1 (ESRI 2011) was used to mosaic multibeam and LiDAR data into a single raster dataset. A comparison of the differences in depth between multibeam and LiDAR products, using 10,000 randomly placed points within the multibeam/LiDAR overlap area, showed an average offset of 0.29 m between the data products (Young et al. 2015).

Derivatives of the seabed terrain were extracted using the Spatial Analyst (ArcGIS 10.5.1)(ESRI Software Inc.; Redland, California) and the Benthic Terrain Modeller tools for ArcGIS (Walbridge et al. 2018). Derivatives used included bathymetry, vector ruggedness measure (VRM), slope, rugosity, aspect (northness and eastness), bathymetric position

index (BPI), curvature, and distance to reef (Table 1). Average wave orbital velocity data were also obtained from a 25-year hindcasted wave model developed by Water Tech (Ierodiaconou et al. 2018).

To prepare the data for modelling, the *Extract Multi Values to Points* tool in ArcGIS was then used to extract the underlying seafloor variables at each site of interest (e.g. BRUV deployment, lobster pot location, towed video still photo location, etc.). Pearson correlations were used to remove highly correlated variables (> 0.6). One major grouping that was consistently correlated were measures of complexity including VRM, rugosity, curvature, slope and standard deviation of bathymetry. Multiple scales of bathymetric position index were also correlated (Inner and Outer radius of 10-30, 25-50 and 100-200). Finally, mean bathymetry was highly correlated with average wave orbital velocity and sea surface temperature with the year of sampling. As all variables from these groupings are correlated, a single representative from each was chosen and a total of seven uncorrelated variables were retained for final analysis (Table 1).

Table 2. Description of bathymetric variables tested in this study. All derivatives of bathymetry were made using the Benthic Terrain Modeller tool for ArcGIS (Walbridge et al. 2018).

Derivatives	Description
Bathymetry	Elevation of a plane passed through its closest grid point.
Rugosity	A measure of topographic roughness, which relates ratio of surface area to planar area.
Slope	Maximum change in elevation between each cell and cells in a specified surrounding neighbourhood.
Curvature	Second derivative of the bathymetric surface, or the first derivative of slope, computed in ArcGIS using the method of (Zevenbergen & Thorne 1987).
Bathymetric Position Index	Measure of a location's elevation relative to the overall landscape. Calculated by using an annulus to compare elevation of a cell with the mean elevation of surrounding cells at various neighborhood sizes.
Aspect (Northness and Eastness)	Azimuthal direction of the steepest slope through points in an analysis window. Northness relates to the sine component of the azimuthal direction, and Eastness relates to the cosine.
Distance to Reef	Reef position was obtained from a substrate layer classified into rock and sediment derived from the bathymetry/backscatter data. Euclidean distance tool (ArcGIS 10.1) was used to create raster of distance to reef. Sites on reef had a distance value of 0 m.

2.2.2 Sea Surface Temperature

Sea-surface temperature data were sourced from the Integrated Marine Observing System (IMOS) (IMOS 2018). IMOS is a national collaborative research infrastructure, supported by

the Australian Government. These data were downloaded in NetCDF format, at monthly intervals, and converted into individual ArcGIS rasters for analysis. Annual and summer means in SST were computed from 1992 to 2018 from the monthly SST datasets. To assess patterns in SST within Point Addis MNP, the mean and standard deviation of annual and summer SST were calculated for each year and plotted through time.

2.2.3 Reef Life Survey for shallow subtidal reefs

Reef Life Survey methods were completed at all historic subtidal reef monitoring program sites associated within the Point Addis Marine National Park (4 sites within the MPA and 4 reference sites, Woods et. al 2014) for 2017 and 2018 to continue the time-series. In recent years, Reef Life Survey (RLS) has become a common method for completing underwater visual census surveys of shallow subtidal reefs. Globally, the RLS technique has allowed approximately 2,000 sites to be surveyed using a standard set of survey methods, described in detail in an online methods manual (Reef Life Survey methods manual. http://reeflifesurvey.com/files/2008/09/NEW-Methods-Manual_15042013.pdf). Briefly, SCUBA divers swim along a 50 m transect line laid along a depth contour on hard substrate (coral or rocky reef). All fish species observed within 5 m of the transect line are recorded on a waterproof datasheet as divers swim slowly along the line (at approximately 2 m/min). On the same transect, all macroinvertebrates and cryptic fish larger than 2.5 cm within 1 m of the transect tape are recorded. A series of 20 photoquadrats are also collected at 2.5 m intervals. These quadrats are later scored, in our case using TransectMeasure software (SeaGIS), in which 20 randomly-placed points are classified per photoquadrat, allowing algae, sessile invertebrates and substratum type to be recorded and stored for later re-analysis if needed. Each point is scored using an adapted CATAMI classification scheme (Althaus et al. 2015). At each site, divers complete two 50 m transects in opposite directions along the same depth contour. This means that for each location, an area of 1,000 m^2 is surveyed for fish and 200 m^2 for invertebrates. The main differences in this survey approach compared with previous SRMP methods, is the replacement of *in situ* quadrat surveys with photo quadrats and a reduced survey effort is from 200m total transect distance in SRMP to 100 m at each site in RLS. To account for these differences in quadrat scoring, this study only compared canopy-forming species to previous SRMP observations, as understory communities are likely to be obscured in photos. Data was also normalised to account for differences in area covered by the two techniques and results were compared.

2.2.4 Baited Remote Underwater Video (BRUV)

Fish assemblages at this site were sampled using BRUVs on three occasions. An initial survey took place in April and May 2013 as part of a previous RPP “Understanding links between seafloor physical characteristics and biological communities: Integrating LiDAR, multibeam sonar and observation techniques for full coverage assessment of Marine National Parks”.

For this survey, sample sites were stratified using existing seafloor bathymetry data and habitat maps to ensure habitat variability across the site was captured (See Section 2.2.1). A further two surveys took place in March of 2017, and March and April of 2018. Sample sites for these surveys were selected using observations from the 2013 survey to haphazardly stratify drops across complexity and depth. A power analysis of existing BRUV data from the Point Addis Marine National Park and other MPAs was used to help inform the design of 2017 and 2018 surveys (Appendix 2). For this, the sample site was split into four groups (Infralittoral reef, infralittoral sediment, circalittoral reef and circalittoral sediment). The statistical power of BRUVs to detect change in species richness and total abundance was calculated for each habitat using a one-way ANOVA in a post-hoc power analysis. The power of BRUVs to detect a change of 20 and 50 % in species richness and total abundance using a significance criterion of 0.05 was estimated using mean and variance for each of the univariate variables in all habitats (Langlois et al. 2010, Harvey et al. 2012, Warnock et al. 2016). Non-central F probabilities were calculated for each analyses using the G*Power programme (Faul et al. 2007). An 80% chance of detecting a change in either of the univariate variables is commonly considered sufficient (Winer 1991). Furthermore, BRUV surveys aimed to target fish communities on deeper (> 10 m depth) algal dominated reefs to complement fish data collected using RLS methods on shallow subtidal reefs inside and outside of the MPA. An unbalanced sampling design was therefore implemented for the 2017 and 2018 surveys to maximise data capture with the MNP whilst limiting the impact associated with power to detect change in comparison to adjacent waters. To achieve this, a progressively unbalanced t-test was completed in G*Power to test how much of a difference could be present between the number of samples inside and outside of the MPA (Appendix 2). It was found that to achieve a power greater than 0.8 when assessing total abundance on macroalgal reef habitat, a minimum of 36 BRUV samples should be completed, with a ratio higher than 2:1 ratio between locations inside and outside of the MPA.

For all surveys, two high definition video cameras (Sony Legria HF G10 or M300 cameras) were fitted on each of six BRUV frames. The pairs of cameras were mounted 0.7 m apart and angled towards each other at 8^{o} to allow for stereo imaging, which can be used to calculate length of fishes and distance from the camera (Langlois et al. 2018). A synchronizing diode was placed in the field of view so the camera frames could be synced for size measurements. Each BRUV frame was calibrated in a pool before undertaking fieldwork. A bait bag made up of 1 kg of pilchards (*Sardinops sagax*) was suspended 1.2 m in front of the cameras. The locations of BRUVs were separated by at least 300 m to minimize potential movement of fish between sites and bait plume overlap. Sixty minutes of footage on the seafloor was analysed for each drop location. Post-processing of BRUVs footage was completed using the program EventMeasure (SeaGIS). For each video, the MaxN (maximum number of individuals of a particular species in the frame at any given time) was recorded, providing a conservative measure of relative abundance. MaxN is a widely recognized way of obtaining fish population data from BRUVs and ensures that no individual is double-

counted (Cappo et al. 2004). The total length of each individual fish counted in the MaxN for each species in each video was then measured using 5 mm as the maximum uncertainty accepted for each measurement. Total species richness, total abundance of individual functional feeding groups and both abundance and mean length of key species were then evaluated for each drop location.

Functional information was compiled for all species of fish present in this study. Specific traits, such as functional feeding group, were selected to include a range of attributes that influence the role of species within a community. Information was compiled following procedures of Stuart-Smith et al. (2013), in which data was predominantly extracted from FishBase (http://www.fishbase.org, Froese and Pauly (2010)). When information on a particular species was not available, it was assigned based on the combined knowledge of the authors for that species, or an appropriate congener from the same genus. This information was ultimately used to split the assemblage into subgroups of herbivore, invertivore and carnivore species for further modelling (Appendix 1). Three individual species were also included in this study to investigate if variations in model trends were present within functional groups. Species included were *Chrysophrys auratus*, *Notolabrus tetricus* and *Meuschenia hippocrepis*. These species are all common invertivores at the site and were further chosen as they have either been previously monitored at this site or are commercially important for the area (Woods et al. 2014).

Generalised additive models (GAMs) were used to investigate and model the effect of environmental variables on various subsets of the fish assemblages captured using BRUVs. GAMs were selected for use in this study because of their ability to allow for nonlinear relationships (Yee & Mitchell 1991, Austin 1998), as well as being a conventional and well-developed method for modelling fish-habitat relationships (Valavanis et al. 2008, Galaiduk et al. 2017). Before running GAMs, spatial autocorrelation of the response variables was tested using a spline correlogram generated in the R package 'ncf' (Bjørnstad 2009). The R package 'mgcv' (Wood 2015) was then used to run GAMs, using species richness as a response variable for multi-species analyses, and abundance for single-species analyses. In GAMs, the number of predictor variables able to be included is limited by the ability of the sample size to capture the variability across the study region. Bolker et al. (2009) recommend using a rule of thumb of > 10-20 samples per experimental unit. Deployments from all three years of sampling were included in a single model (n = 181 deployments). All combinations of the 9 predictor variables selected (n = 511 combinations) were modelled to obtain the highest possible model performance. These 9 variables included the 7 uncorrelated environmental variables as well as the year of sampling and MPA status as factor variables. Model selection was conducted using the "MuMIn" package in R (Barton 2016), in which all models were ranked based on a number of model parameters including Log-likelihood, AICc, ΔIC and Akaike weights. To assess the spatial ecology of species interactions with the surrounding environment, modelling in this study was completed using environmental derivatives extracted at multiple spatial scales (5 m, 10 m, 25 m, 50 m, 75 m,

100 m, 150 m, 200 m, 250 m, 300 m, 400 m and 500 m) around each BRUV deployment location. We randomly selected 75 % (n = 138) of BRUV deployments for training of models, reserving the remaining 25 % (n = 45) for testing the accuracy of predictions. Pearson's correlations were used to assess the accuracy of the predicted data compared with observed data. To assess individual variable importance, models with the best performance for each subset of the assemblage were run with and without each variable included to single out the contribution of the variable in question. Individual contributions were then summed and a percentage of relative importance in the model was derived. The R package "raster" (Hijmans & van Etten 2014) and the raster calculator tool in ArcGIS was used to create predictive maps extrapolating relative species richness and abundance predictions over the entire study area.

2.2.5 Towed video and Downward Facing Imagery

Towed video was employed to obtain transect data on benthic habitats extending beyond diving depths within the MNP. Two towed video surveys (2017 and 2018) were conducted as part of this study. These surveys used a VideoRay remotely operated vehicle (ROV), modified to function as a drift camera by inserting it into a stainless steel frame and adding a micro-wing attachment to assist in drifting across the seafloor. Forward-facing high-definition footage was obtained from 2 GoPro Hero 3+ cameras fastened to the top of the frame in a custom built stereo housing with a 40 cm base bar. To reduce the distorting effect of the fisheye lens in the cameras, footage was recorded with medium field-of-view, at a resolution of 1920 × 1080 pixels and 60 frames per second (FPS). The position of the unit in the water column was tracked at 1 s intervals using a Tracklink 1500MA ultra-short baseline (USBL) acoustic tracking system. The unit was flown approximately 1 m above the seafloor using a winch system while observing a live-feed obtained via an umbilical cable from the ROV unit. During both surveys, the boat speed was kept between 0.5 and 1.0 knots (0.26 to 0.5 m/s) for the majority of the transect. Time synchronization between the live towed video, stereo GoPro HD data and USBL system enabled measurement of the geographical location of benthic habitat observations along transects. For all transects, cameras were positioned at a 45° angle to the seabed. A downward facing camera with an attached strobe light was additionally used to create photoquadrats every 10 seconds. Pictures are then synchronized with time stamps from the GPS feed and positioned using the USBL system. These detailed images make it possible to obtain high-resolution taxonomic identification. Furthermore, this project had access to a towed video dataset acquired in 2005 by Holmes et al. (2008). This dataset was used to firstly prioritise survey locations for 2017 and 2018 surveys, as well as to assess temporal changes in the extent of key habitat groups.

Post-processing of towed video observations was conducted using the program TransectMeasure (SeaGIS). Georeferenced downward-facing stills were overlayed on

previously mentioned environmental variables (Section 2.1), allowing depth to be extracted for each image. Images were subsequently grouped into 5 m depth bins, where 40 images were randomly chosen per depth category. Five randomly spaced points were classified for each image using an adapted CATAMI classification scheme (Althaus et al. 2015). From this, differences in contribution of each biotic component at the lowest taxonomic resolution possible was identified for each depth strata.

In an attempt to rapidly assess whether changes in the extents of key habitat groups have occurred between 2015, 2017 and 2018 surveys, oblique video was analysed. Firstly, data was subset to include transects that had overlap between multiple years to enable direct comparisons to be made. These transects were then analysed by classifying a still image approximately every 15 m (dependent on the speed of tow), for presence or absence of key habitat groups. For the Point Addis MNP, key groups selected for analysis were *Ecklonia radiata* and rhodolith beds. Once classified, points could then be plotted on top of each other to allow for direct comparisons in extent to be made between years.

2.2.6 Fisheries Independent Southern Rock Lobster Survey

Southern Rock lobster (*Jasus edwardsii*) have previously been identified as an essential indicator of the health of subtidal reefs, as well as a proxy for the effect of poaching in marine national parks and sanctuaries. Rock lobster surveys can further offer valuable information about 'secondary' ecosystem services provided by the park to the rock lobster fishery, as well as being used to inform ecosystem-based management of the fishery. Southern Rock Lobster (SRL) have previously been surveyed as part of the Subtidal Reef Monitoring Program (Woods et al. 2014), however, it has been difficult to accurately sample rock lobster populations as monitoring sites rarely overlapped with prime rock lobster habitat. As an alternative, this study used standardized fishery assessment trapping methods to provide fine-scale SRL population information within and adjacent to the Point Addis Marine National Park. Lobster pots were baited with 1 kg of locally available bait and escape gaps were wired shut (Woods & Edmunds 2013, Young et al. 2016, Ierodiaconou et al. 2018). The sampling design was created in conjunction with local commercial lobster fisherman, who provided a wealth of knowledge in the local area, having fished there for 20 years, including reefs within the Point Addis Marine National Park prior to it becoming protected in 2002. A total of 240 pots were deployed during this survey, with 120 being placed inside the park and 120 outside. For each day's sampling, pots outside the park were deployed in areas of similar habitat to those deployed inside the park to accurately test the effect the park has on the local SRL population. All captured SRL were counted and sexed, females were assessed for reproductive condition, and all lobsters were measured for carapace length (CL). A genetic sample linked to individual morphometrics was also taken for potential analyses beyond the scope of this project. By-catch were recorded for each pot location before promptly being returned to the water. To calculate SRL biomass, we

used the length-weight relationship provided in Punt (2003): $W = aCL^b$, where W is the weight in kilograms, CL is carapace length and a and b are coefficients related to sex and size class (Females: a = 0.000271, b = 3.135; Males: a = 0.000285, b = 3.114). For each potlift, a pre-recruit index was developed by calculating the percentage of lobsters below the sex-specific size limits for this region (Male = 110 mm CL, Female = 105 mm CL) (Bentley et al. 2005).

The purpose of this SRL survey was to compare populations inside and outside the MPA and determine the role of environmental drivers on the spatially-explicit catch observed. Generalised additive models (GAMs) were further used to investigate the effect of environmental variables on SRL at this site. Methodology for implementation of GAMs was adapted from those used previously in this study for BRUV observations. GAMs were run using various groupings of abundance and biomass as response variables. Deployments from inside and outside of the MPA were included in a single model (n = 120 deployments). All combinations of the eight predictor variables selected (n = 255 combinations) were modelled in order to obtain the highest possible model performance. Model selection was conducted using the "MuMIn" package in R (Barton 2016), in which all models were ranked based on a number of model parameters including Log-likelihood, AICc, ΔIC and Akaike weights. We randomly selected 75 % (n = 90) of deployments for training of models, reserving the remaining 25 % (n = 30) for testing the accuracy of predictions. Pearson's correlations were used to assess the accuracy of the predicted data compared with observed data.

2.3 Control Charts

Parks Victoria, in collaboration with the University of Melbourne and Deakin University, have developed a series of control charts to provide timely, accurate, and reliable information on the condition of natural assets, level of threats and management effectiveness. These charts form part of Parks Victoria's State of the Parks evaluation. These charts depict a simple line graph tracking an indicator through time, with a zone of acceptable change identified, plus upper and/or lower control limits to flag values where a management response should be considered.

Control limits (CL) around the zone of acceptable change are calculated to reflect the statistical properties of the chart (Montgomery 2007) as follows:

$$CL_{upper} = LAC_{upper} + \frac{Z_\alpha \sigma}{\sqrt{n}}$$

$$CL_{lower} = LAC_{lower} - \frac{Z_\alpha \sigma}{\sqrt{n}}$$

where UL_{upper} = upper Control Limit, CL_{lower} = lower Control Limit, LAC_{upper} = upper Limit of Acceptable Change, LAC_{lower} = lower acceptable population mean, Z_{α} = multiplier for number of standard deviations to correspond with desired Type I error rate α, σ = weighted average standard deviation, and n = modal sample size to allow for possibly unequal sample sizes.

In the Point Addis Marine National Park dataset, the lower limit of acceptable change (LLAC, change to yellow) was initially identified as the minimum value inside the MPA from SRMP surveys in 2003, 2005 and 2006. For some indicators, modification of this lower LAC was needed to ensure the lower control limit remained above zero. Each chart was then plotted over the entire survey period including SRMP surveys from 2012, 2013, with current surveys in 2017 and 2018. For the BRUV data, the LLAC was chosen as the minimum value from the reference site over the two surveys. For *Hormosira banksii* (dominant algae on intertidal reefs), the LLAC was chosen as the three Sigma for Pt Lonsdale (42%), which represents the limit of natural mean variation of *H. banksii* in the area. This is also roughly the lowest value at the MPA site at Pt Addis prior to the last survey in 2013. However, it is worth noting that at 30% (which is the LCL), *H. banskii* recovery can take multiple (e.g. 1 – 3) years (Povey & Keough 1991, Keough & Quinn 1998, Schiel & Taylor 1999). The lower control limit (LCL, change to red) was then calculated from the LLAC and taking into account the variation in the data (Standard deviation) and number of sites surveyed (n) over the entire survey period. For ease of interpretation, zones of acceptable change on charts were shaded green, control limits were indicated by dashed horizontal lines, and areas outside the control limits were shaded red.

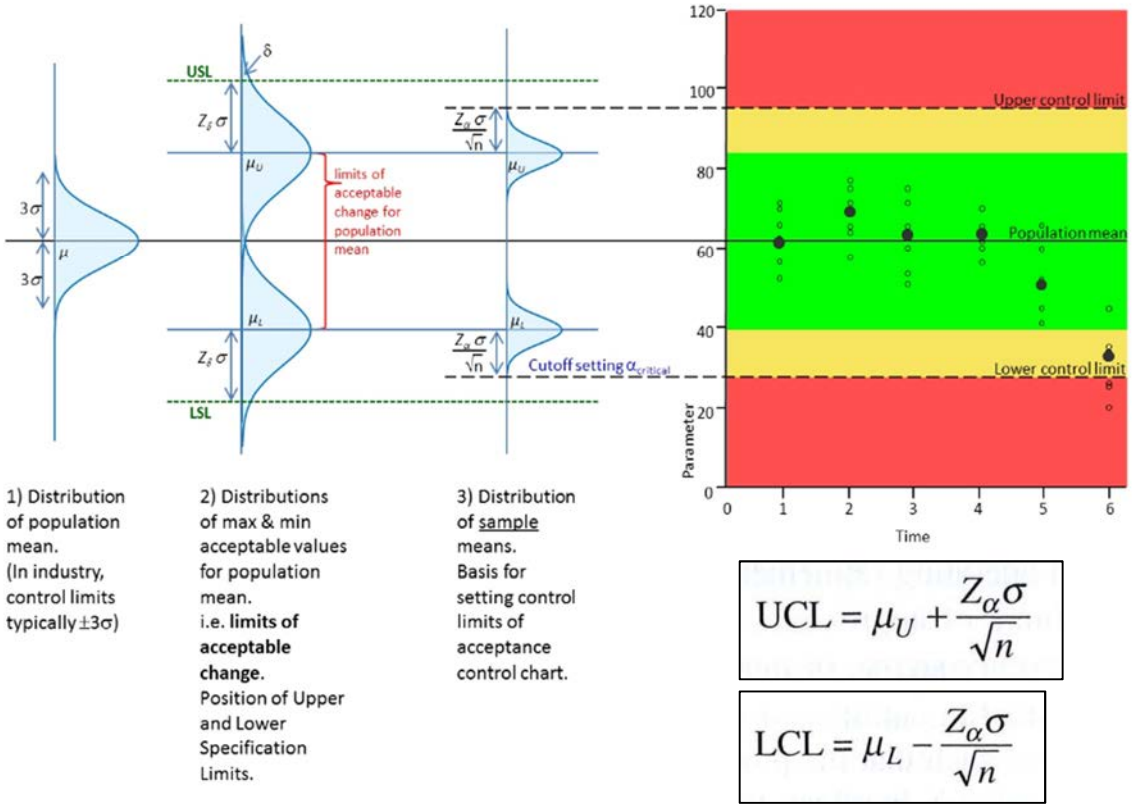

Figure 4. Principles behind the Acceptance Control Chart as applied to the Pt Addis MNP data, based on Montgomery (2009) (pg. 439-443).

3. Results

3.1 Seabed of Point Addis MNP and adjacent waters

For use in this study a high-resolution (5 metre horizontal resolution) bathymetric grid, was obtained for the Point Addis Marine National Park and surrounding areas of interest (an area of approximately 100 km^2). From this, eight derivatives of bathymetry were calculated to further our understanding of seafloor features. Derivatives created included depth, vector ruggedness measure (VRM), slope, rugosity, aspect (northness and eastness), bathymetric position index (BPI), and curvature (Table 1, Figure 6 and Figure 7). From this high-resolution grid, the extents of low and high-profile reef within the park were estimated, totalling an area of approximately 21 km^2, of which approximately 5 km^2 was classed as high-profile reef.

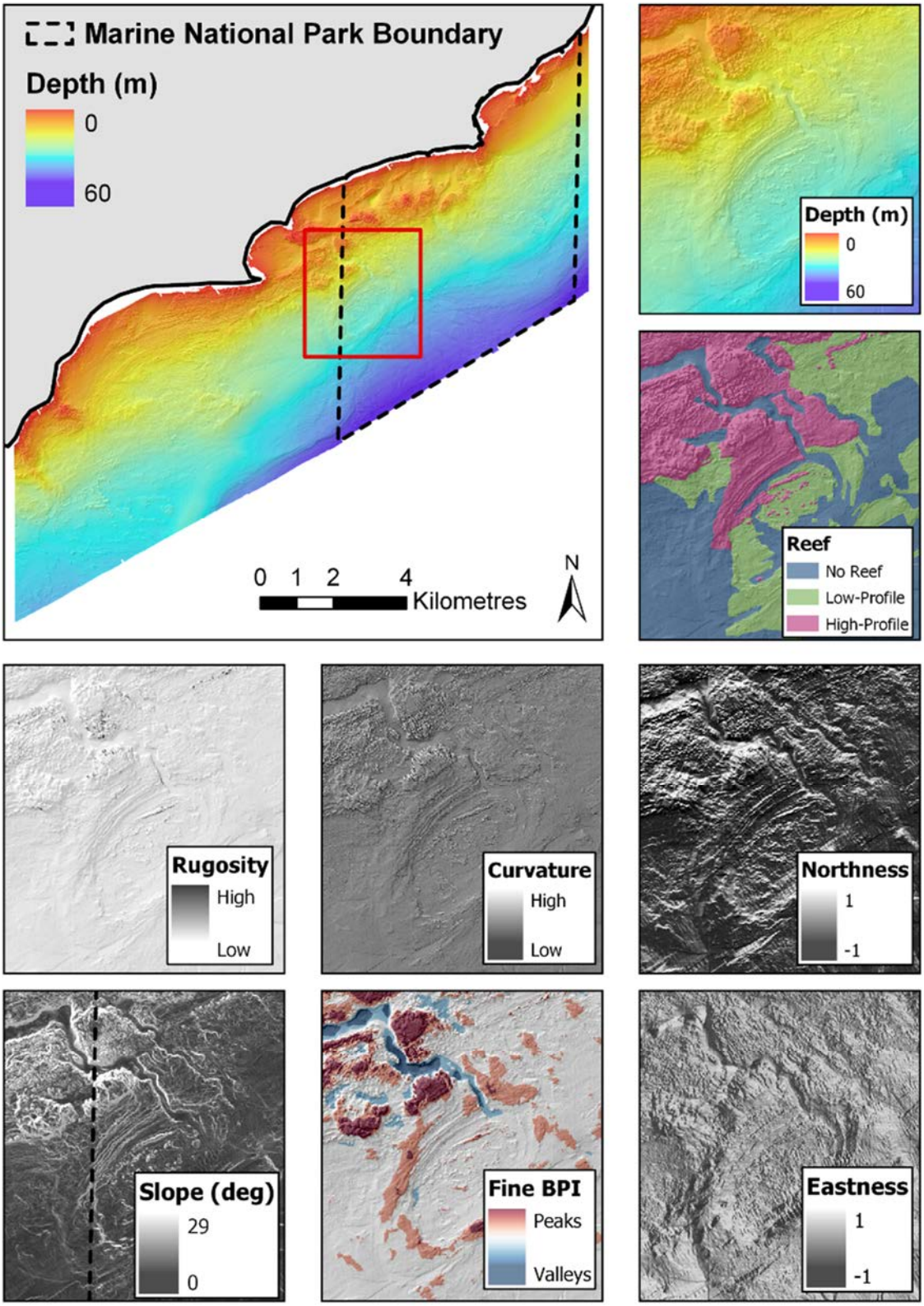

Figure 5. Overall map of bathymetry data available for this study with subset images of example derivatives used to characterise seafloor structure. Red box in large map indicates area for smaller windows shown.

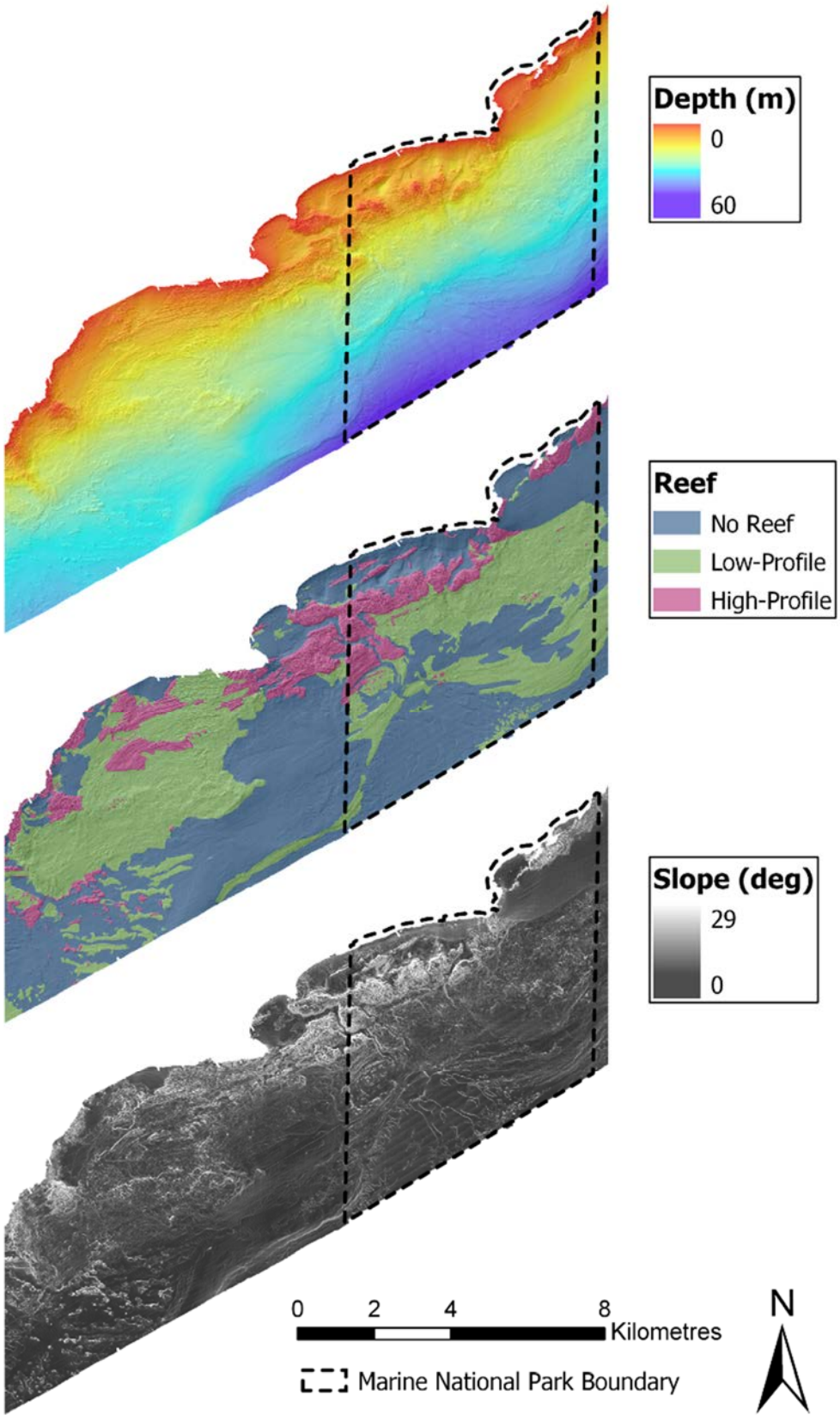

Figure 6. Examples of bathymetry (top), reef extents (middle) and slope (bottom) data available used to inform analysis within this study.

3.2 Patterns of Sea Surface Temperature change through time

Mean sea surface temperature (SST) varies seasonally and temporally in the Point Addis MNP with higher mean temperatures during summer. The SST has experienced an overall mean increase since 1992 in both annual and summer time series; however, this trend is not linear with oscillations in temperatures occurring through time. During the summer months, the SST in the park experienced a marked increase in SST in 2018 following a slightly negative trend since 2010. These trends also show that SST does not vary much throughout the park with very low standard deviations.

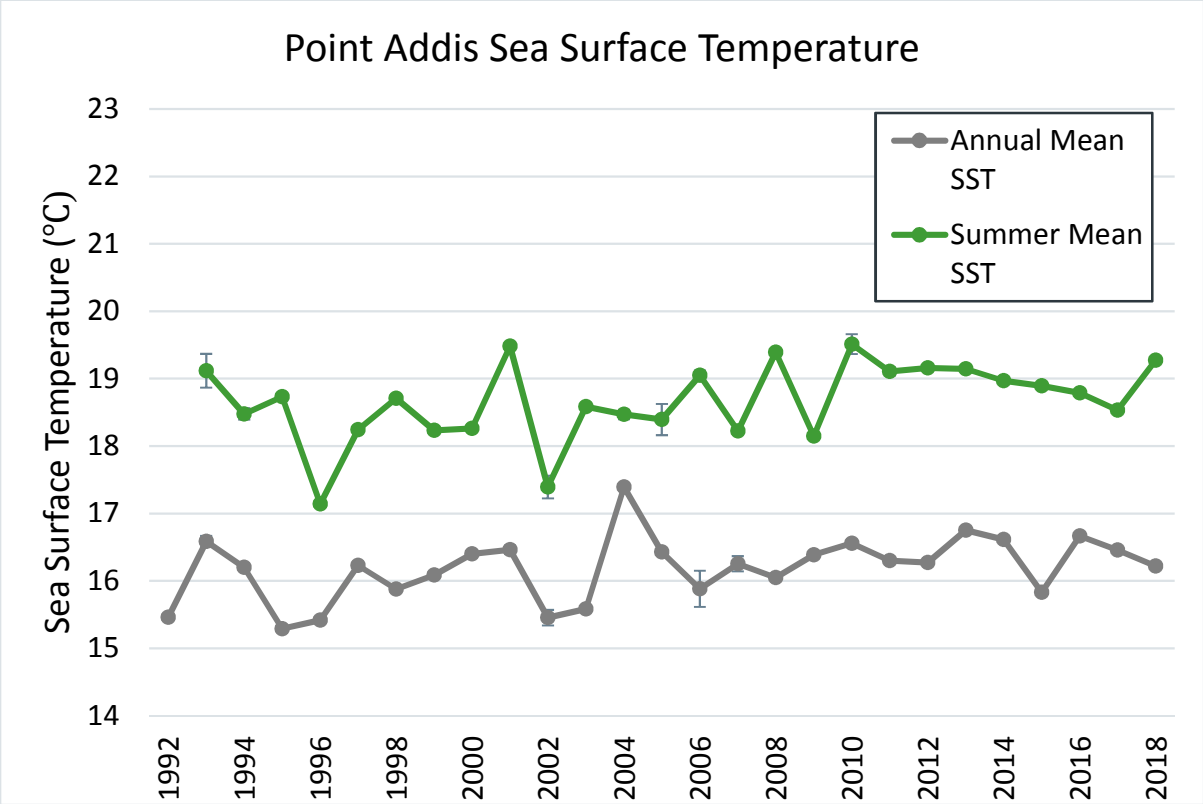

Figure 7. Sea Surface Temperature (SST) trends through time for annual and summer means in the Point Addis MNP. The standard deviations of the means across the park are represented as error bars.

3.3 Reef Life Survey for shallow subtidal reefs

A total of 888 mobile fish observations and 313 macroinvertebrates, across a total of 91 taxa were observed from Reef Life Surveys in this study (Table 6). Observations came from thirty-two 50 m transects, at 16 sites, allowing a total area of 1.6 hectares to be sampled for fish and 0.16 hectares to be sampled for macroinvertebrates and cryptic fish species. Notable fish species observed in this survey included *Achoerodus gouldii* (Western Blue Groper), *Aetapcus maculatus* (Warty Prowfish), *Orectolobus maculatus* (Spotted Wobbegong), *Chrosphyrs auratus* (Snapper), *Seriola lalandi* (Yellowtail Kingfish) and *Siphonognathus*

beddomei (Pencil Weed Whiting). Notable macroinvertebrates species included *Haliotis laevigata* (Greenlip Abalone), *Haliotis rubra* (Blacklip Abalone) and *Jasus edwardsii* (Southern Rock Lobster). A further 12800 random points were classified for benthic substrate from 640 photoquadrats taken during surveys. Predominant macroalgal species observed using this method included *Acrocarpia paniculata*, *Seirococcus axillaris*, *Cystophora* sp. and *Phyllospora* sp., as well as a range of foliose red algae (predominantly unable to be identified to species level using this method).

Table 3. Summary of Reef Life Survey sampling and observations across all years.

	2017	2018	Total
Number of sites completed	8	8	16
Area surveyed for fish (m^2)	16000	16000	32000
Area surveyed for invertebrates (m^2)	1600	1600	3200
No. of random points classified for benthic habitat	6400	6400	12800
No. of fish observations	888	790	1678
No. of fish species observed	33	33	43
No. of invertebrates and cryptic fish observations	313	441	754
No. of invertebrate and cryptic fish species observed	36	36	48

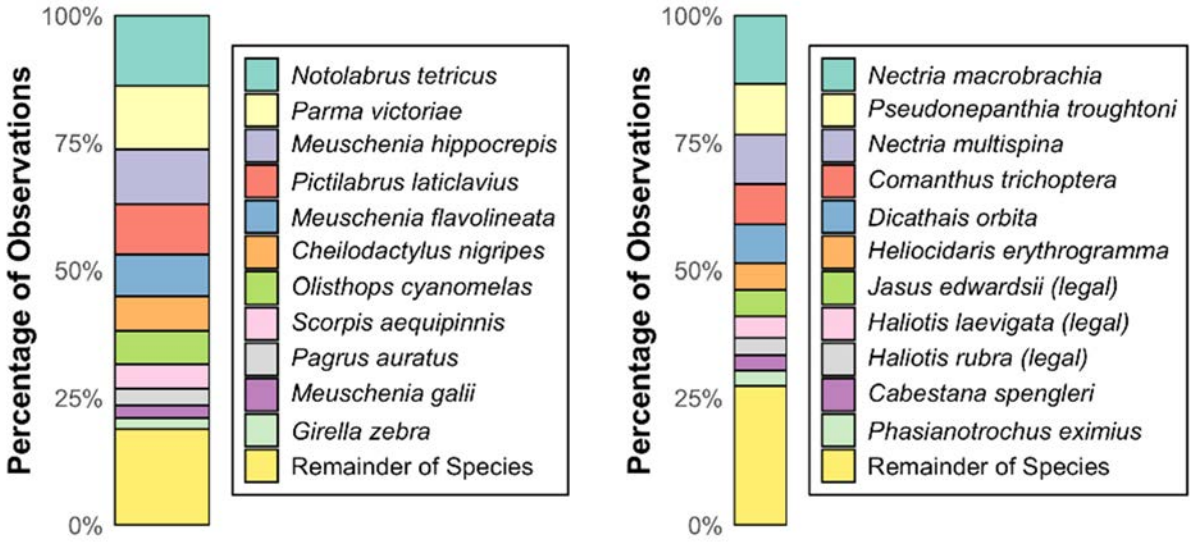

Figure 8. Proportions (as percentages) of the total observations of fish (left) and invertebrate (right) species made in the 2017 and 2018 RLS surveys completed in this project.

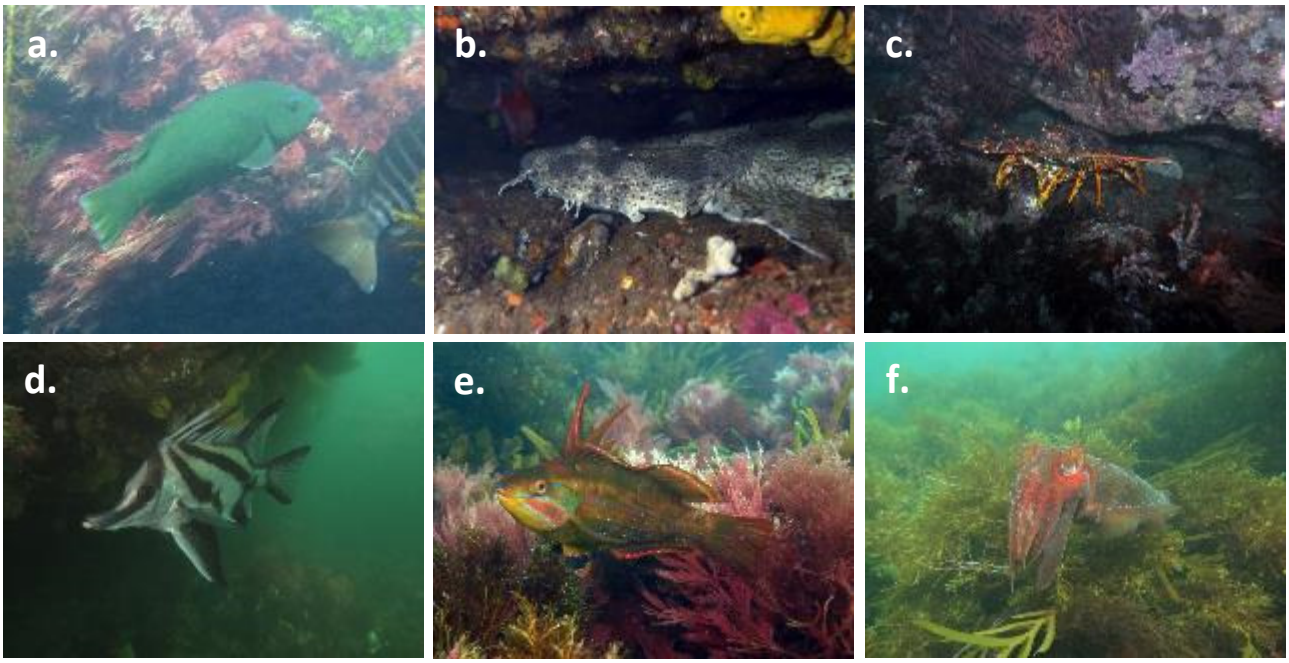

Figure 9. Example photos of fish and invertebrates observed in Reef Life Survey transects. (a) *Achoerodus gouldii* (b) *Orectolobus maculatus* (c) *Jasus edwardsii* (d) *Pentaceropsis recurvirostris* (e) *Odax acroptilus* (f) *Sepia apama*

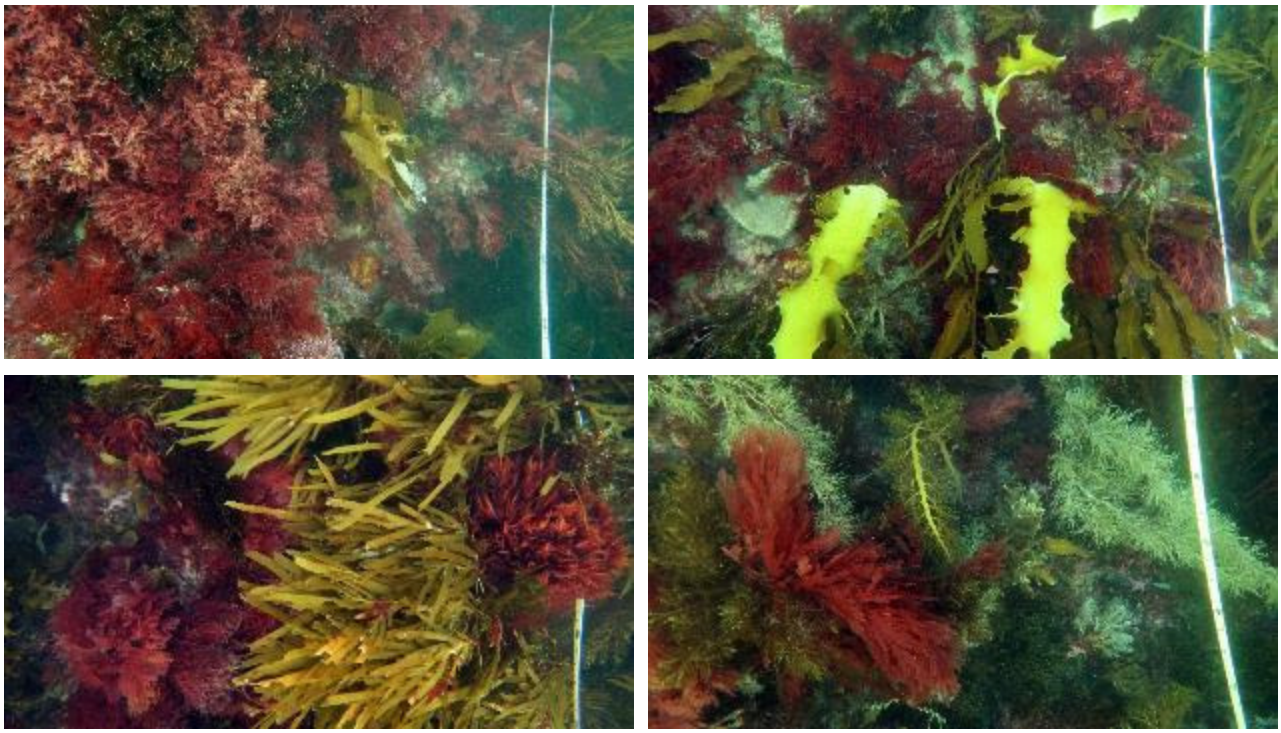

Figure 10. Example photoquadrats taken on Reef Life Survey transects. Such photos are subsequently classified using 20 random points and allow for detailed habitat classifications to be made and continuation of metrics for control charts for canopy forming algae at SRMP sites.

3.3.1 Key Mobile Fish Species

Control charts indicate that the current status of all key mobile fish species is healthy (above the lower control limit) with all species analysed currently being within the zone of 'good' condition (Figure 19). The size of individual fish species was generally similar between MPA and reference sites over time, with all species well above the LLAC (yellow zone). *N. tetricus*, *M. flavolineata* and *M. hippocrepis* showed increases in the mean number present in MPA sites between 2012 and 2018. While abundances of *Scorpis aequipinnis* have maintained similar numbers inside the MPA, the references sites have continued to show low numbers over time.

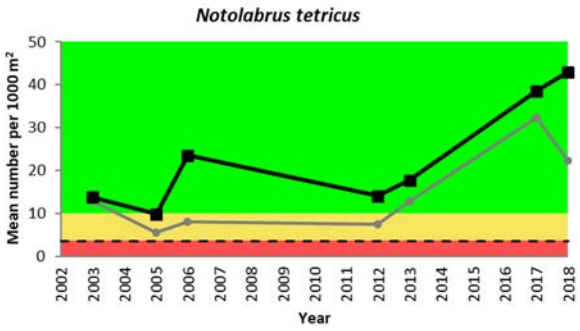

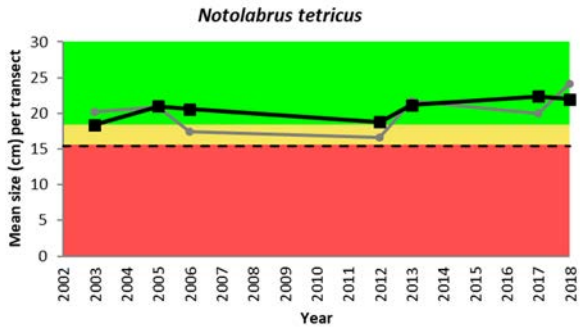

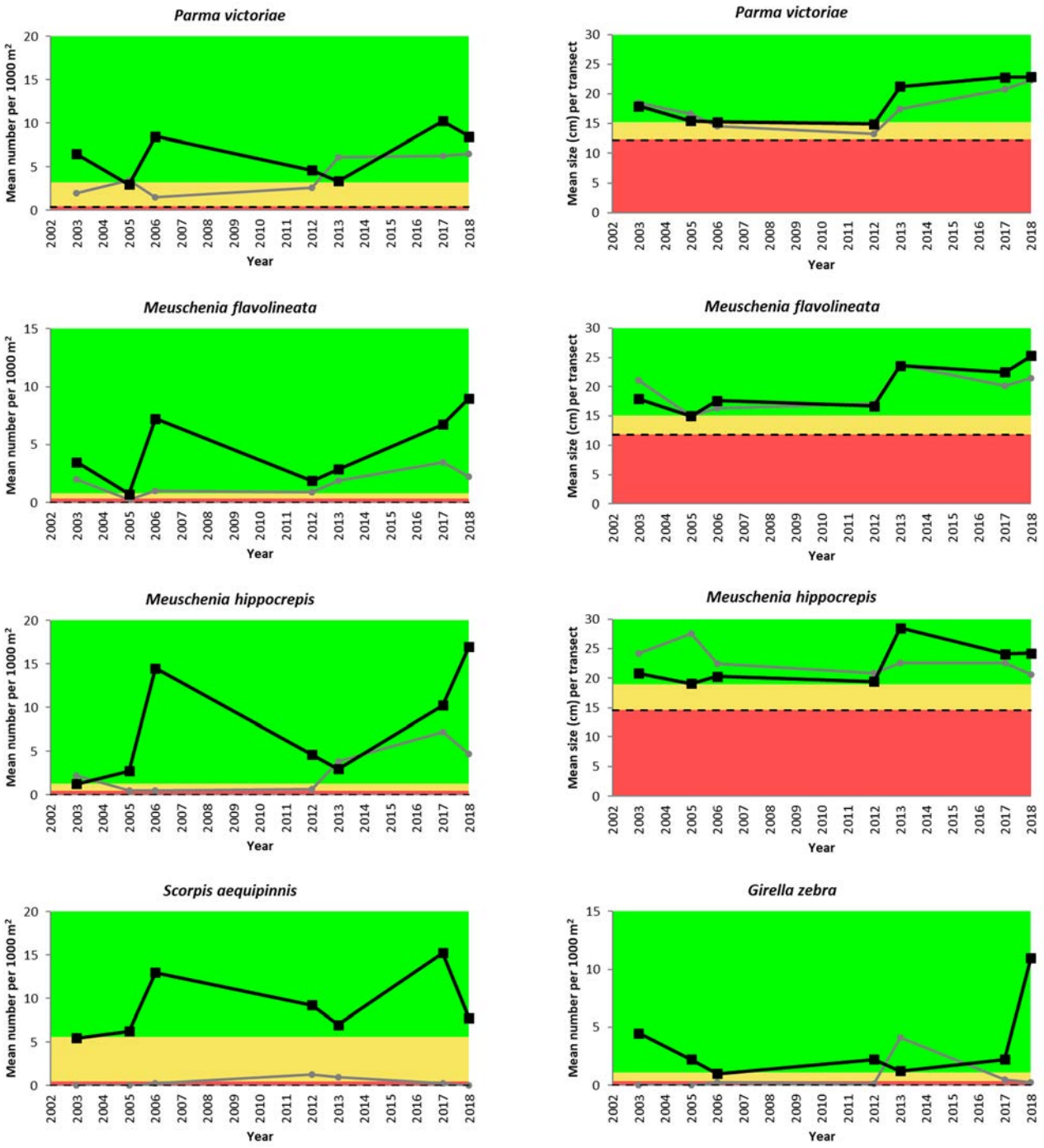

Figure 11. Control charts showing change in abundance and size of key mobile fish species within the Point Addis Marine National Park (black line) and reference sites (grey line). Observations for these charts were sourced from SRMP and Reef Life Survey diver transects. These charts have a lower limit of acceptable change (LLAC, yellow line - set as the minimum value inside the MPA from SRMP surveys in 2003, 2005 and 2006) and lower control limit (LCL, red line) based on the variation from surveys, which indicates the level when conditions are sufficiently poor that some management response is required.

3.3.2 Key Macroinvertebrates

The current (2018) status of *Haliotis laevigata* and *Nectria* spp. were found to be in good condition (well above LLAC) (Figure 20). However, consistent declines over the last 15 years were observed in *Haliotis rubra* and *Lunella undulata*. *Haliotis rubra* has been below its lower control limit of 4.6 individuals per 200 m^2 since 2012, and prior to this, from 2003 to 2006, the average abundances inside the MPA reduced from 70 to 30. A similar trend was also seen for *Lunella undulata*, with its highest abundances occurring between 2003 and 2006. Since then, it has been below its LLAC of 17.5 individuals per 200 m^2. It has not crossed its lower control limit, because this is currently calculated to be zero, due to high variability in its numbers between sites. *Haliotis laevigata* has shown highly variable patterns between years, resulting in low values for the LLAC and LCL. As a result, *H. laevigata* is currently classed as being in good abundance. *Nectria* spp. has maintained good abundance since 2002. Despite approaching the LLAC in 2017, the 2018 mean abundances of *Nectria* spp. returned to within acceptable levels.

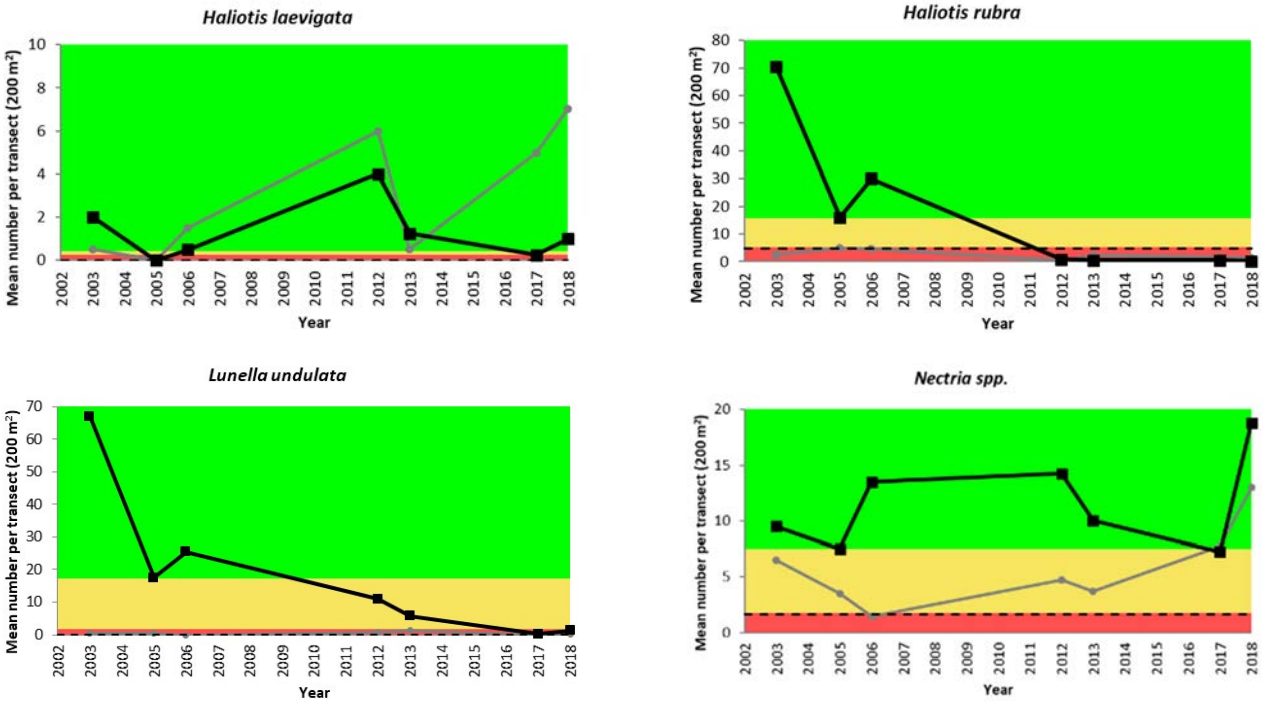

Figure 12. Control charts showing change in abundance and size of key motile macroinvertebrate species within the Point Addis Marine National Park (black line) and reference sites (grey line). Observations for these charts were sourced from Reef Life Survey diver transects. These charts have a lower control limit (set as the minimum value inside the MPA from SRMP surveys in 2003, 2005 and 2006) indicating the level when conditions are sufficiently poor that some management response is required.

3.3.3 Macroalgal Beds

The most notable change in the subtidal reef macroalgal communities of the Point Addis Marine National Park has been the decline of the common kelp *Ecklonia radiata* (hereafter *Ecklonia*) since 2012 (Figure 21). This has exceeded the lower control limit in the 2013, 2017 and 2018 surveys. This decline in *Ecklonia* has been followed by an increase in *Acrocarpia paniculata* and *Seirococcus axillaris*. These two large fucoid algae have increased from covering between 2 - 12 % of the reef between 2003 and 2006, to now each covering on average 20 % of the survey sites inside Point Addis Marine National Park. The other species of interest, *Phyllospora comosa*, has seen an increase. *Phyllospora comosa* showed very little percentage cover in surveys between 2003 and 2013, but covered 10 % of the reefs inside the Marine National Park in the 2018 survey. The one macroalgal group that has shown little patterns of change is the thallose red algae, which maintained reef cover of between 25 – 35 % between 2003 and 2018. When all the canopy-forming brown algae are plotted together we see that there has been a noticeable decline overall in the 2013, 2017 and 2018 surveys, currently being below the lower control limit.

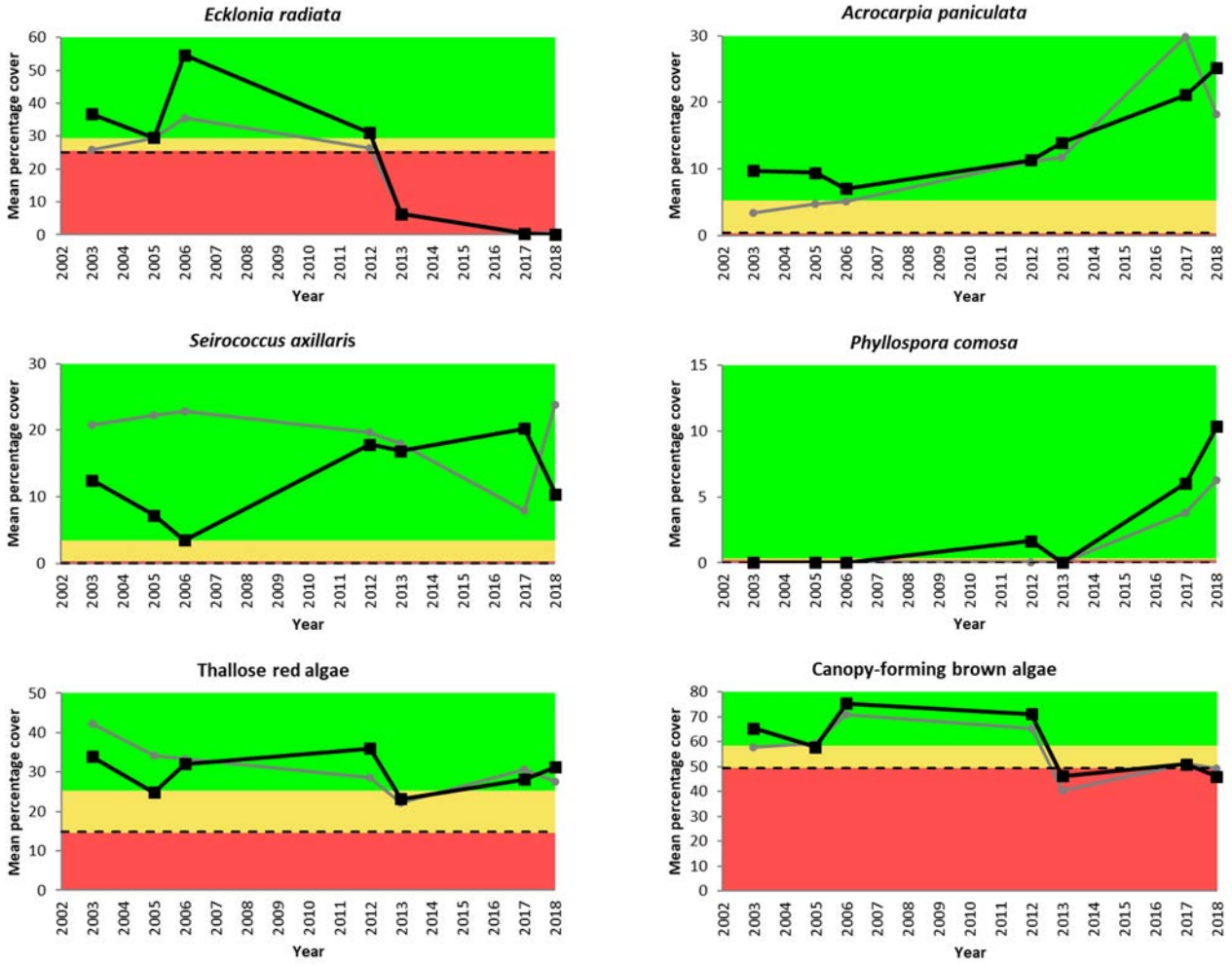

Figure 13. Control charts showing change in percentage cover of algal species within the Point Addis Marine National Park (black line) and reference sites (grey line). Observations for these charts were sourced from Reef Life Survey diver photoquadrats. These charts have a lower control

limit (set as the minimum value inside the MPA from SRMP surveys in 2003, 2005 and 2006) indicating the level when conditions are sufficiently poor that some management response is required. "Canopy-forming brown algae" is a combination of *Ecklonia radiata*, *Acrocarpia paniculata, Seirococcus axillaris and Phyllospora comosa.*

3.3.4 Summary of Control Charts Derived from Diver Surveys

When results for each section of the site were summarised (Figure 22), all fish examined were found to be in good abundance while both motile invertebrates and macroalgal beds were found to be in fair condition. The condition of macroinvertebrates was found to be in good condition between 2003 and 2006, however, a drop to fair condition was observed between 2006 and 2012, driven by the declines in both *Lunella undulata* and *Haliotis rubra*. While being stable for the past four sampling years, the abundance of macroinvertebrates remains fair. The condition of macroalgal beds within the Point Addis Marine National Park was consistently good between 2003 and 2012, however, has decreased since 2012, due to declines in *Ecklonia* and again in 2018, due to overall declines in "canopy-forming brown algae".

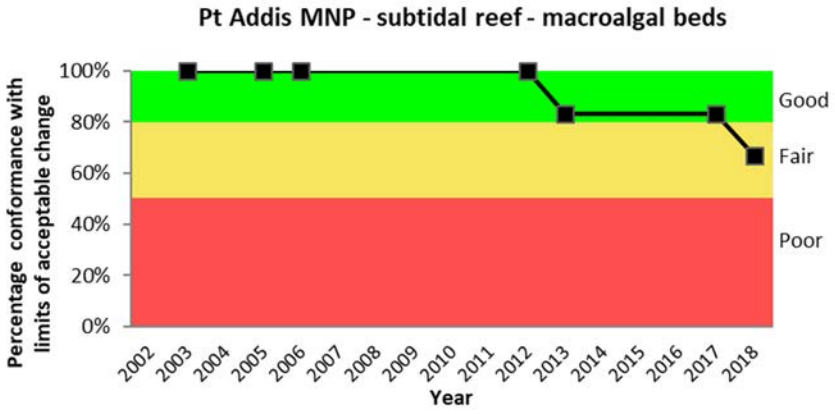

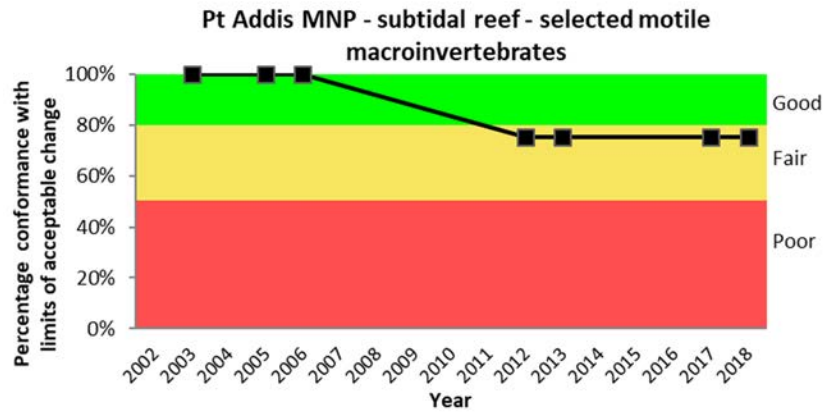

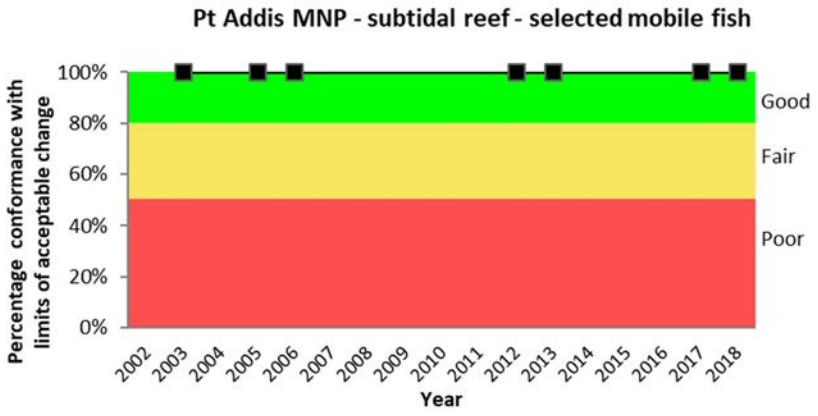

Figure 14. Control charts showing change in percentage conformance with limits of acceptable change for selected algal, macroinvertebrate and mobile fish species within the Point Addis Marine National Park (black line). This was calculated as the percentage of key species that were in good/poor condition. For example if four species were observed and only one was in 'poor' condition, this would be 3/4 = 75 %. Observations for these charts were sourced from Reef Life Survey diver surveys. These charts have a lower control limit (set at 50 % conformance) indicating the level when conditions are sufficiently poor that some management response is required.

3.4 Baited Remote Underwater Video Stations (BRUVS)

A total of 8,233 fish observations across 83 taxa belonging to 51 families were observed in this study (Table 7). Observations came from 181 BRUV deployments, with depths of sample sites ranging from 3 to 55 m (Figure 5). Eighty-one of these locations sampled sediment habitat and 137 sampled reef substratum (Table 7). The most abundant families observed were Carangidae (26.5 %), Sparidae (17.8 %), Serranidae (15.9 %), Monacanthidae (14.6 %) and Labridae (8.6 %) (Figure 24). The most abundant species in this study were *Trachurus* sp. (25.4 %), *Chrysophrys auratus* (17.8 %), *Caesioperca* sp. (15.8 %), *Meuschenia hippocrepis* (6.4 %) and *Notolabrus tetricus* (6.0 %) (Figure 24 and Table 8).

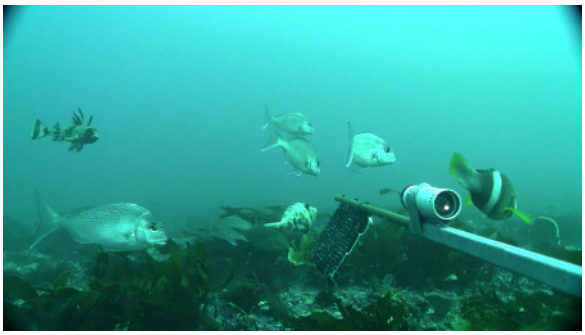

Figure 15. Screen grabs from high-definition BRUV video exhibiting the diversity of habitat and species that can be sampled by this method.

Table 4. Summary of successful baited remote underwater video (BRUV) observations across all years, and all habitats sampled.

	2013	2017	2018	Total
Total No. of Individuals	2268	2725	3240	8233
Total No. of Taxa	64	63	65	83
Total No. Deployments	75	48	58	181
No. Deployments Inside MPA	42	30	37	109
No. Deployments Outside MPA	33	18	21	72
No. Deployments with Reef Present	64	34	39	137
No. Deployments with Sediment Present	36	21	24	81
No. Deployments with Infralittoral Reef Present	36	34	39	109
No. Deployments with Circalittoral Reef Present	34	11	18	63

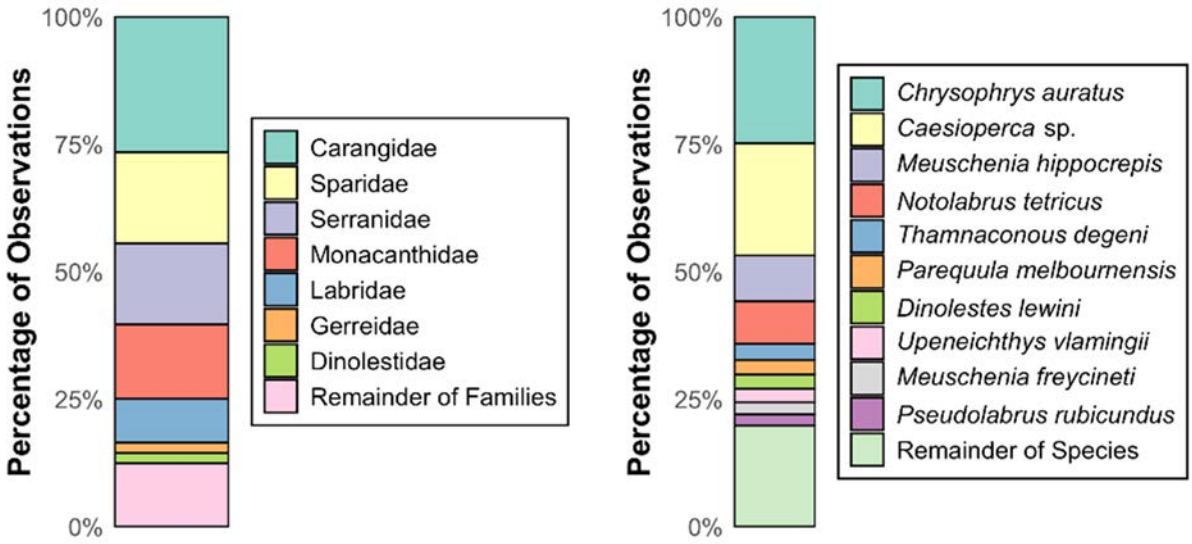

Figure 16. Proportions (as percentages) of the complete fish assemblage (across all three years of BRUV sampling) based on family (left plot) and species (right plot).

Table 5. Proportions (as percentages) of the total abundance of fish observed by BRUV surveys, across three years of sampling (2013, 2017 and 2018). Note that this is not a complete species list. This list only contains top contributors (See full list in Appendix 1.1).

Species	2013	2017	2018
***Trachurus* sp.**	26.70	31.56	19.20
Chrysophrys auratus	12.29	21.25	18.92
***Caesioperca* sp.**	15.53	15.12	16.67
Meuschenia hippocrepis	5.76	5.36	7.78
Notolabrus tetricus	4.67	5.28	7.65
Thamnaconus degeni	4.28	1.50	1.45
Parequula melbournensis	4.07	1.10	1.42
Upeneichthys vlamingii	2.86	1.06	1.91
Dinolestes lewini	0.13	2.24	3.18
Meuschenia freycineti	1.34	1.72	1.91
Pseudolabrus rubicundus	2.55	0.70	1.60
Neosebastes scorpaenoides	1.99	0.95	0.62
Meuschenia scaber	1.82	0.48	1.23
Meuschenia flavolineata	1.08	0.92	1.48
Pictilabrus laticlavius	1.21	0.70	1.05
***Pseudocaranx* sp.**	1.00	1.03	0.86
Cheilodactylus nigripes	0.91	0.73	0.93
Thyrsites atun	0.69	0.95	0.34
Meuschenia galii	0.65	0.37	0.77
Girella zebra	0.52	0.33	0.77
Mustelus antarcticus	0.65	0.22	0.71

Pempheris multiradiata	0.78	0.11	0.68
Heterodontus portusjacksoni	0.26	0.40	0.86
Enoplosus armatus	0.13	0.62	0.62
***Parma* sp.**	0.56	0.37	0.31
Scobinichthys granulatus	0.95	0.11	0.15
Olisthops cyanomelas	0.52	0.15	0.49
Acanthaluteres vittiger	0.35	0.37	0.40
Cephaloscyllium laticeps	0.48	0.40	0.15

Table 6. Proportions (as percentages) of the total biomass of fish observed by BRUV surveys, across three years of sampling (2013, 2017 and 2018). Note that this is not a complete species list. This list only contains top contributors (See full list in Appendix 1.1)

Species	2013	2017	2018
Notorynchus cepedianus	30.58	18.94	11.95
Chrysophrys auratus	8.99	19.71	9.90
Myliobatis australis	2.18	6.77	28.61
Mustelus antarcticus	12.01	5.68	10.30
***Dasyatis* sp.**	9.78	4.16	8.17
***Caesioperca* sp.**	5.66	9.15	4.47
***Trachurus* sp.**	6.09	10.04	2.67
Meuschenia hippocrepis	3.16	3.63	2.62
Cephaloscyllium laticeps	2.04	2.98	0.46
Alopias vulpinus	3.52	0.00	1.70
Orectolobus maculatus	0.57	0.00	4.37
Heterodontus portusjacksoni	0.70	1.52	2.64
Thyrsites atun	1.15	2.12	0.33
Trygonorrhina fasciata	0.20	0.95	2.45
Dipturus whitleyi	1.65	1.06	0.75
Neosebastes scorpaenoides	1.73	1.27	0.34
Meuschenia freycineti	0.76	1.50	0.83
Notolabrus tetricus	0.62	1.10	0.65
Dinolestes lewini	0.06	1.43	0.83
Cheilodactylus nigripes	0.55	0.80	0.42
Meuschenia scaber	0.79	0.47	0.45
Girella zebra	0.57	0.48	0.49
Dactylophora nigricans	0.75	0.51	0.21
***Pseudocaranx* sp.**	0.39	0.68	0.33
Thamnaconus degeni	0.76	0.41	0.21
Upeneichthys vlamingii	0.68	0.36	0.28
Seriola lalandi	0.08	0.14	1.08
Meuschenia flavolineata	0.34	0.44	0.30

3.4.1 Key Mobile Fish Groups / Species

Control charts indicate that the current status of all key mobile fish species is healthy with none of the species analysed being in 'poor' condition (Figure 25). However, it should be noted that as these charts are based on only three surveys (using the lowest value from the reference sites as the LLAC), these surveys have helped establish a baseline for on-going monitoring, rather than being a true assessment of their current condition. Mean abundances and sizes of fish in unprotected waters, were found to be either equal with, or higher than those within protected areas. Groups where numbers are different between inside and outside the MPA included species richness on circalittoral reef, herbivores and planktivores. Species richness on circalittoral reefs was found to be on the rise since 2013, however, it is still in the 'fair' zone and has consistently lower richness than outside the MPA. The abundance of herbivores within the MPA showed low 'fair' to 'poor' performance in 2013 and 2017 surveys, with circalittoral reef classed as 'fair' for the first time in 2018. Higher abundances of herbivores have consistently been found at reference sites, compared with protected sites. There was only one occurrence in three years of sampling that control charts showed a higher abundance of herbivores within protected sites. Planktivore abundance, while still classed as 'good', have shown declines between 2017 and 2018, in which abundances at reference sites have become appreciably higher than those within the MPA. Strong consistent positive trends in abundance were observed for carnivores on circalittoral reef, invertivores, *C. auratus,* and *N. tetricus*.

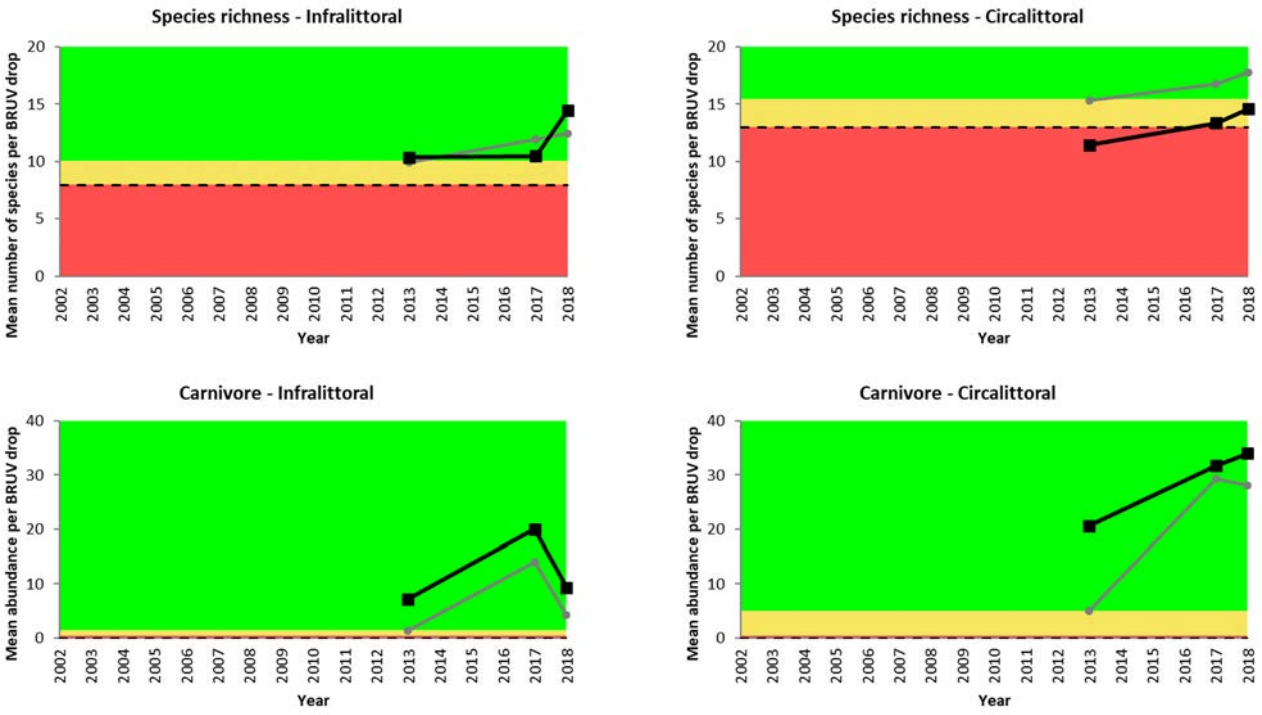

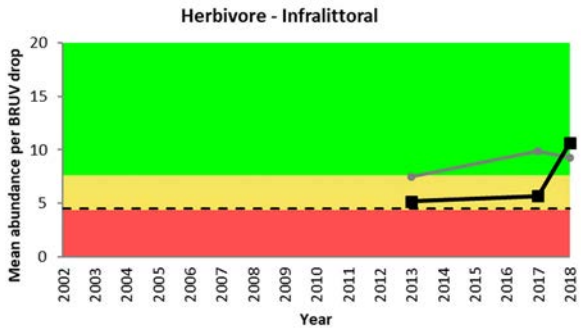
Herbivore - Infralittoral
Mean abundance per BRUV drop
0
5
10
15
20
2002 2003 2004 2005 2006 2007 2008 2009 2010 2011 2012 2013 2014 2015 2016 2017 2018
Year

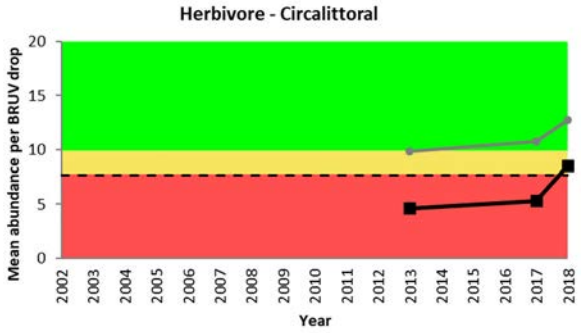
Herbivore - Circalittoral
Mean abundance per BRUV drop
0
5
10
15
20
2002 2003 2004 2005 2006 2007 2008 2009 2010 2011 2012 2013 2014 2015 2016 2017 2018
Year

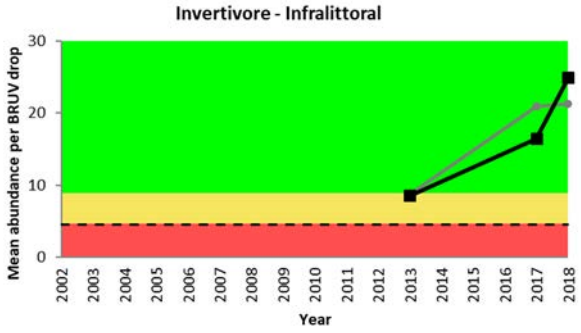
Invertivore - Infralittoral
Mean abundance per BRUV drop
0
10
20
30
2002 2003 2004 2005 2006 2007 2008 2009 2010 2011 2012 2013 2014 2015 2016 2017 2018
Year

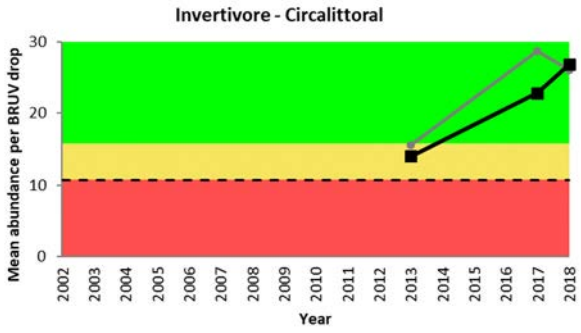
Invertivore - Circalittoral
Mean abundance per BRUV drop
0
10
20
30
2002 2003 2004 2005 2006 2007 2008 2009 2010 2011 2012 2013 2014 2015 2016 2017 2018
Year

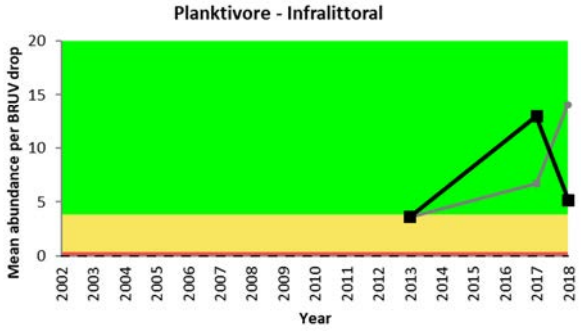
Planktivore - Infralittoral
Mean abundance per BRUV drop
0
5
10
15
20
2002 2003 2004 2005 2006 2007 2008 2009 2010 2011 2012 2013 2014 2015 2016 2017 2018
Year

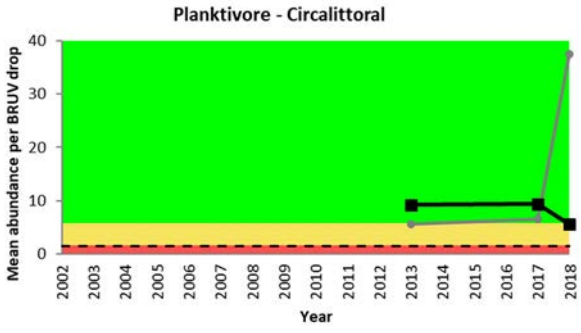
Planktivore - Circalittoral
Mean abundance per BRUV drop
0
10
20
30
40
2002 2003 2004 2005 2006 2007 2008 2009 2010 2011 2012 2013 2014 2015 2016 2017 2018
Year

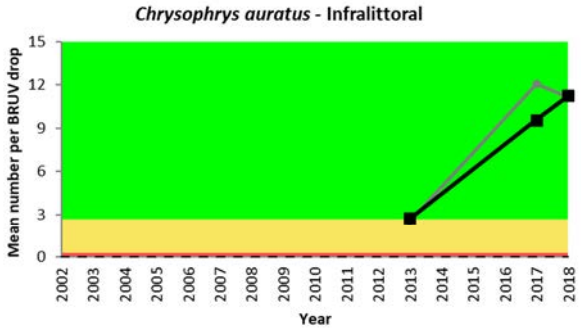
Chrysophrys auratus - Infralittoral
Mean number per BRUV drop
0
3
6
9
12
15
2002 2003 2004 2005 2006 2007 2008 2009 2010 2011 2012 2013 2014 2015 2016 2017 2018
Year

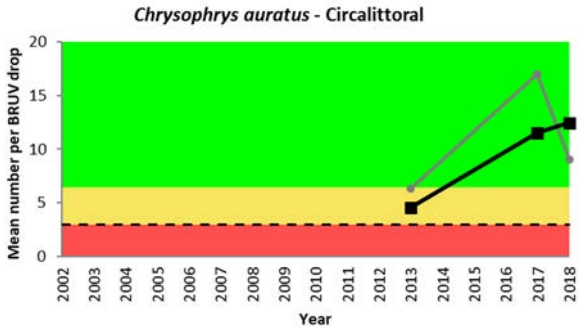
Chrysophrys auratus - Circalittoral
Mean number per BRUV drop
0
5
10
15
20
2002 2003 2004 2005 2006 2007 2008 2009 2010 2011 2012 2013 2014 2015 2016 2017 2018
Year

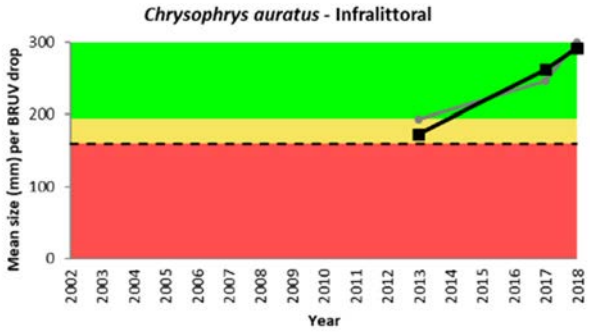
Chrysophrys auratus - Infralittoral
Mean size (mm) per BRUV drop
0
100
200
300
2002 2003 2004 2005 2006 2007 2008 2009 2010 2011 2012 2013 2014 2015 2016 2017 2018
Year

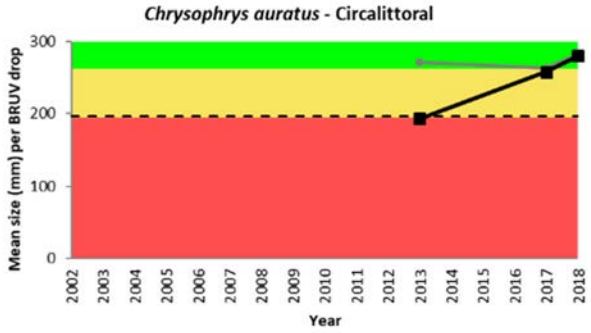
Chrysophrys auratus - Circalittoral
Mean size (mm) per BRUV drop
0
100
200
300
2002 2003 2004 2005 2006 2007 2008 2009 2010 2011 2012 2013 2014 2015 2016 2017 2018
Year

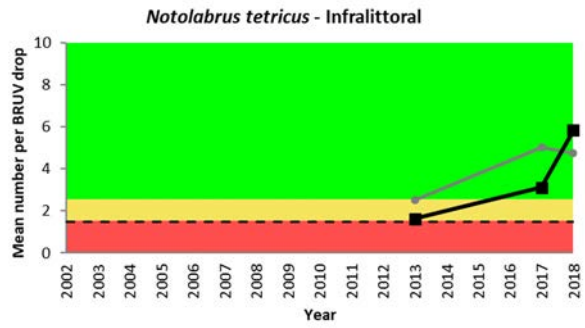
Notolabrus tetricus - Infralittoral
Mean number per BRUV drop
Year

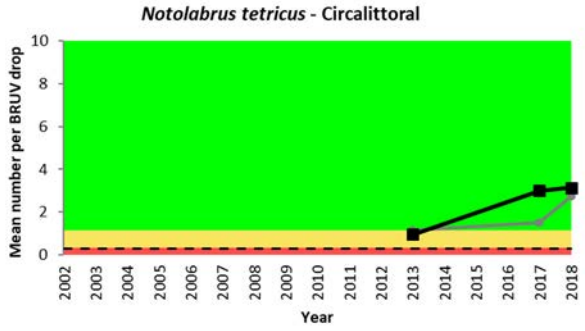
Notolabrus tetricus - Circalittoral
Mean number per BRUV drop
Year

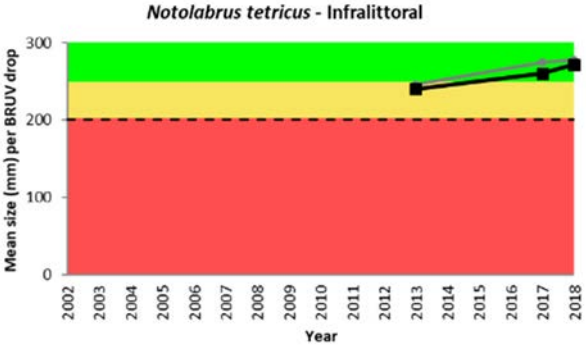
Notolabrus tetricus - Infralittoral
Mean size (mm) per BRUV drop
Year

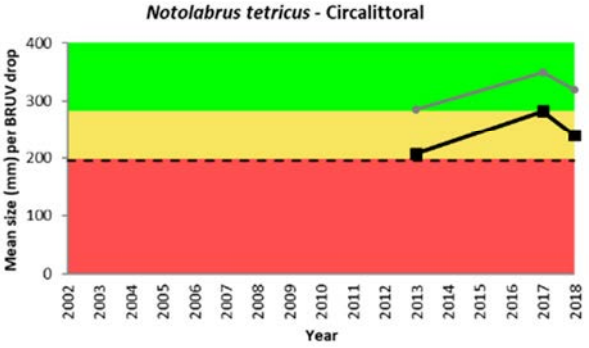
Notolabrus tetricus - Circalittoral
Mean size (mm) per BRUV drop
Year

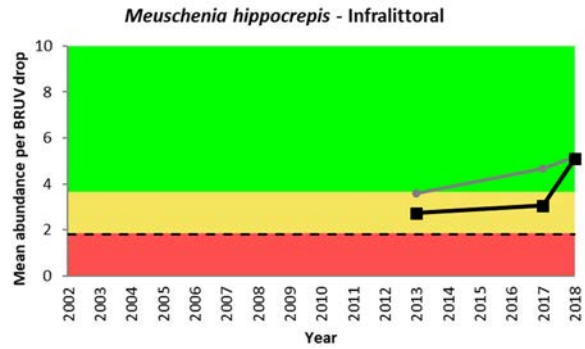
Meuschenia hippocrepis - Infralittoral
Mean abundance per BRUV drop
Year

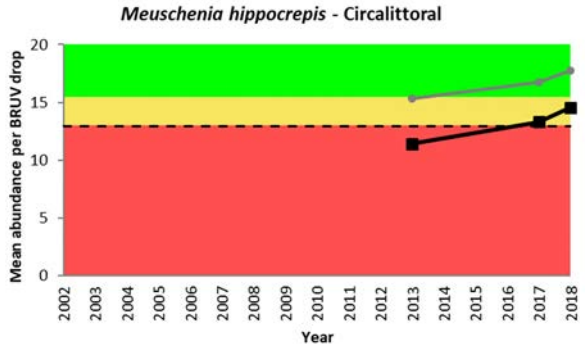
Meuschenia hippocrepis - Circalittoral
Mean abundance per BRUV drop
Year

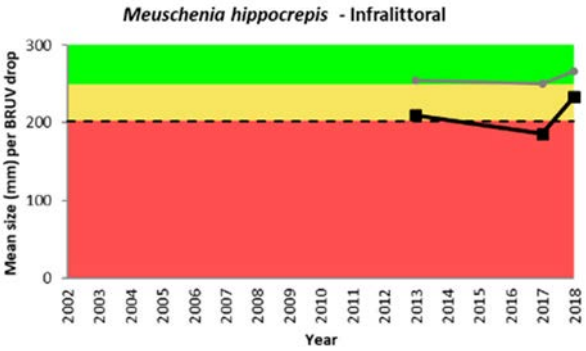
Meuschenia hippocrepis - Infralittoral
Mean size (mm) per BRUV drop
Year

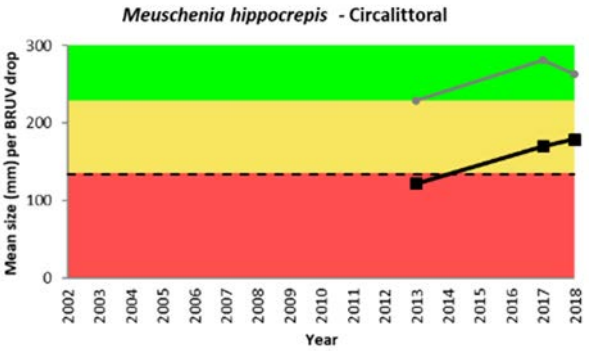
Meuschenia hippocrepis - Circalittoral
Mean size (mm) per BRUV drop
Year

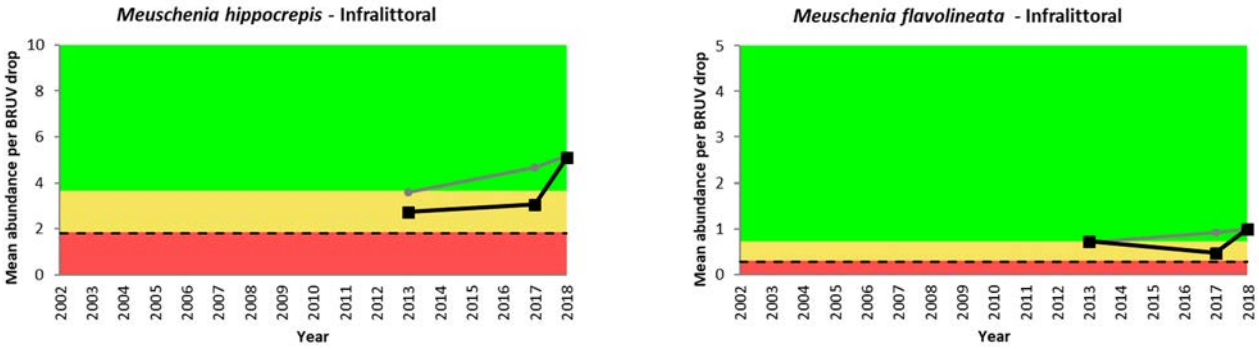

Figure 17. Control charts showing change in abundance and size of key mobile fish species within the Point Addis Marine National Park (black line) and reference sites (grey line). Observations for these charts were sourced from Baited Remote Underwater Video (BRUV). These charts have a lower control limit (set at the lowest value observed at reference sites outside of the MPA) indicating the level when conditions are sufficiently poor that some management response is required.

3.4.2 Performance of Species Distribution Models using BRUVs data

We used species distribution models to develop full coverage maps of components of the fish assemblage by combining the observations from BRUVS and statistical relationships with environmental variables (e.g. seafloor structure from multibeam sonar at different scales) to model distribution patterns beyond the extent of finite sample locations. Overall, when species richness was modelled for the entire assemblage using BRUVs data, best performing models were found when environmental variables at a spatial scale of 25 m were used. In this model, 54.2 % of the deviance in species richness was explained (Table 10). When tested, positive spatial autocorrelation was present up to 1000 m. However, spatial autocorrelation was no longer significant in the residuals after GAMs were run. This suggests that spatial autocorrelation was accounted for within the model via the use of the environmental variables. Models of species richness across the entire assemblage showed similar patterns across all years of sampling, however a general increase in species richness was present between 2013 and 2017/18 (Figure 26).

When samples were limited by broad habitat groups (reef and sediment), best model performance was observed when environmental variables at a spatial scale of 25 m were used for reef and a spatial scale of 50 m for sediment (Table 10). Models using observations from sediment habitats, as opposed to reef, explained 28.7 % more deviation. No major increases in model predictability were found when individual types of reef were modelled. Both infralittoral and circalittoral reef presented best model performance at fine spatial scales of 10 and 25 m spatial scales and explained 50 and 46.2 % of deviance respectively.

This consistent trend of small scales explaining the greatest deviance continued when species modelled were limited to invertivores (Table 10). A total of 43.2 % of the deviance in invertivores was best explained at a scale of 25 m. Furthermore, 33.7 % of the deviance in

herbivores was explained at a scale of 10 m (where ΔIC = 0). Conversely, when carnivorous species were modelled, only 22.1 % of deviance could be explained.

When abundances of individual species were modelled, considerable variation was present (Table 10). *N. tetricus* showed the highest performance at the 5 m scale where a deviance of 68.43 % was obtained. Conversely *C. auratus* showed the highest performance at a scale of 25 m where it explained a deviance of 46.2 %. *M. hippocrepis* showed highest model performance at a spatial scale 150 m where it explained 63.1 % of the deviance in *M. hippocrepis* abundance.

Table 7. Summary statistics of best performing generalised additive models (GAMs) completed at spatial scales of 5 m, 10 m, 25 m, 50 m, 75 m, 100 m, 150 m, 200 m, 300 m, 400 m and 500 m. Best descriptor variables are identified by (+).

Subset	Optimal Radius Scale (m)	Year	MPA Status	Bathymetry	Distance to Reef	Rugosity	Curvature	Fine BPI	Eastness	Northness	AICc	Deviance Explained (%)	Test Data Correlation
Entire Assemblage	25	+	+	+	+	+					691.83	54.26	0.49
Pelagic Species Removed	25	+	+	+	+	+					677.97	51.39	0.42
Mobile Species Removed	25	+	+	+	+	+					677.52	51.44	0.41
Reef	10	+	+	+	+	+					547.99	47.78	0.31
Sediment	50	+	+	+	+	+			+		304.19	83.37	0.56
Circalittoral Reef	400				+		+	+			216.66	49.66	0.01
Infralittoral Reef	50	+			+		+	+		+	442.21	46.20	0.09
Carnivores	100	+		+			+	+			270.15	24.36	0.34
Herbivores	25	+	+	+	+	+	+			+	446.47	38.97	0.42
Invertivores	50	+		+	+			+	+	+	561.05	48.80	0.46
C. auratus	25	+	+	+	+				+		869.27	46.23	0.31
N. tetricus	5	+		+	+			+	+		497.06	68.43	0.79
M. hippocrepis	150	+	+			+	+		+		581.22	63.15	0.35

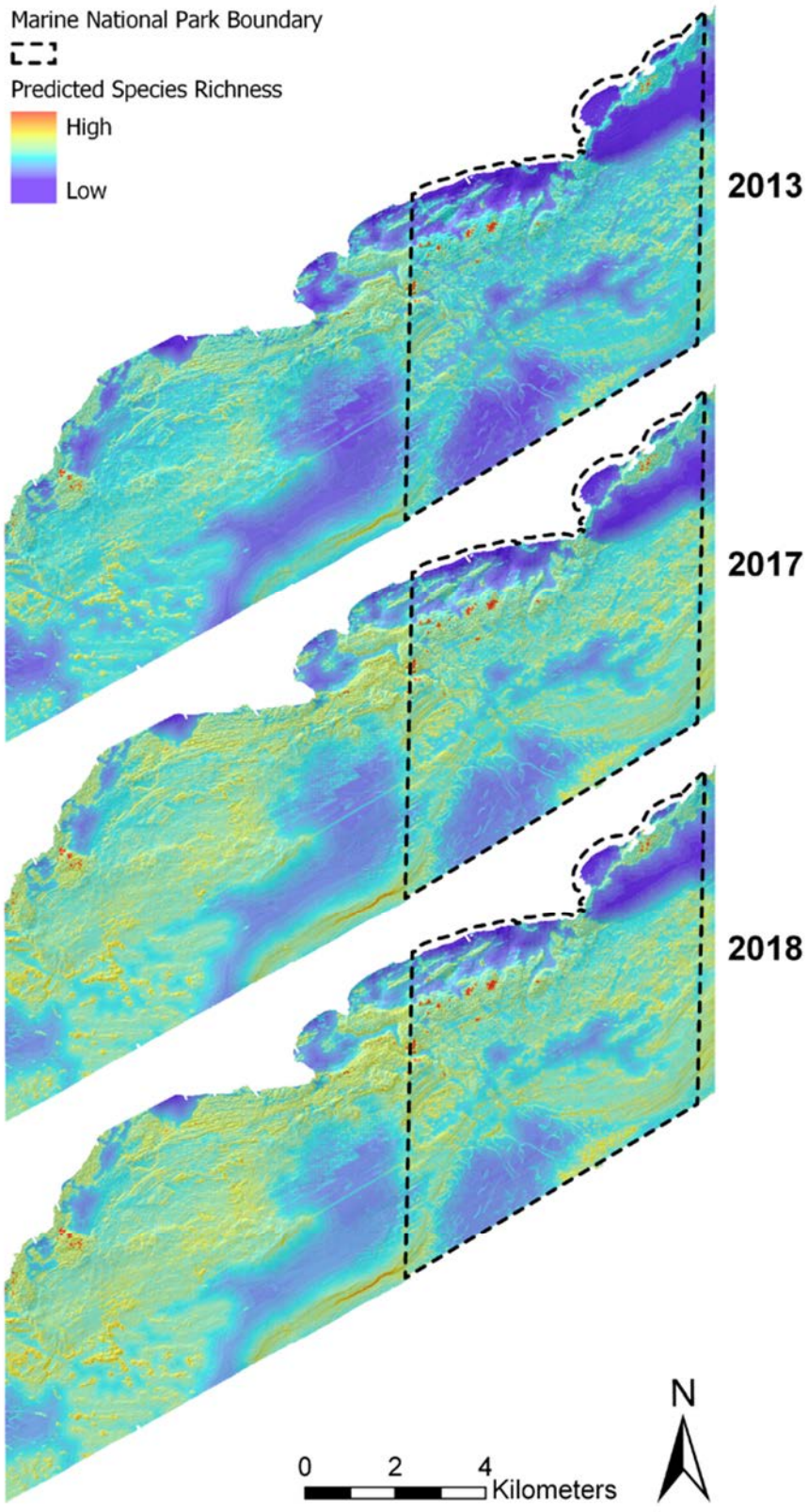

Figure 18. Predicted species richness for BRUV sampling across the whole study site, displayed by year of sampling (2013, 2017 and 2018).

3.4.3 Environmental Drivers of Fish Assemblage

When the environmental drivers of the fish assemblages present in this study were assessed, year of sampling was found to be the most significant predictor variable across all subsets tested except circalittoral reef (Figure 27). Control charts found species richness to increase between all years, with the difference between 2013 and 2018 being significant (Figure 25). The importance of year decreased the more the assemblage was split into subgroups. Variation was observed for models of individual species where *C. auratus* showed the most significant importance of year, followed by *N. tetricus* (Figure 27). Control charts for *C. auratus* abundance throughout the years of sampling showed a consistent increase through 2013, 2017 and 2018 (Figure 25). The same was observed for abundance of *N. tetricus* through the years, where abundance in 2017 and 2018 was higher than in 2013. (Figure 25). The second and third most common variables across all subsets of the assemblage sampled were bathymetry and distance to reef, respectively (Figure 27). These findings were reflected by trends observed in bubble plots (Figure 28 and Figure 29), where the most evident trend was that highest species richness and total biomass varied strongly across years of sampling. Within both plots, species richness and total biomass were generally highest in the 2018 survey. Furthermore, some differences were observed between sites within the MPA compared to the reference site. For the 2018 survey, species richness and total biomass were generally higher inside the MPA.

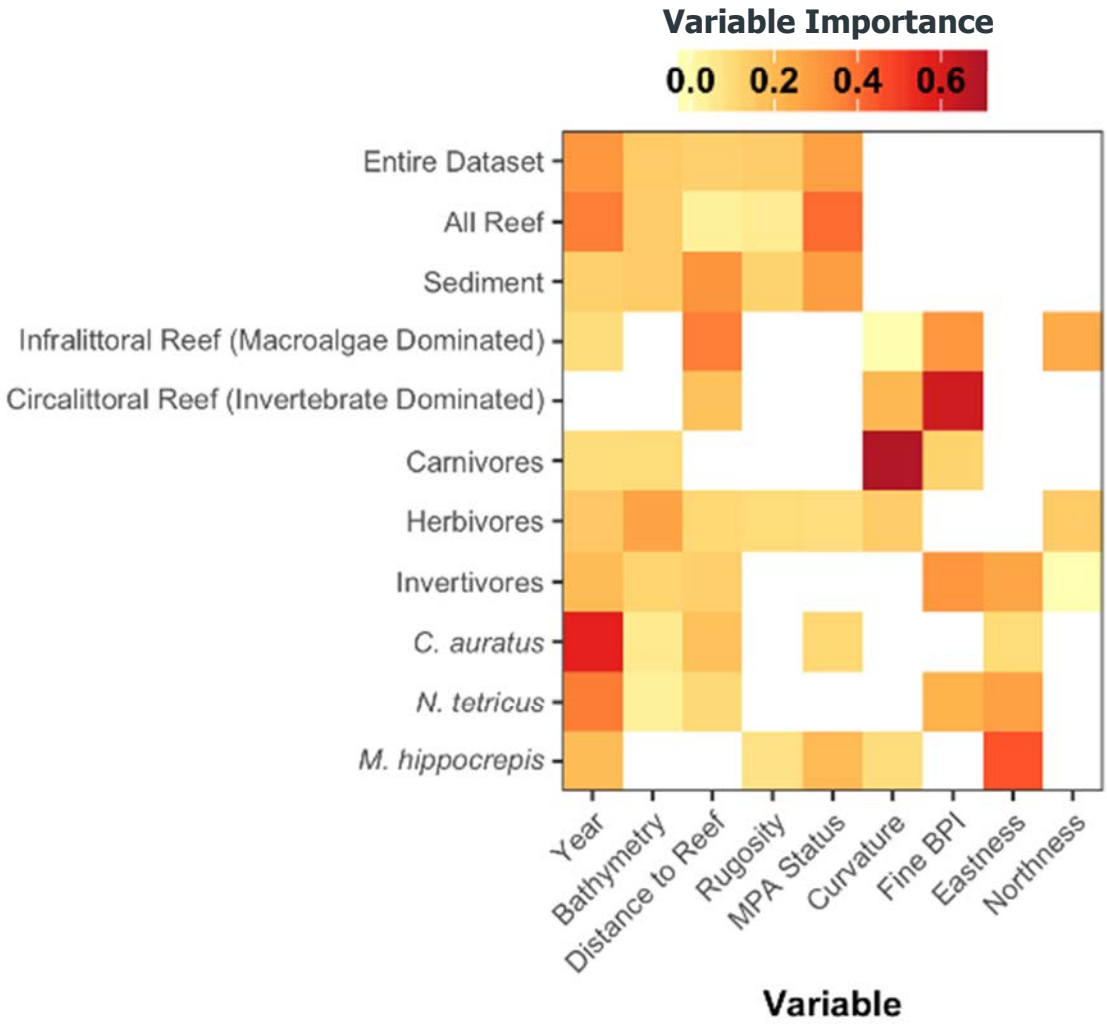

Figure 19. Heatmap showing predictor variables (x-axis) used in each of the model subsets used in this study (y-axis). Colour gradient denotes the relative importance of each variable in its respective model. Values are on a scale from pale yellow (low importance) to dark red (high importance).

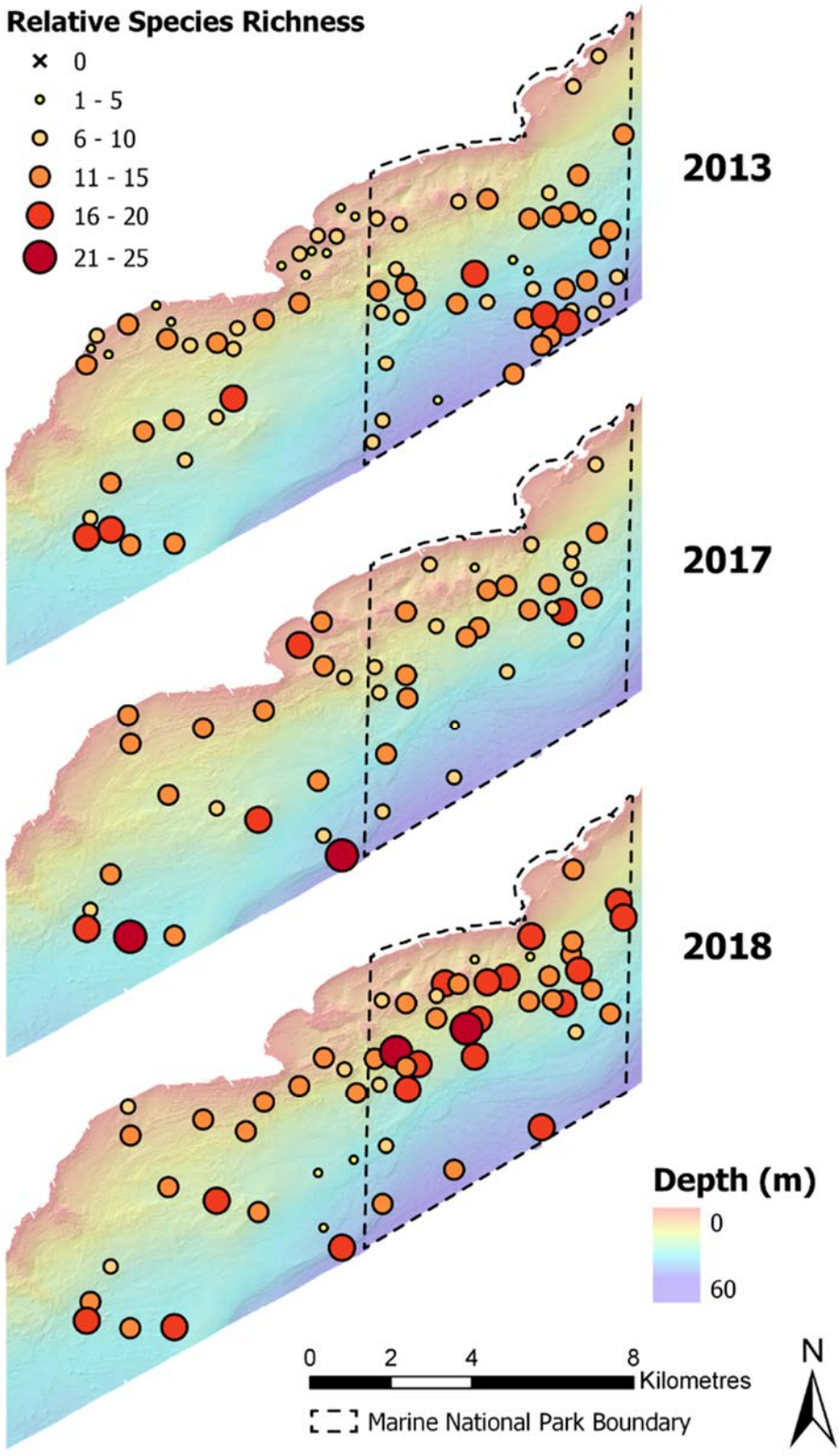

Figure 20. Bubble plot showing the sites of all BRUV deployments. The colour of each site marker corresponds to the relative species richness of fish observed at that site. These sites are overlayed on hillshaded bathymetry of the study area, coloured by depth.

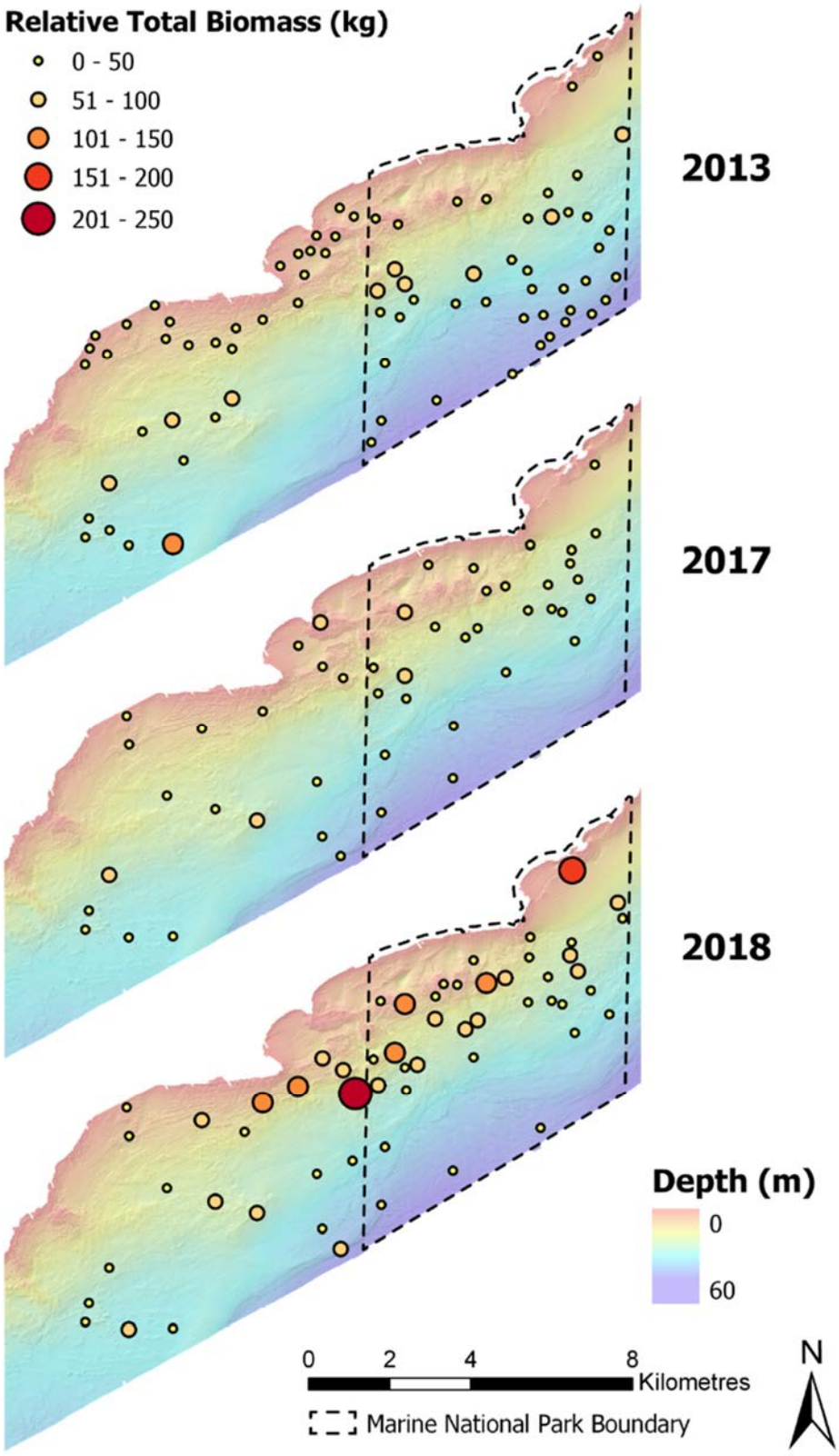

Figure 21. Bubble plot showing the sites of all BRUV deployments. The colour of each site marker corresponds to the estimated relative total biomass (kg) of fish observed at that site. These sites are overlayed on hillshaded bathymetry of the study area, coloured by depth.

3.4.4 Dynamics of Habitat Used by Functional Feeding Groups

Varying trends were found between functional groups across the entire site (Figure 30). Highest richness of carnivores was observed in deep waters (> 30 m) within the MPA and was generally much lower in shallow water. Habitat predictions for herbivores showed strong affinity to certain habitats. Shallow, near-shore reef, synonymous with the presence of macroalgae, presented highest species richness of this group. There was also a discrete boundary of high and low species richness that followed the transition between reef and sediment, with low species richness of herbivores present on soft sediment. Finally, species richness of invertivores followed reef coverage throughout the study area in the same fashion as herbivores, except invertivores were more predominant on deeper circalittoral reef dominated by sessile invertebrates.

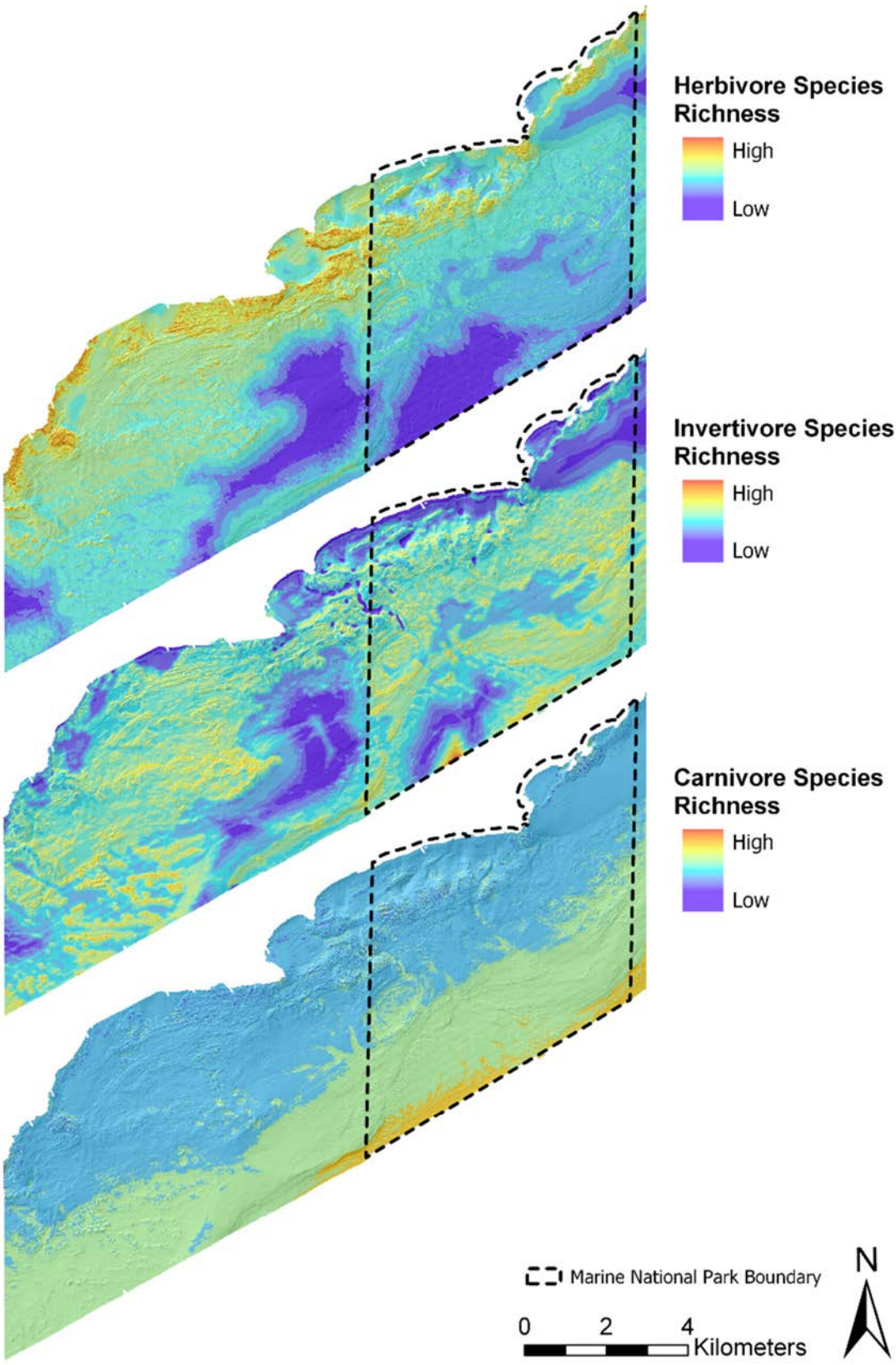

Figure 22. Predicted species richness for 2018 sampling across the whole study site, split into functional feeding groups (carnivores, herbivores and invertivores).

3.4.5 Dynamics of Habitat Used by Key Fish Species

Similar to functional feeding groups, trends of habitat use observed at the individual species level were species-specific (Figure 31). Apart from being slightly higher in deeper habitats, the abundance of *C. auratus* was observed to be fairly uniform across the study site. Conversely, whilst models showed some abundance on deeper circalittoral reefs and supported by BRUV observrvations, *N. tetricus* showed strong trends of highest abundance on shallow macroalgal-dominated reef. Similar to herbivores, *N. tetricus* also observed a sharp distinction between areas of reef and sediment, with little to none found in areas of sediment. Finally, *M. hippocrepis* was predicted to have highest abundances on shallow, near-shore infralittoral reef. This species, however, was also wide-ranging, having its presence on all broad habitats measured including both infralittoral and circalittoral reef, as well as areas of soft sediment.

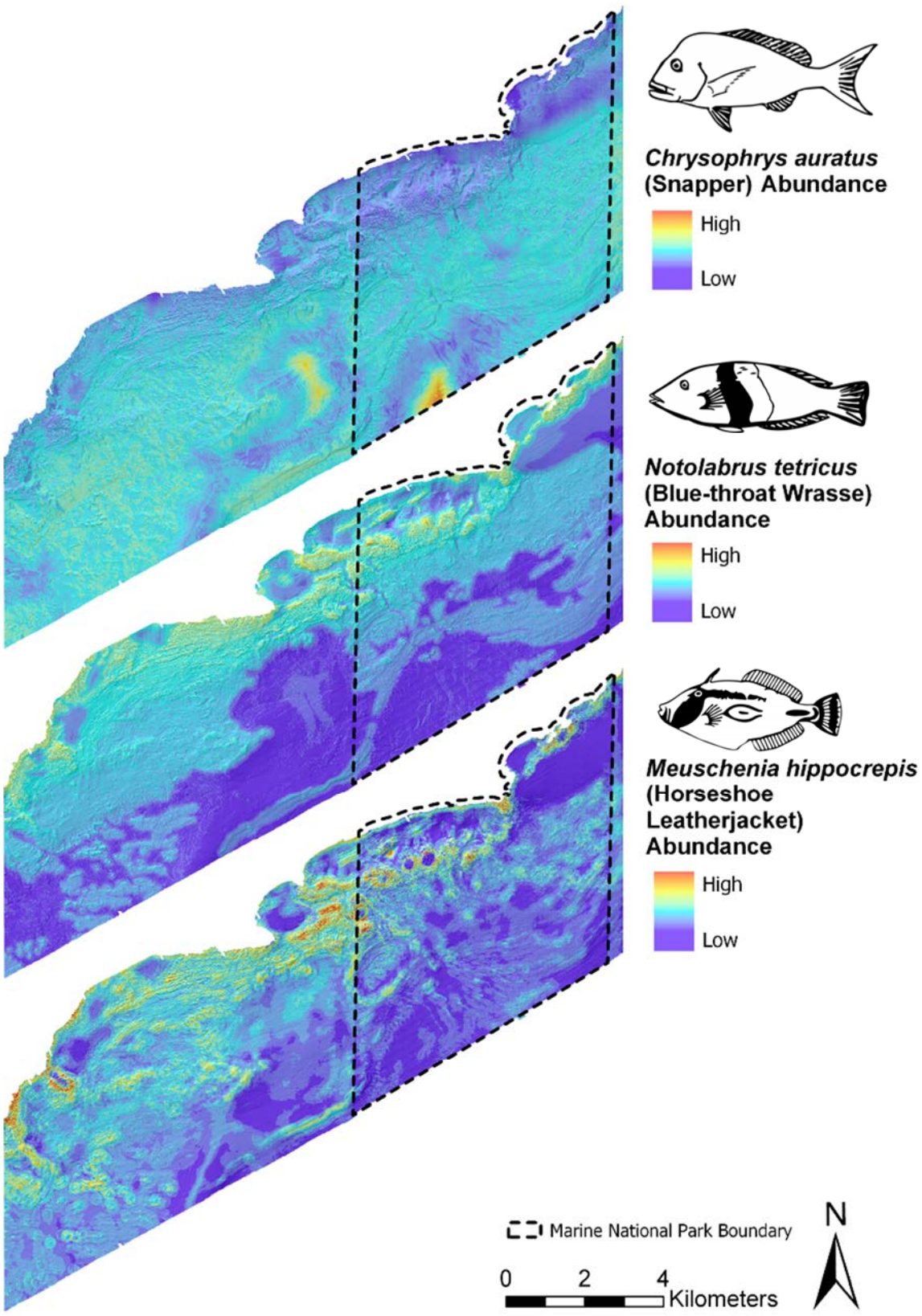

Figure 23. Predicted abundance for 2018 sampling across the whole study site for three key species (*Chrysophrys auratus*, *Notolabrus tetricus* and *Meuschneia hippocrepis*).

3.5 Towed video and downward facing imagery

This study achieved extensive towed video coverage across the entire Point Addis Marine National Park and surrounding subtidal reef monitoring sites. Between 2017 and 2018, 56 transects were completed totalling 126.5 linear km of observations. Coverage was achieved across all major habitat groups within the MPA. Furthermore, within these transects, 8,932 downward facing stills were successfully acquired. From this data, 40 georeferenced still images were classified for each 5 m depth strata. This process was completed for both surveys allowing for the classification of 800 georeferenced stills. Additionally, across the 3 surveys that oblique video was recorded (2005, 2017 and 2018), 3,478 still images were extracted and classified to allow extents of key habitat groups to be visualised.

Table 8. Summary of distances covered, number of transects completed and number of downward facing stills successfully collected using towed video in this study.

	2005	2017	2018	Total
Distance Towed (km)	58	63	63	126
Transects Completed	24	28	28	56
Downward Facing Stills Acquired	-	4893	4039	8932
Classified Downward Facing Stills	-	400	400	800
Classified Georeferenced Oblique Stills	1302	1298	886	3478

Figure 24. An example downward-facing georeferenced still image collected using towed video. This image contains a typical shallow infralittoral reef community composed of green and red algal species within the Point Addis Marine National Park.

Figure 25. An example downward-facing georeferenced still image collected using towed video. This image contains a typical infralittoral reef community composed of foliose brown and red algal species with sparse sessile invertebrates and calcareous red algae, within the Point Addis Marine National Park.

Figure 26. An example downward-facing georeferenced still image collected using towed video. This image contains a typical infralittoral reef community composed of foliose brown and red algal species with sparse sessile invertebrates, within the Point Addis Marine National Park.

Figure 27. An example downward-facing georeferenced still image collected using towed video. This image contains an example of the dense rhodolith beds present within the Point Addis Marine National Park.

Figure 28. An example downward-facing georeferenced still image collected using towed video. This image contains an example of a sessile invertebrate complex present within the Point Addis Marine National Park.

Figure 29. An example downward-facing georeferenced still image collected using towed video. This image contains an example of a sessile invertebrate complex present within the Point Addis Marine National Park.

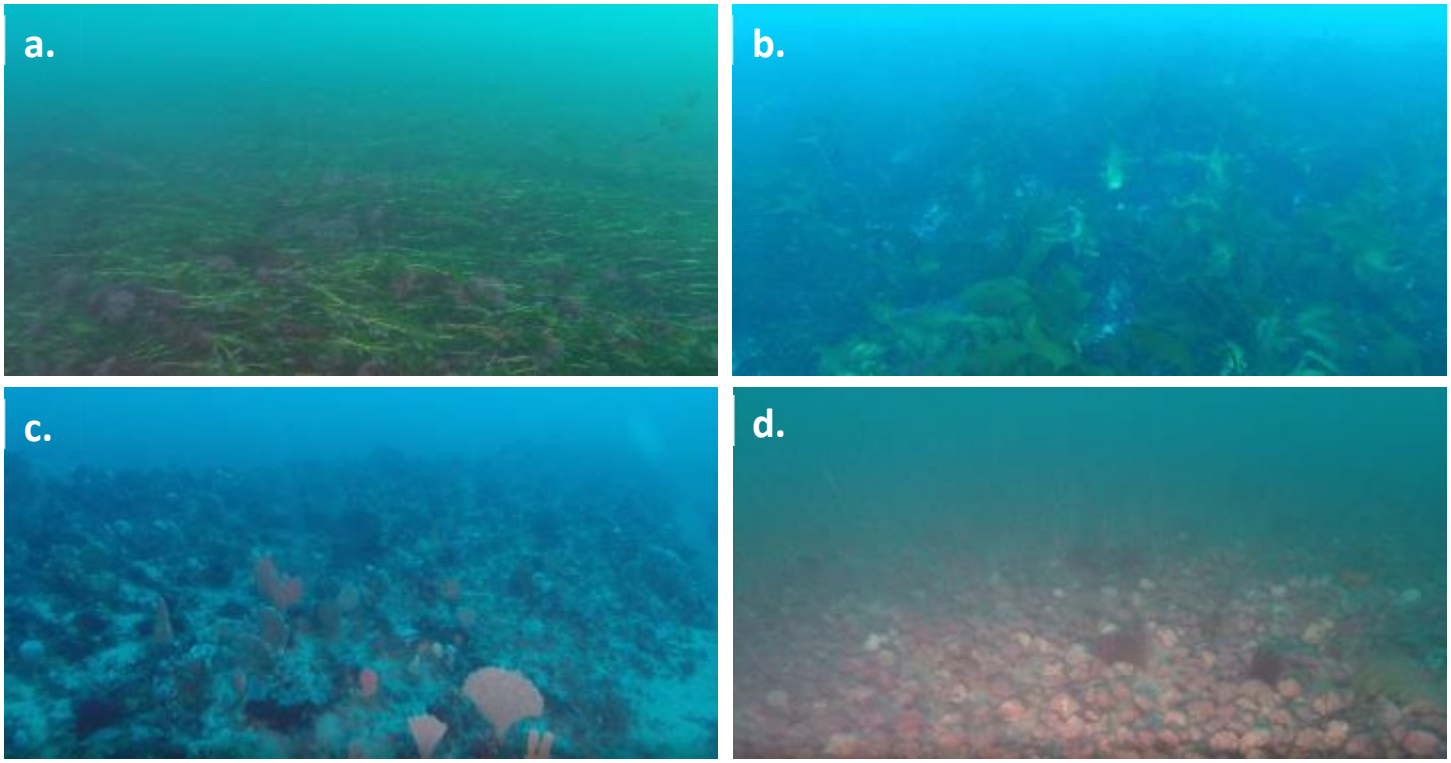

Figure 30. Screen grabs of high-definition GoPro images sourced from towed video surveys. (a) Seagrass with a mixed red algae understory (b) *Ecklonia* with mixed red algae understory (c) Sponge community (d) Rhodolith bed

3.5.1 Depth-related Patterns of Habitat Composition

Classification of georeferenced downward-facing stills revealed similar patterns in dominant cover types between 2017 and 2018 (Figure 39). *Amphibolis antarctica* made a sizeable contribution of 11 % of total percentage cover (across both years) at depths between 5 and 10 m. Brown macroalgal species (dominated by *Seirococcus axillaris*, *Acrocarpia paniculata*, *Sargassum* sp. and *Ecklonia radiata*) were prevalent (~ 50 % of percentage cover across both years of sampling) to depths of 30 m. Rhodophyta (red algae) was prevalent (≥50 % of percentage cover) to 50 m, however highest dominance was between 25 m and 50 m, with rhodoliths making up ~25% cover. Porifera (sponges) were observed to be prevalent at depths below 20 m. This group, however, only became the dominant biota at depths below 50 m (Figure 39).

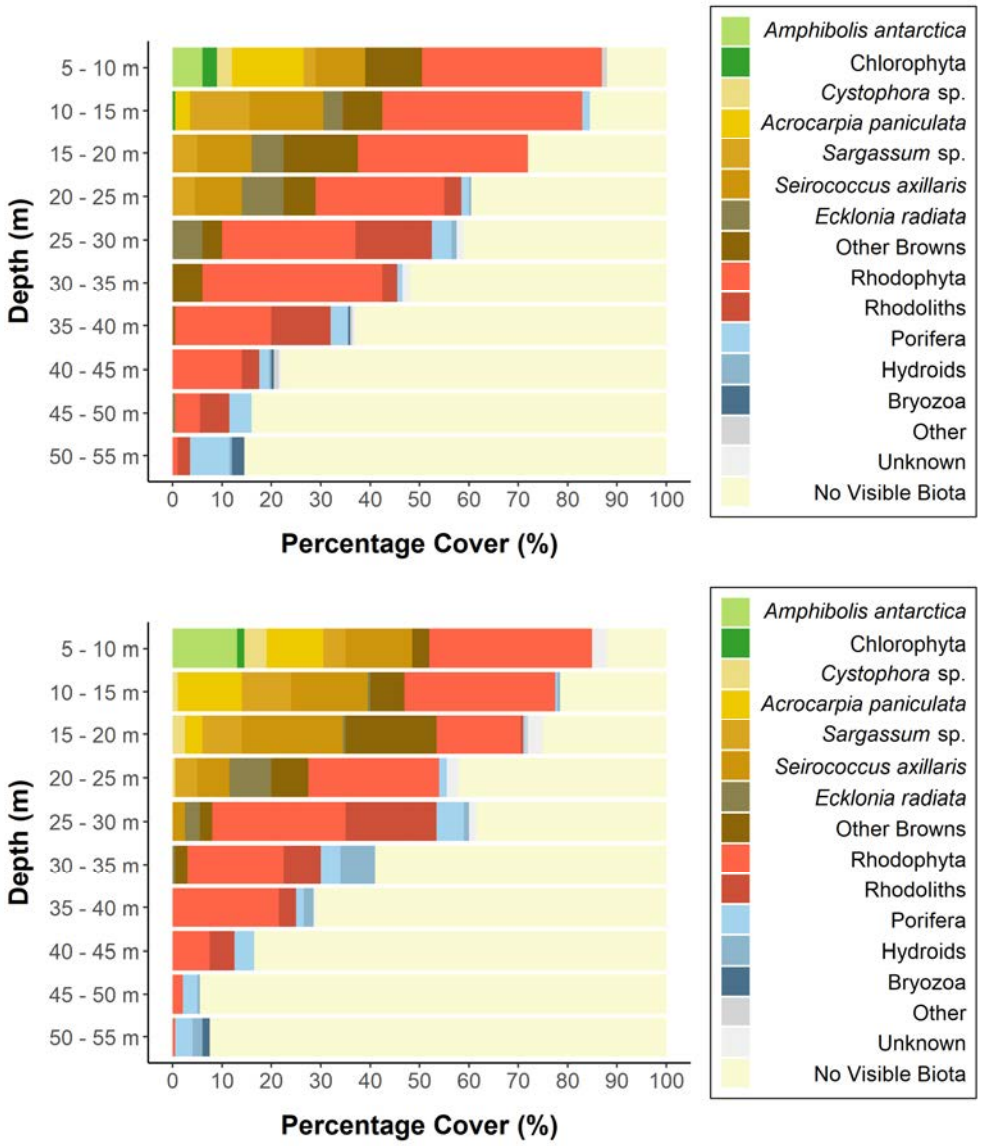

Figure 31. Depth zonation of broad reef habitat categories for 2017 (top) and 2018 (bottom) observed by classifying downward facing still images collected using towed video.

The one-way ANOSIM detected differences in the dominant benthic community assemblages across the five depth strata within the Point Addis Marine National Park (Global R= 0.018, P < 0.001) (Figure 40). Pairwise comparisons indicated that the degree of variation across the depth strata varied. All adjacent depth strata were significantly different to one another with the largest differences, as indicated by the larger R value, between the shallower and deeper depths as expected (i.e. comparisons between 5-15m and 35-55m).

The large R value in comparison of these shallower depths indicates that there is a larger degree of variation in the dominant benthic community assemblage at the shallower

locations of the Point Addis MNP. Conversely, the relatively small R values for the comparison between depth strata shallower than 35 m and depth strata deeper than 35 m suggest that there is strong difference among shallow (< 35 m) and deeper (> 35 m) habitats.

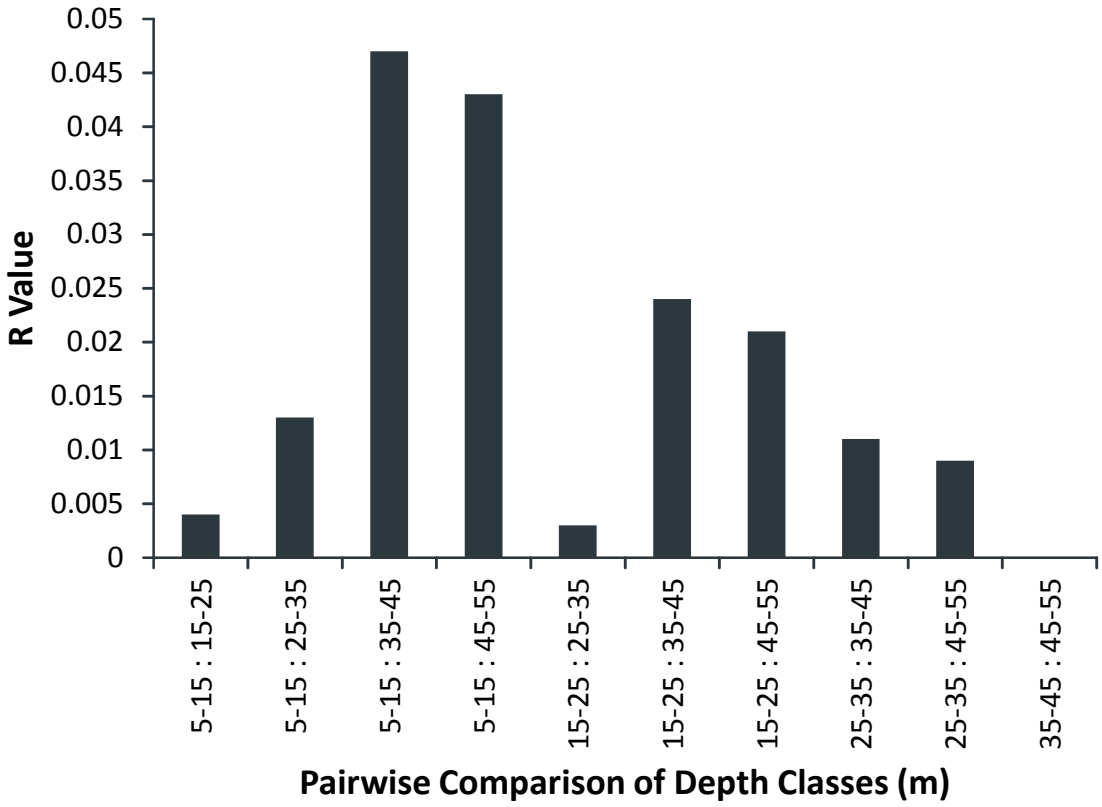

Figure 32. Pairwise comparisons of dominant benthic community assemblages for each depth strata generated from a one-way ANOSIM for the Point Addis site. All comparisons were significantly different (P < 0.01).

3.5.2 Extents of Key Habitat Groups

Classification of oblique video from towed video allowed for rapid identification of the extents of key habitat groups, *Ecklonia radiata* and rhodolith beds, throughout the Point Addis MNP. When these observations were plotted against the position in which they were taken, overlap in the presence and absence of the groups was clearly observed (Figure 41 and Figure 43). Overall, very little change in habitat extents were identified for both *Ecklonia* and rhodolith beds between 2005, 2017 and 2018 (Figure 42 and Figure 44). Strong overlap in transects was achieved on the western side of the MPA, however due to low visibility (especially during the 2018 survey) a limited amount of transects were classified.

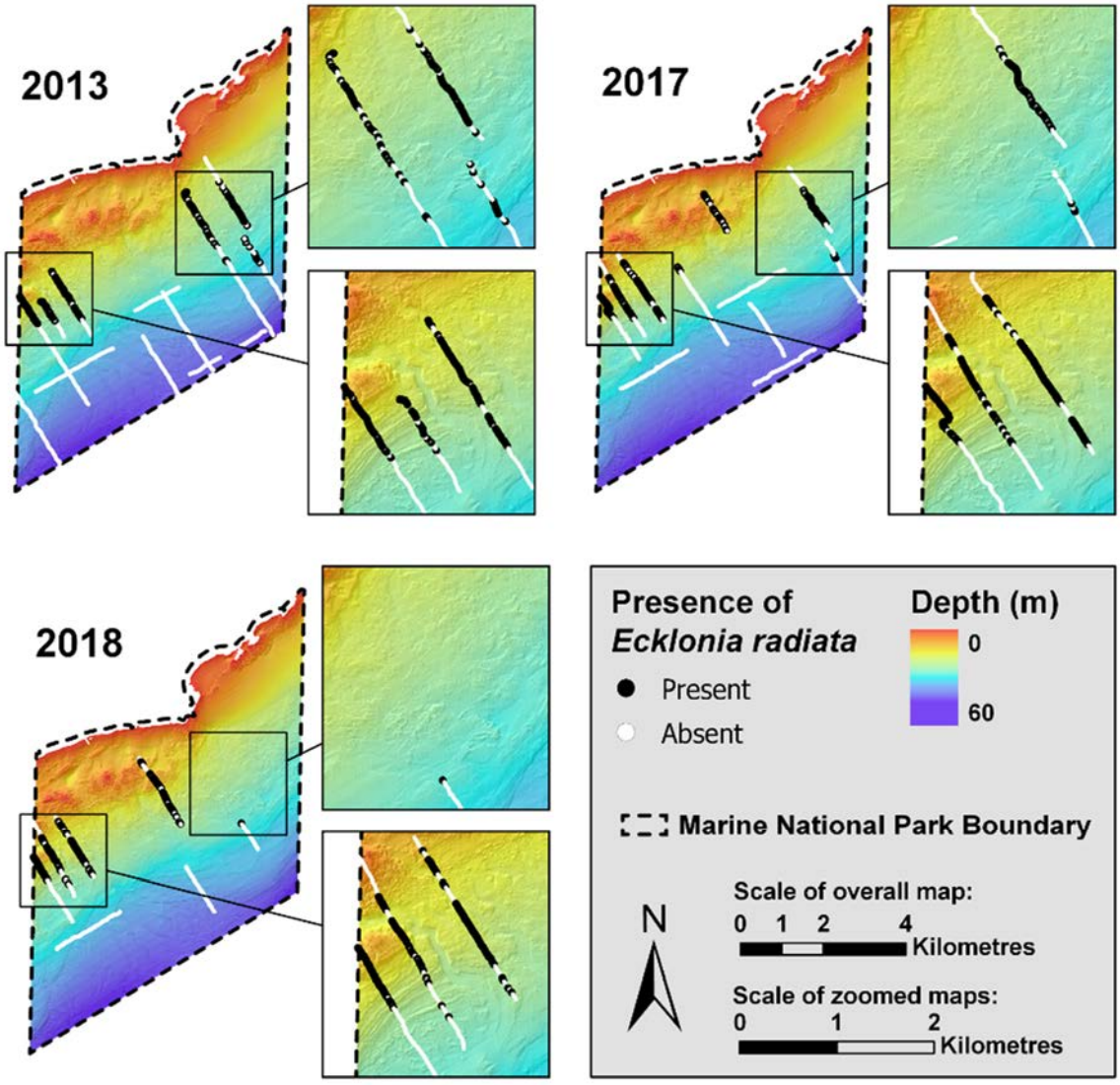

Figure 33. Presence (black) and absence (white) of *Ecklonia radiata* across three years of sampling (2013, 2017 and 2018). Observations were made from oblique video collected using towed video. Extents of overall maps and zoom windows are consistent across all year, to enable direct comparisons of extent change to be made.

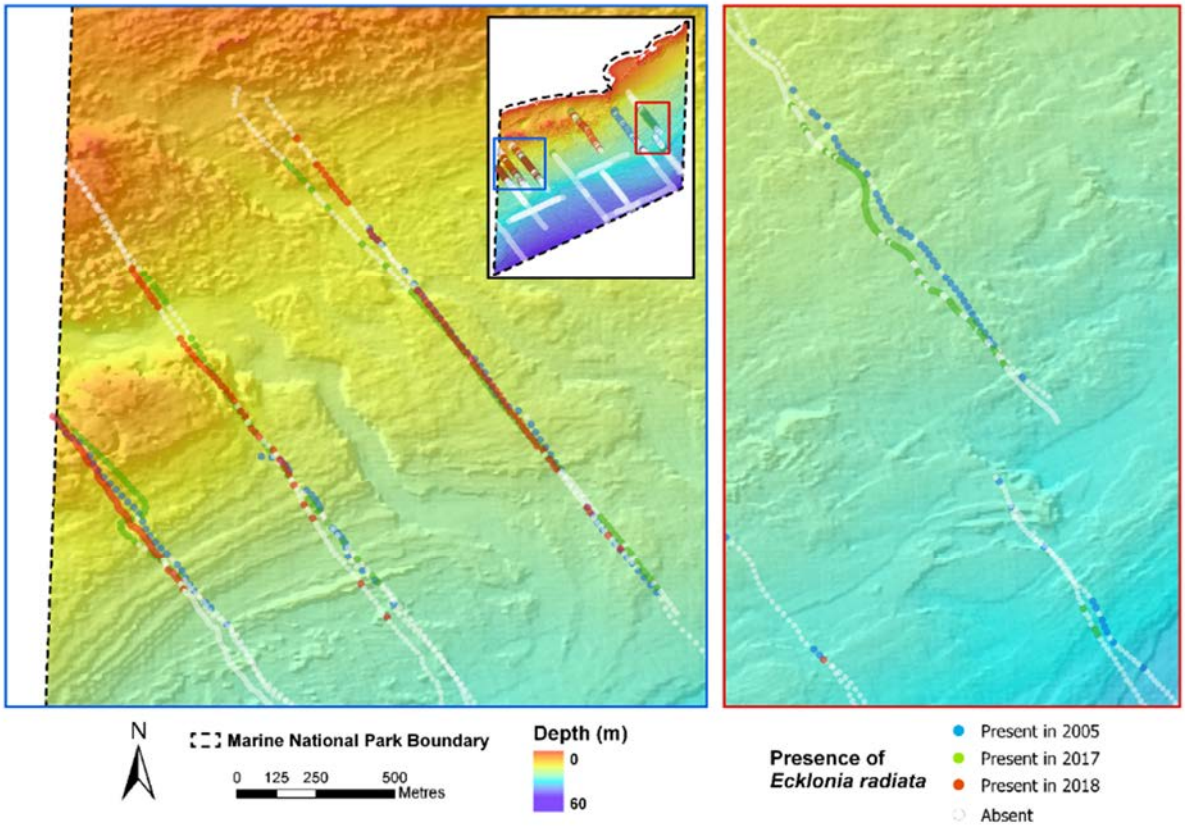

Figure 34. Presence (coloured by year) and absence (white) of *Ecklonia radiata* across three years of sampling (2013, 2017 and 2018). Observations were made from oblique video collected using towed video.

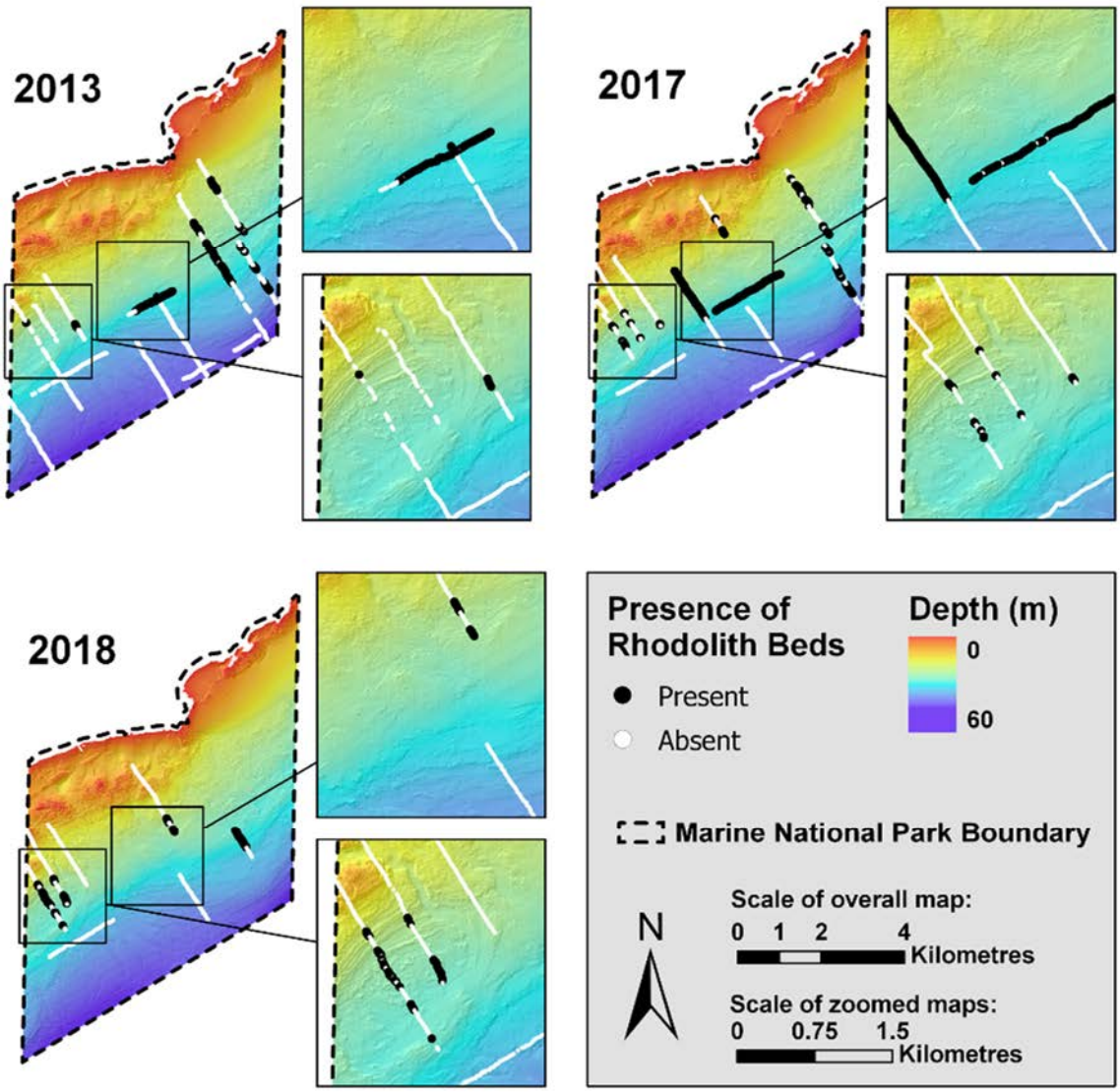

Figure 35. Presence (black) and absence (white) rhodolith beds across three years of sampling (2013, 2017 and 2018). Observations were made from oblique video collected using towed video. Extents of overall maps and zoom windows are consistent across all year, to enable direct comparisons of extent change to be made.

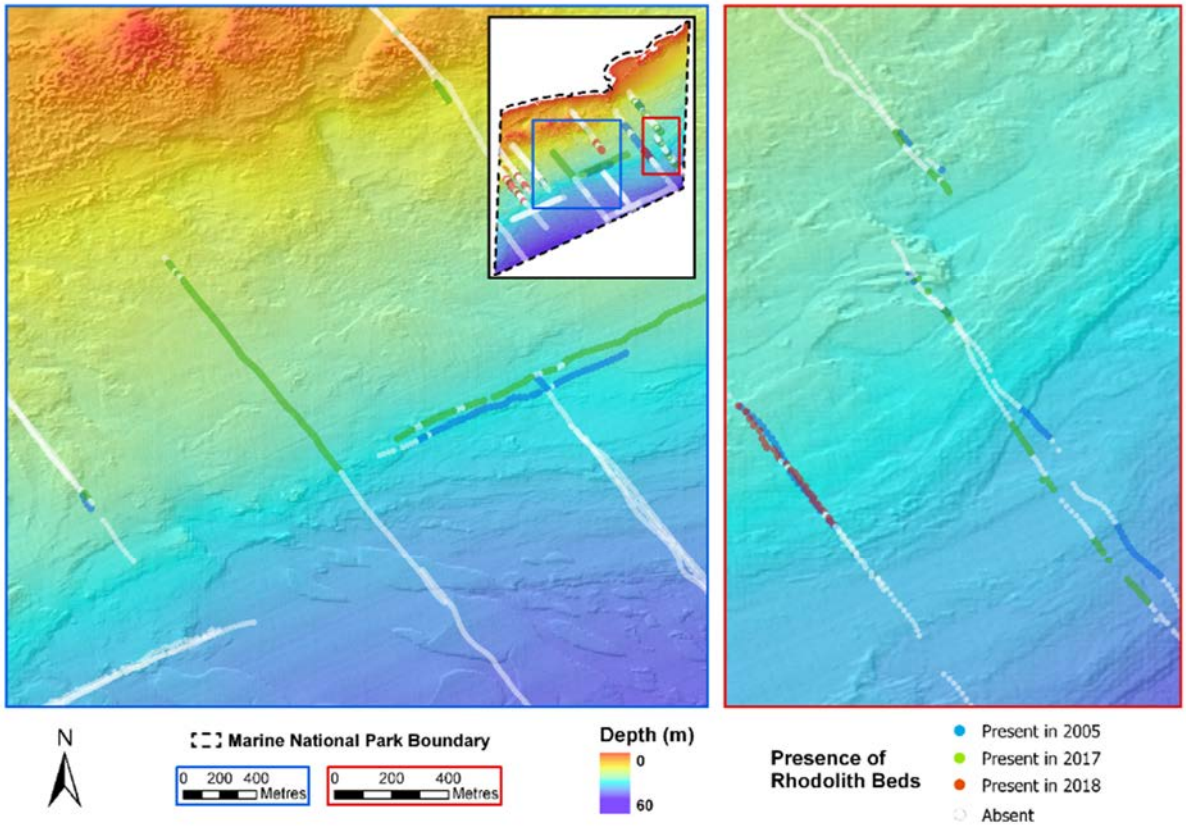

Figure 36. Presence (coloured by year) and absence (white) of rhodolith beds across three years of sampling (2013, 2017 and 2018). Observations were made from oblique video collected using towed video.

3.6 Fisheries Independent Southern Rock Lobster Survey

A total of 240 spatially referenced lobster pots were placed equally inside and outside of the marine national park between the 16th and 20th of November 2018 (Figure 5). A total of 373 Southern Rock Lobster, at an estimated biomass of 328.3 kg, were caught and examined during this study. While sampling effort was equal inside and outside of protected waters, 295 lobsters were caught within the MPA, as opposed to 78 in fished waters (Figure 45). Significantly more lobsters above legal size were found within the MPA (n = 282) in comparison to outside (n = 62) (Figure 45 and Table 13). A small pre-recruit index was present with an average of 0.12 for the entire study with similar values inside/ outside the park (MPA = 0.11, outside MPA = 0.13). Lobsters caught within the park were also found to be on average larger than in fished areas, with a difference of 9 mm carapace size and 210 g weight being present between means inside and outside of the MPA. No significant depth related trends were observed for abundance and average carapace length, across the gender and legal size status (Figure 43).

Overall, bycatch numbers were relatively low in this study, with an average of less than one organism being caught per pot (mean bycatch per pot = 0.625). Velvet crabs (28.7%),

horseshoe leatherjacket (26.7%) and sixspine leatherjackets (20%), made up the vast majority of all bycatch (Table 12). All species were returned to the water without harm. A slightly higher amount of bycatch was caught outside of the MPA (n = 86), compared with inside the MPA (n = 64).

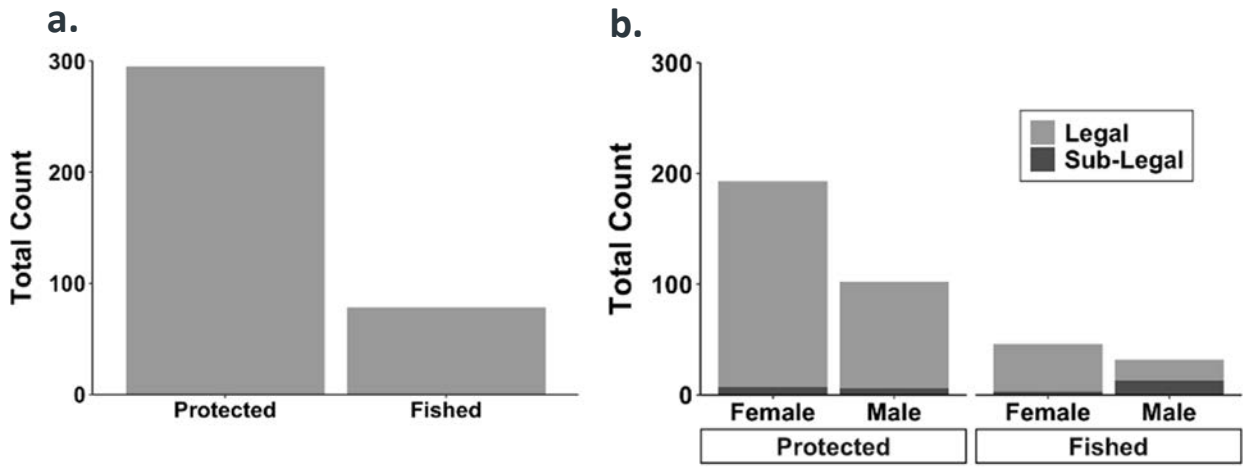

Figure 37. Summary of the total lobster counts from potting surveys within the Point Addis MNP. Charts compare the total number of lobster caught in protected against non-protected areas for all lobsters caught (left plot) and by gender and legal size (Male = 110 mm CL, Female = 105 mm CL) (right plot).

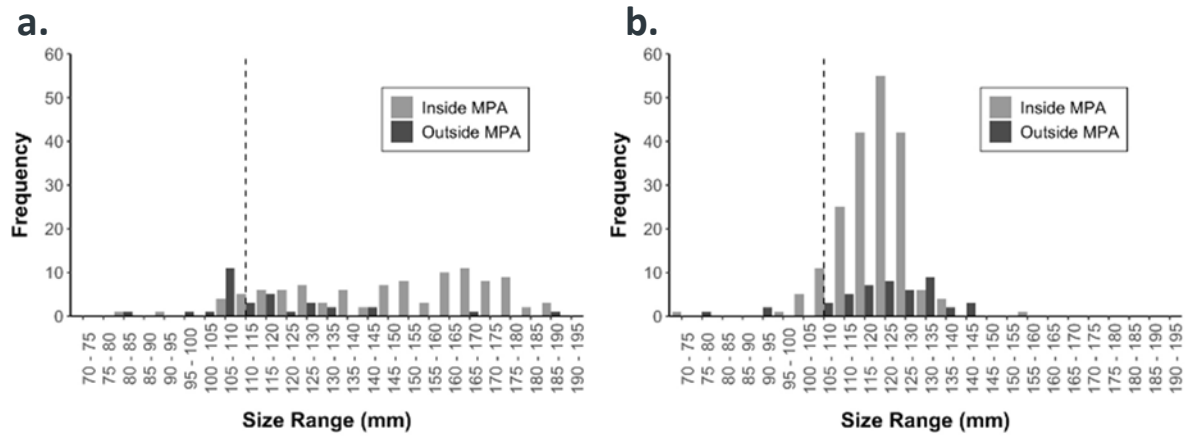

Figure 38. Southern Rock Lobster (*Jasus edwardsii*) male and female size distributions (carapace length in mm) inside and outside the Point Addis Marine National Park with the length of legal size for males (a) and females (b) displayed as a dashed grey line in each distribution plot.

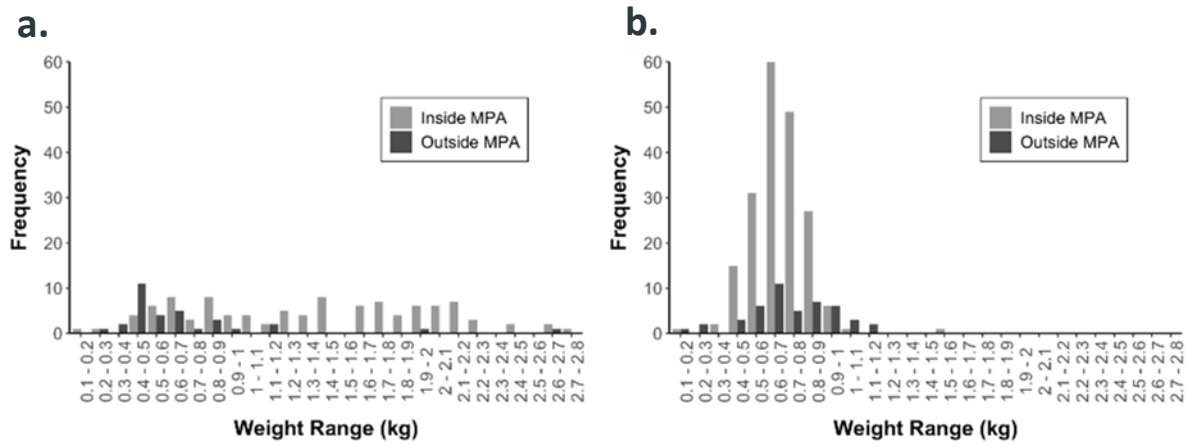

Figure 39. Southern Rock Lobster (*Jasus edwardsii*) male and female size distributions (total weight in kg) inside and outside the Point Addis Marine National Park with the length of legal size for males (110 mm CL) (a) and females (105 mm CL) (b) displayed as a dashed grey line in each distribution plot.

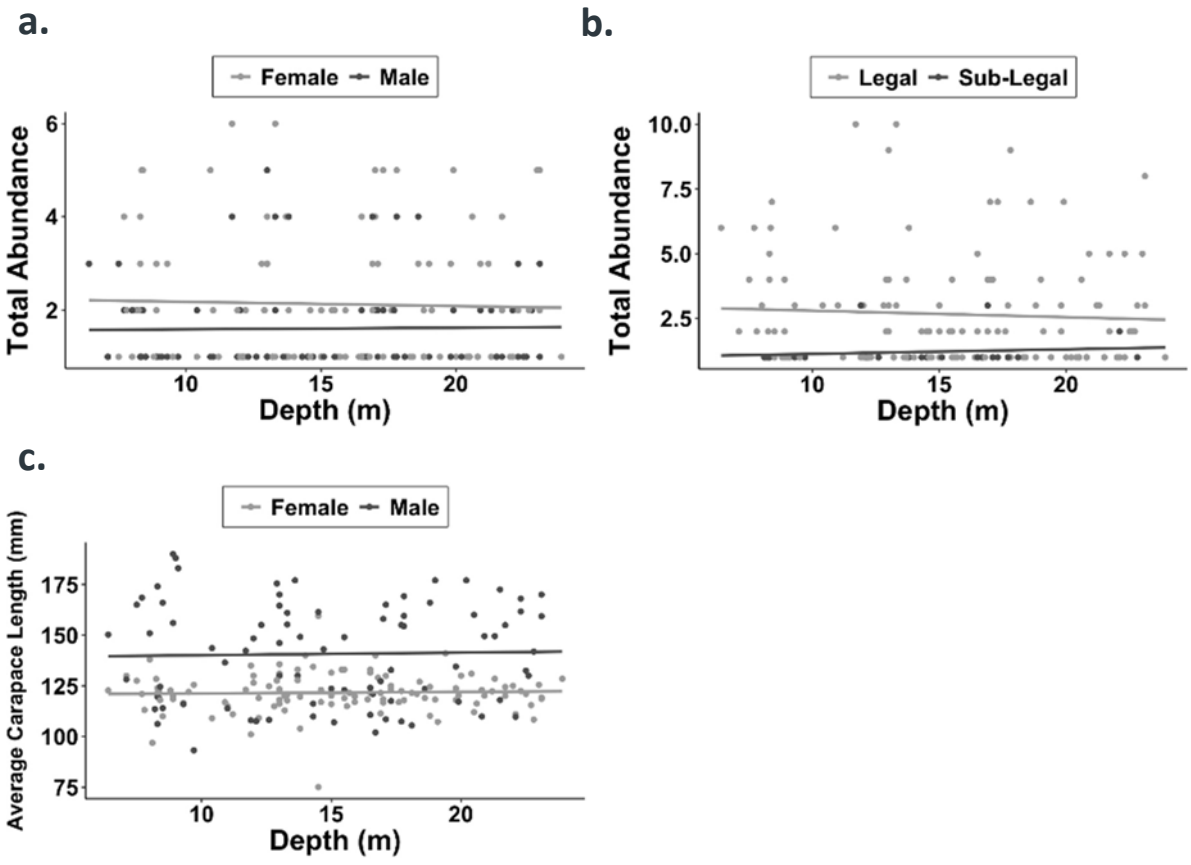

Figure 40. Size and depth related trends of abundance and mean carapace length (mm) per pot lift of lobsters with and adjacent to the Point Addis MNP.

Table 9. Bycatch observed from lobster potting using research pots with no escape gaps in the Point Addis MNP and adjacent fished reference locations. All bycatch observed was identified, measured and promptly return to the water.

Bycatch Species	MPA	Fished
Velvet Crab	9	34
Horseshoe Leatherjacket	11	29
Six Spine Leatherjacket	12	18
Undefined Leatherjackets	18	0
Blue Throat Wrasse	6	4
Octopus	2	1
Hermit Crab	3	0
Port Jackson Shark	1	0
Mosaic Leatherjacket	1	0
Perch	1	0

3.6.1 Environmental Drivers of Southern Rock Lobster Observations

Results of generalised additive models showed varying success in understanding the environmental drivers of various groupings of *Jasus edwardsii* (Table 14). A deviance of approximately 42 % (± 3 %) was explained by the models the number of individuals and total biomass per pot lift, for both all lobsters and subsets of female lobsters. Performance of models of male lobster abundance and biomass was poor, with a maximum correlation of 0.04 between predictions and observations for a test dataset. Standard deviation of depth (a measure of seafloor complexity) was significant in explaining the variation in all groups tested. Depth and distance from the MPA were also significant in explaining variation in number of individuals and total biomass per pot lift, for both all lobsters and subsets of female lobsters. These findings were strongly reflected by trends observed in bubble plots (Figure 49, Figure 50, Figure 51 and Figure 52), where highest abundances were associated with area presented by the bathymetric hillshade as highly complex. Across all four bubble plots, locations where no lobster were caught are commonly presented by the hillshade as relatively low-profile and potentially sand-inundated reef. Clear differences can also be observed between pot locations inside and outside of the MPA, where pot locations inside the MPA caught lobster more commonly and with higher abundances than those outside of the MPA. Similarly, lobster above the minimum legal size limits were much more common, and in higher numbers within the MPA (Figure 46).

Table 10. Comparison of Southern Rock Lobster statistics inside (n = 120) and outside (n = 120) the Point Addis Marine National Park.

Protection Status	Sex	No. of Individuals	No. of Legal Size Individuals	Pre-Recruit Index	Average Carapace Length (mm)	SD of Average Carapace Length	Biomass (kg)	Average Weight (kg)	SD of Average Weight	No. of Reproductive Females
Inside Park	Male	102	96	0.05	149	24.4	141.9	1.39	0.6	181
	Female	193	186	0.06	121	8.6	130.7	0.68	0.1	
	Total	295	282	0.11	130	20.9	272.6	0.92	0.5	
Outside Park	Male	32	19	0.11	119	20.1	22.6	0.71	0.5	36
	Female	46	43	0.03	122	13.7	33.1	0.72	0.2	
	Total	78	62	0.13	121	16.5	55.7	0.71	0.3	

Table 11. Results from generalised additive models (GAMs) used to associate Southern Rock Lobster population characteristics with habitat and protection status inside and outside of the Point Addis Marine National Park.

Group	Depth	Std. Deviation of Depth	Distance to MPA	Fine BPI	Profile Curvature	Plan Curvature	AIC	Deviance Explained (%)	Test Data Correlation
# of Individuals per pot lift	+	+	+			+	439.7	39.1	0.225
Total Biomass per pot lift	+	+	+	+	+		438.2	43.4	0.106
# of Females per pot lift	+	+	+		+	+	297.2	45.3	0.172
# of Males per pot lift		+					172.4	14.3	0.040
Female Biomass per pot lift	+	+	+			+	229.1	41.3	0.123
Male Biomass per pot lift		+					232.0	23.8	0.004

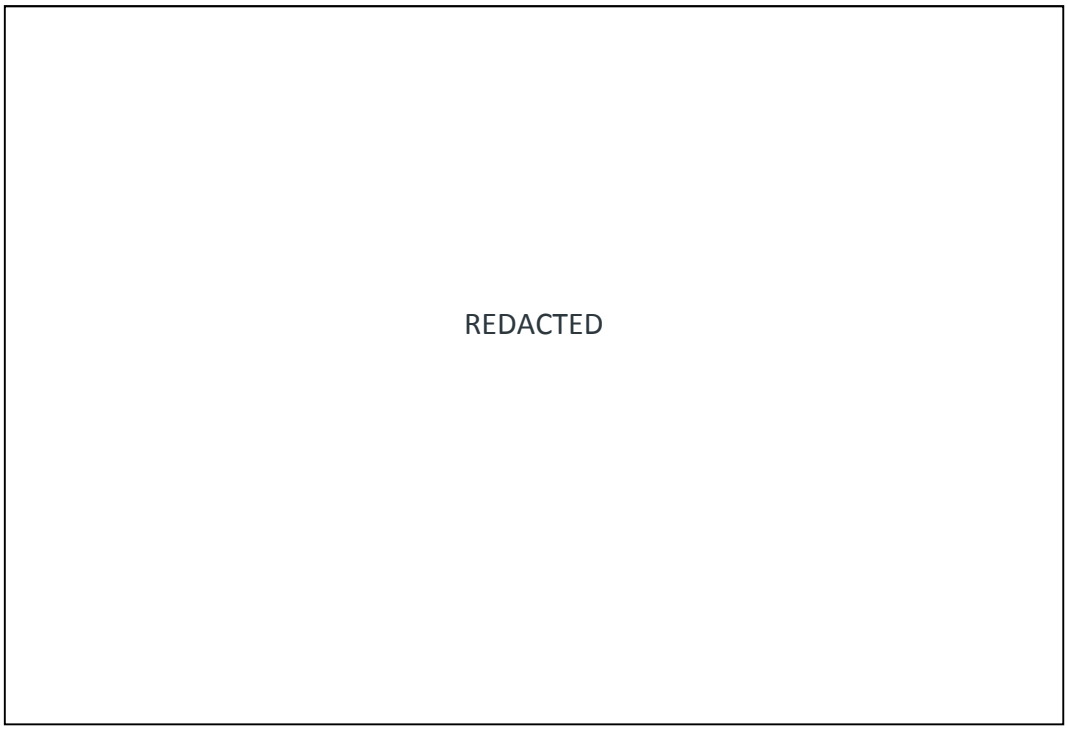

Figure 41. Bubble plot showing the sites of all lobster pot deployments. The size of each site marker corresponds to the total abundance of *Jasus edwardsii* observed at that site. These sites are overlayed on hillshaded bathymetry of the study area and coloured by depth.

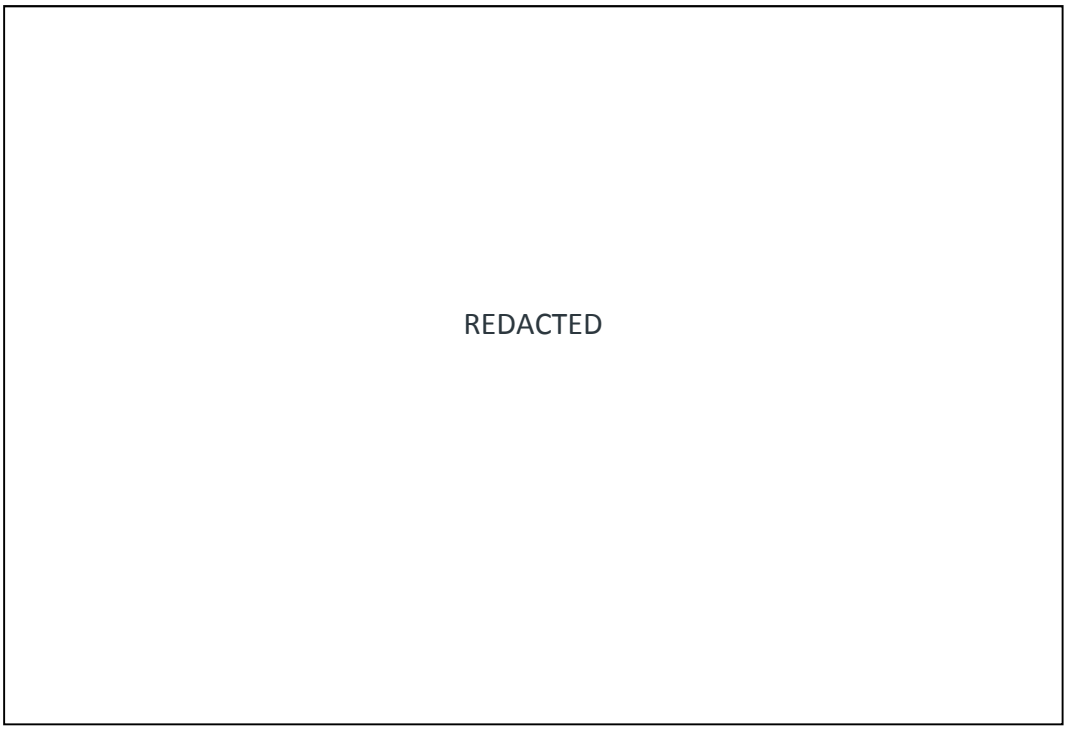

Figure 42. Bubble plot showing the sites of all lobster pot deployments. The size of each site marker corresponds to the abundance of *Jasus edwardsii* above the minimum legal size limit (Male = 110 mm CL, Female = 105 mm CL), observed at that site. These sites are overlayed on hillshaded bathymetry of the study area and coloured by depth.

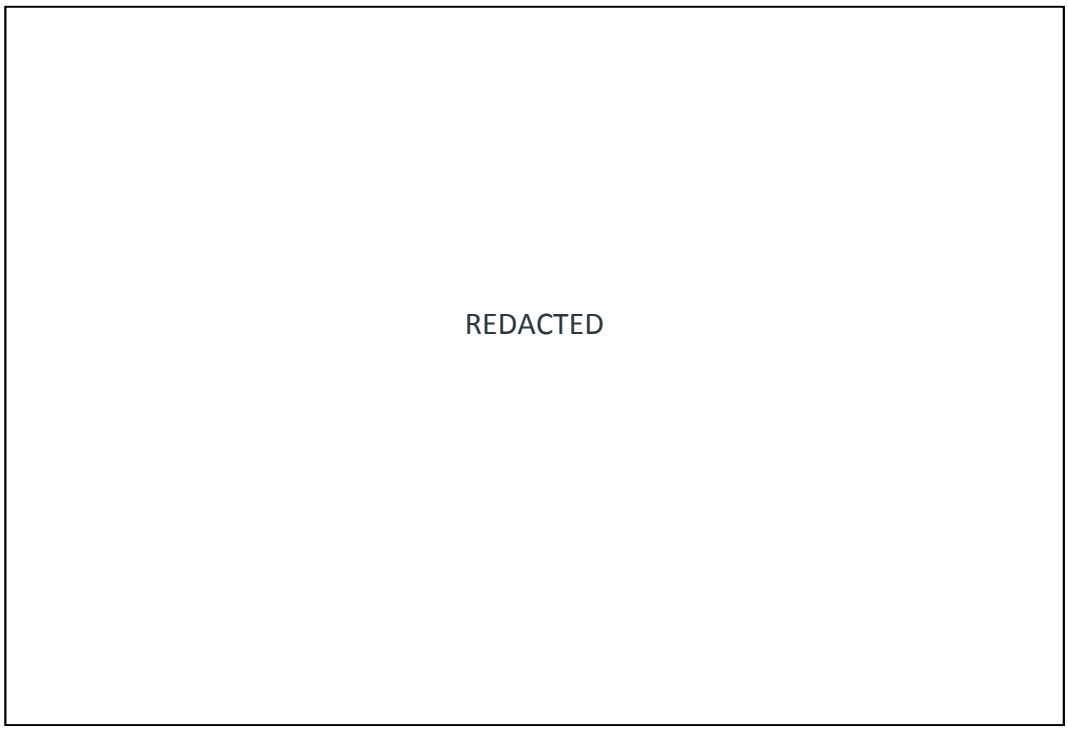

Figure 43. Bubble plot showing the sites of all lobster pot deployments. The size of each site marker corresponds to the abundance of *Jasus edwardsii* observed at that site. These sites are overlayed on hillshaded bathymetry of the study area and coloured by depth.

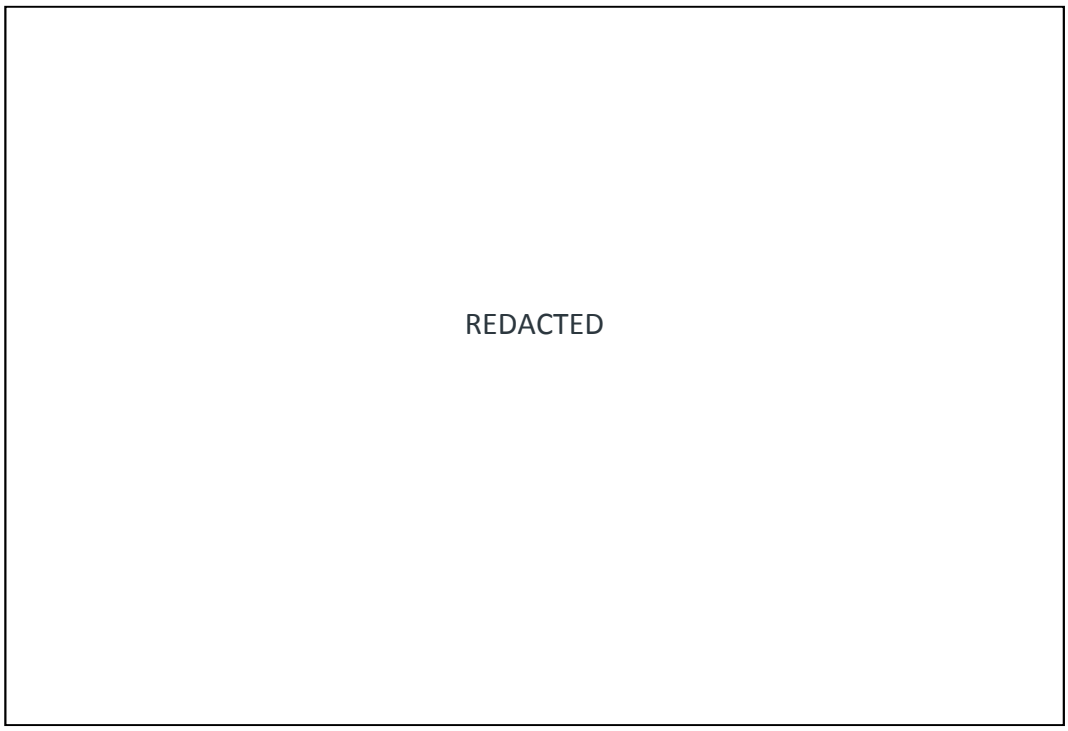

Figure 44. Bubble plot showing the sites of all lobster pot deployments. The size of each site marker corresponds to the abundance of male *Jasus edwardsii* observed at that site. These sites are overlayed on hillshaded bathymetry of the study area and coloured by depth.

3.7 Intertidal Reefs

3.7.1 Unmanned Aerial Vehicle surveys of intertidal reefs

UAV operations were successfully conducted on April 21st 2018 and March 28th 2019. Lighting conditions likely drove differences in data capture rate between surveys. There were lower light conditions on April 21st 2018 and bright sunshine on March 28th 2019. There was also a two-fold difference in the resolution captured by the Parrot Sequoia and higher resolution Micasense Red Edge M multispectral camera. Furthermore, there is a difference in image clarity. Image clarity refers to attributes such as image detail, colour depth, and image distortion (Figure 8). Intermittent GPS functionality in the Parrot Sequoia also created complications in the processing, and greater time and manual processing was required to generate the final spectral maps.

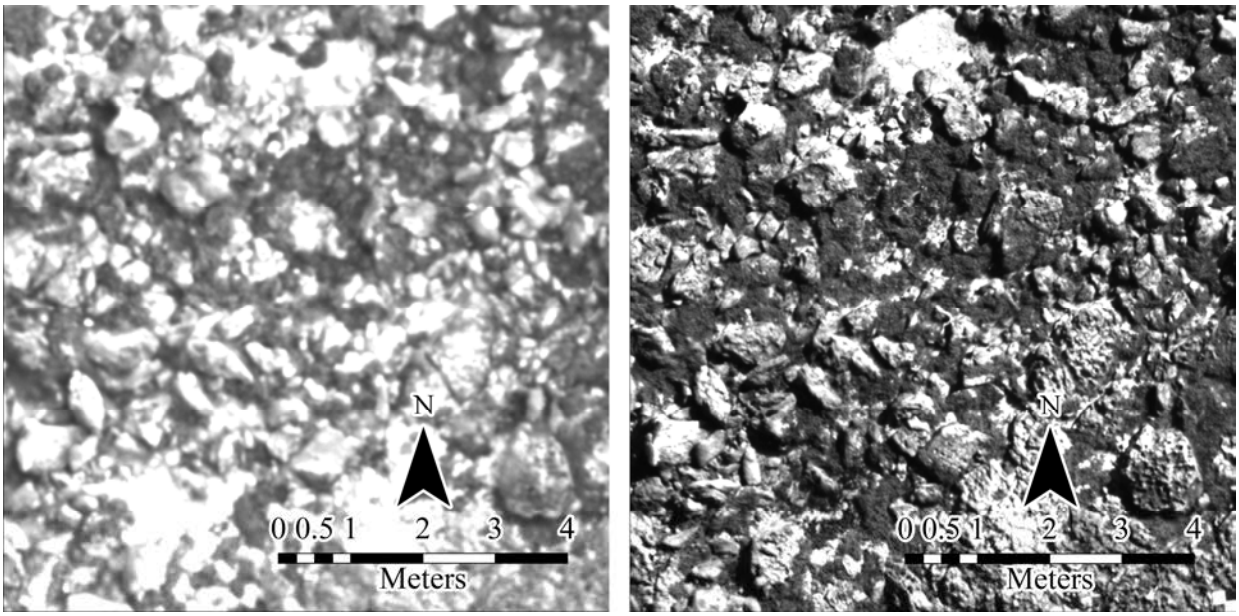

Figure 45. A comparison of the same section of Point Addis intertidal platform represented in the red reflectance band of the Parrot Sequoia spectral camera is a 1280 x 960 resolution, 10 bit colour depth, 4.0 mm Focal Length, 4.8mm x 3.6mm Imager size, and 61.9° Horizontal FOV (left), and the Micasense Red Edge M spectral camera is a 1280 x 960 resolution, 16 bit colour depth, 5.4 mm Focal Length, 4.8mm x 3.6mm Imager size, and 47.9° Horizontal FOV (right). They have the same resolution, but different clarity.

Spatially accurate orthomosaic and spectral maps were generated for the Point Addis intertidal platform (Figure 9). The coverage extent between the years varied for surrounding rocky outcrops, so an area of 21,738.15 m^2 was determined as the main Point Addis intertidal platform (Table 3). Multispectral analysis generated calibrated reflectance indices which were used to calculate Normalised Difference Vegetation Index (NDVI) maps of the intertidal platform (Figure 11). The resultant *H. banksii* coverage maps are shown in Figure

12. The coverage classification was effective at defining extents of the *H. banksii* where it appeared on reef pavement, but was susceptible to misclassifying similarly shaped and coloured objects on the reef platform such as other algae and seagrasses, or areas in shadow caused by overhangs. Over-classification was also evident at habitat boundaries where areas beyond the extents of the coverage as *H. banksii* were classified. The recorded *H. banksii* coverage was 8% less on the main Point Addis intertidal platform in 2019 compared to 2018 (Table 3). However, much of this reduction may be due to the change in sensor characteristics as the Parrot Sequoia multispectral camera was found to be of lower quality than the Red edge sensor used in 2019.

Table 12. The area of the main Point Addis Intertidal Platform, and the average percentage cover of *H. banksii* recorded on April 21st 2018 and March 28th 2019.

	Area (m^2)	Average *H. banksii* Percentage Cover
Point Addis Intertidal Platform	21,738.15	
2018 *H. banksii*	10,323.72	47.49 %
2019 *H. banksii*	8,553.91	39.35 %

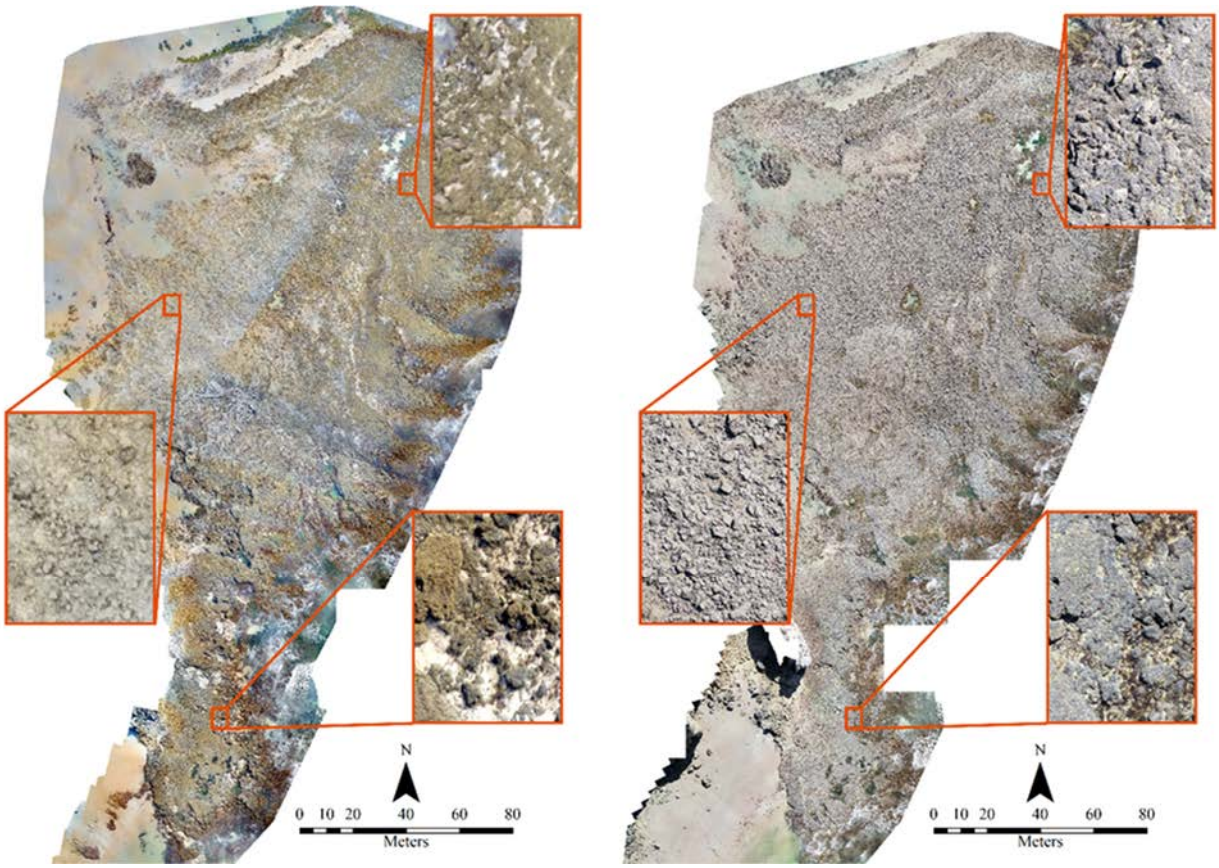

Figure 46. Georeferenced orthomosaic maps of the Point Addis intertidal platform for April 21st 2018 (left) and March 28th 2019 (right).

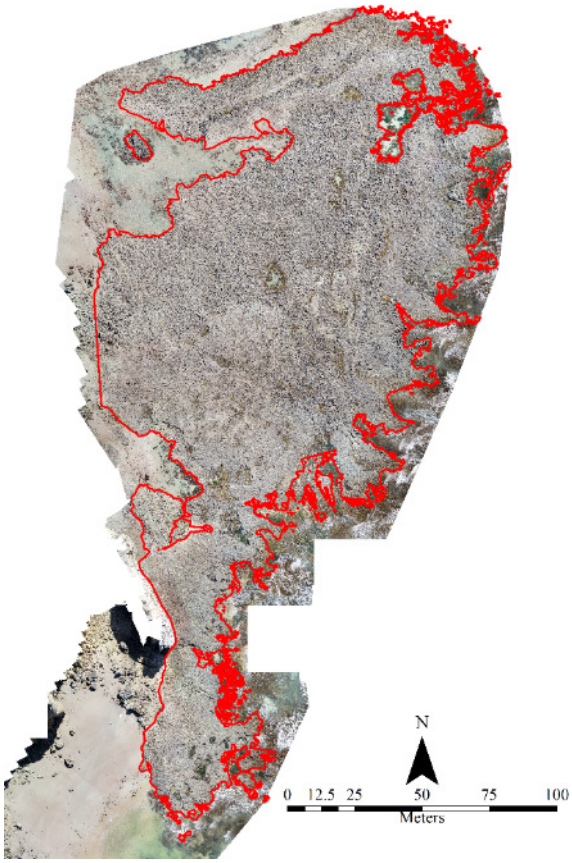

Figure 47. Image of the determined extent of the Point Addis intertidal platform (outlined in red) for all statistical analyses in this report

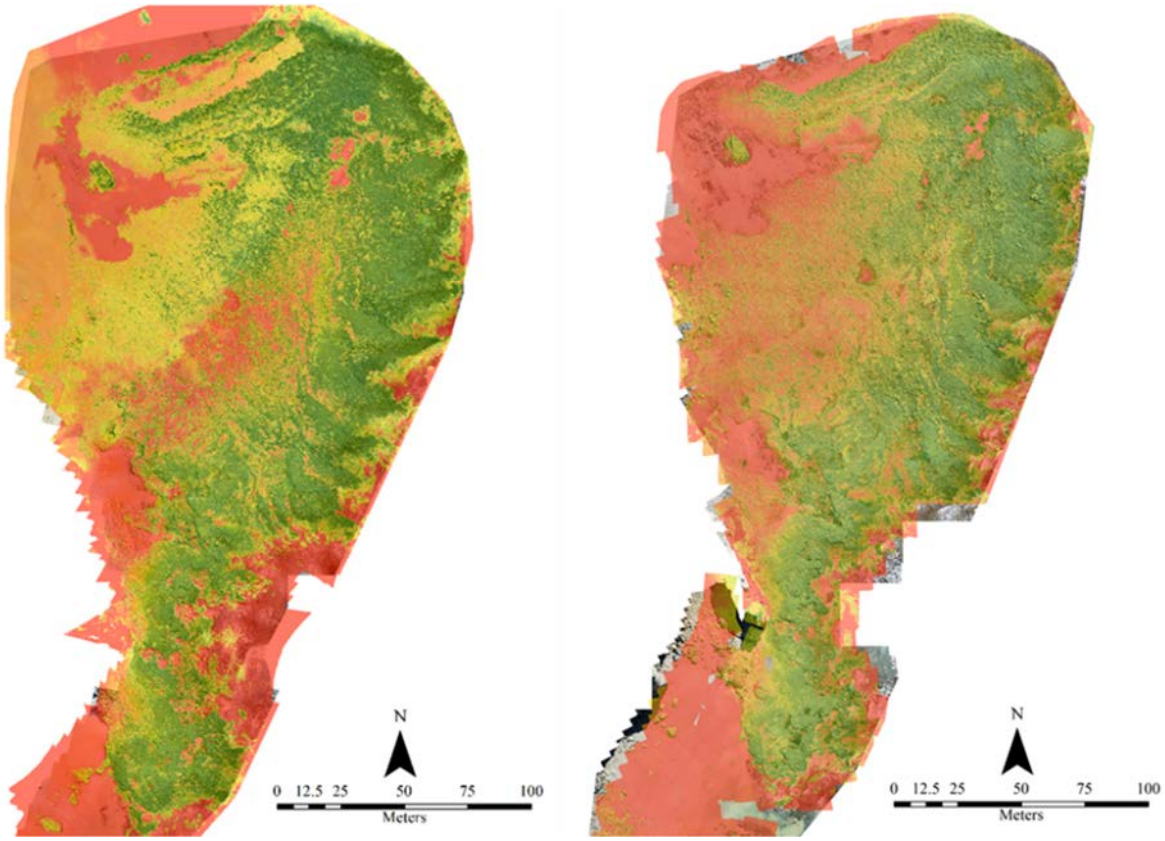

Figure 48. Georeferenced NDVI maps of the Point Addis intertidal platform for April 21st 2018 (left) and March 28th 2019 (right). Red indicated no vegetation, yellow indicates sparse vegetation, and green indicates dense vegetation.

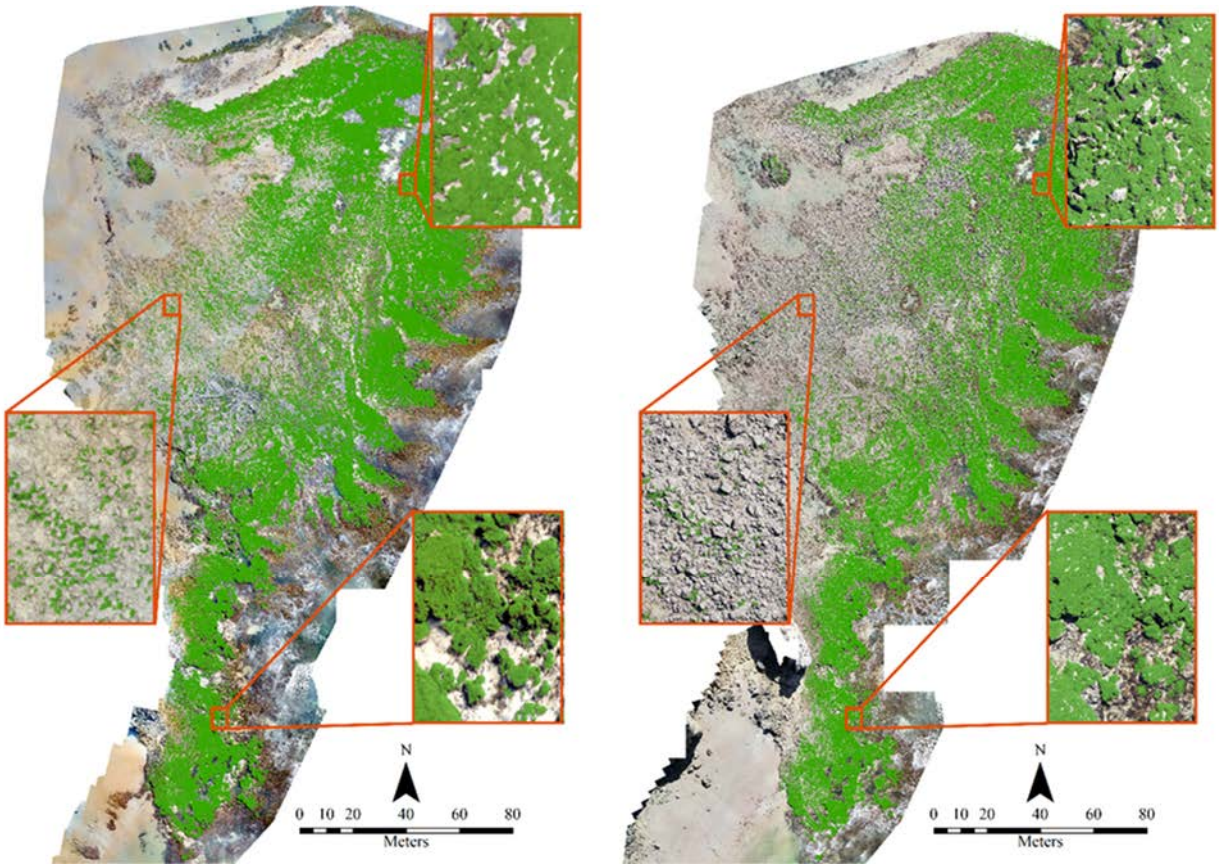

Figure 49. *H. banksii* (indicated in green) coverage maps of the Point Addis intertidal platform for April 21st 2018 (left) and March 28th 2019 (right).

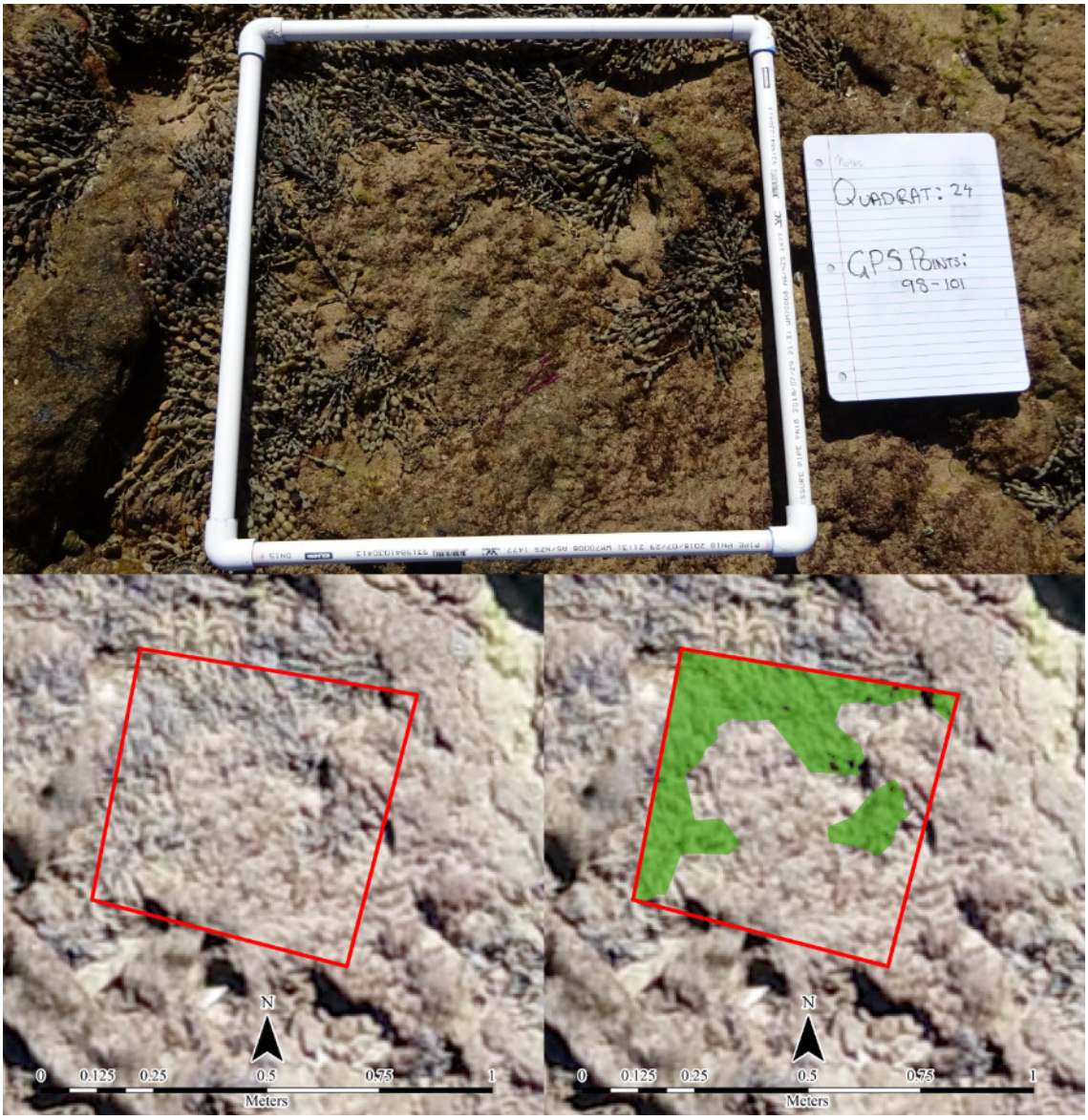

Figure 50. A Comparison of an on-ground photograph (top), virtual quadrat (bottom left), and virtual quadrat with *H. banksii* coverage identification indicated in green (bottom right) for Quadrat 13.

Table 13. The comparison of the percentage cover of *H. banksii* recorded via on-ground quadrat sampling and the same quadrats recreated virtually for RTK GPS points of the quadrat corners for the main Point Addis Intertidal Platform recorded on April 21st 2018 and March 28th 2019.

Quadrat	Virtual Quadrat *H. banksii* Coverage	On-Ground *H. banksii* Coverage	Difference
2018			
Quadrat_Horm01	100.00%	100.00%	0.00%
Quadrat_Horm02	100.00%	100.00%	0.00%
Quadrat_Horm03	100.00%	100.00%	0.00%
Quadrat_Horm04	100.00%	97.96%	2.04%
Quadrat_Horm05	98.80%	89.80%	9.00%
Quadrat_Horm06	96.72%	89.80%	6.92%
Quadrat_Horm07	100.00%	100.00%	0.00%
Quadrat_Horm08	97.45%	93.88%	3.57%
Quadrat_Horm09	100.00%	97.96%	2.04%
Quadrat_Horm10	99.79%	100.00%	0.21%
Quadrat_VLS01	0.00%	0.00%	0.00%
Quadrat_VLS02	17.29%	1.02%	16.27%
Quadrat_VLS03	56.01%	6.12%	49.89%
Quadrat_VLS04	0.00%	8.16%	8.16%
Quadrat_VLS05	18.61%	1.02%	17.59%
Quadrat_VLS06	0.00%	2.04%	2.04%
Quadrat_VLS07	0.00%	6.12%	6.12%
Quadrat_VLS08	4.32%	2.04%	2.28%
Quadrat_VLS09	29.39%	20.41%	8.98%
Quadrat_VLS10	11.39%	4.08%	7.31%
2019			
Quadrat_01	96.82%	97.96%	1.14%
Quadrat_02	93.24%	100.00%	6.76%
Quadrat_07	19.29%	28.57%	9.29%
Quadrat_08	19.30%	10.20%	9.10%
Quadrat_09	1.99%	2.04%	0.05%
Quadrat_10	0.00%	0.00%	0.00%
Quadrat_11	0.00%	0.00%	0.00%
Quadrat_12	83.57%	75.51%	8.06%
Quadrat_13	94.87%	97.96%	3.09%
Quadrat_14	85.78%	89.80%	4.01%
Quadrat_15	99.62%	100.00%	0.38%
Quadrat_16	95.60%	100.00%	4.40%
Quadrat_21	0.00%	0.00%	0.00%
Quadrat_22	11.49%	28.57%	17.08%
Quadrat_22	0.00%	0.00%	0.00%
Quadrat_24	36.91%	40.82%	3.90%
Quadrat_25	0.00%	0.00%	0.00%

Hormosira banksii coverage comparisons between the virtual quadrats and the on-ground quadrats were very similar, with an average 7.12% (± 11.35%) difference in 2018, and 3.96% (± 4.79%) difference in 2019 (Table 4). In both years, there was one quadrat with a greater difference than the others. In 2018, the greatest disparity between virtual and on-ground quadrats is Quadrat_VLS03, which recorded 56.01% in the virtual quadrat, and 6.12% in the on-ground measurement. The disparity of 49.89% is due to misclassification of non- *H. banksii* algae in the virtual quadrat as *H. banksii*. This is likely due to inundation of water on this quadrat during mapping, and quality of data from the Parrot Sequoia multispectral camera. In 2019, the greatest disparity between virtual and on-ground quadrats is 17.08% at Quadrat_22. The difference recorded at this quadrat is most likely due to the difference in size of the virtual quadrats compared to the on-ground quadrats. *H. banksii* is sparse in the region surrounding Quadrat_22, so the additional 25% area covered by the virtual quadrat may account for the disparity.

The landscape pattern indices measured across the nine patch analysis windows (low *H. banksii* coverage (3 windows), moderate *H. banksii* coverage (3 windows), and dense *H. banksii* coverage (3 windows) showed a general trend of higher coverage, less patches, and lower edge density in 2018 (Table 5). Similar to the percentage cover of *H. banksii*, much of this may be due to the lower resolution and lower quality data collected by the Parrot Sequoia multispectral camera. The lower clarity images provided less detail in the coverage maps, which resulted fewer but larger patches (Figure 14). The comparison between virtual quadrats and on-ground quadrats also showed higher variation and greater difference in the 2018 data compared to the 2019 data.

Table 14. The landscape pattern indices of the nine patch analysis windows for the main Point Addis Intertidal Platform recorded on April 21st 2018 and March 28th 2019.

	H. banksii Cover (%)		Number of Patches		Maximum Patch Area (m²)		Mean Patch Area (m²)		Total Perimeter (m)		Mean Patch Perimeter (m)		Edge Density	
	2018	***2019***	***2018***	***2019***	***2018***	***2019***	***2018***	***2019***	***2018***	***2019***	***2018***	***2019***	***2018***	***2019***
Low Cover 01	35.50	17.43	992	1639	155.54	25.28	0.224 (± 4.989)	0.066 (±0.866)	4196.27	3993.46	4.23 (± 83.41)	2.437 (± 25.99)	6.71	6.39
Low Cover 02	18.82	6.54	1730	1744	9.28	1.13	0.068 (±0.325)	0.023 (±0.0505)	2258.10	2280.56	1.305 (± 4.20)	1.308 (± 2.28)	3.61	3.65
Low Cover 03	8.35	2.79	1806	1327	2.01	0.85	0.029 (±0.088)	0.013 (±0.037)	1575.66	1152.97	0.872 (± 2.14)	0.869 (± 1.84)	2.52	1.84
Moderate Cover 01	61.11	34.45	712	1921	348.46	66.44	0.536 (±13.058)	0.112 (±1.909)	3777.25	7024.75	5.305 (± 117.09)	3.657 (± 52.10)	6.04	11.24
Moderate Cover 02	46.39	40.24	757	1409	205.75	146.70	0.383 (±7.5)	0.178 (±3.93)	6445.06	8926.54	8.514 (± 160.30)	6.335 (± 131.20)	10.31	14.28
Moderate Cover 03	24.31	25.46	1190	1796	13.53	55.13	0.128 (±0.64)	0.089 (±1.33)	3803.57	6957.63	3.196 (± 11.50)	3.874 (± 51.03)	6.09	11.13
Dense Cover 01	58.43	59.08	853	969	335.93	340.46	0.428 (±11.501)	0.381 (±10.937)	7173.95	5695.56	8.41 (± 194.99)	5.878 (± 147.99)	11.48	9.11
Dense Cover 02	76.33	67.64	118	611	470.32	413.39	4.043 (±43.292)	0.692 (±16.723)	1949.97	10233.20	16.525 (± 168.80)	16.748 (± 392.25)	3.12	16.37
Dense Cover 03	84.30	63.98	33	479	525.37	391.89	15.966 (±91.446)	0.835 (±17.905)	1092.32	8130.70	33.101 (± 184.97)	16.974 (± 355.22)	1.75	13.01

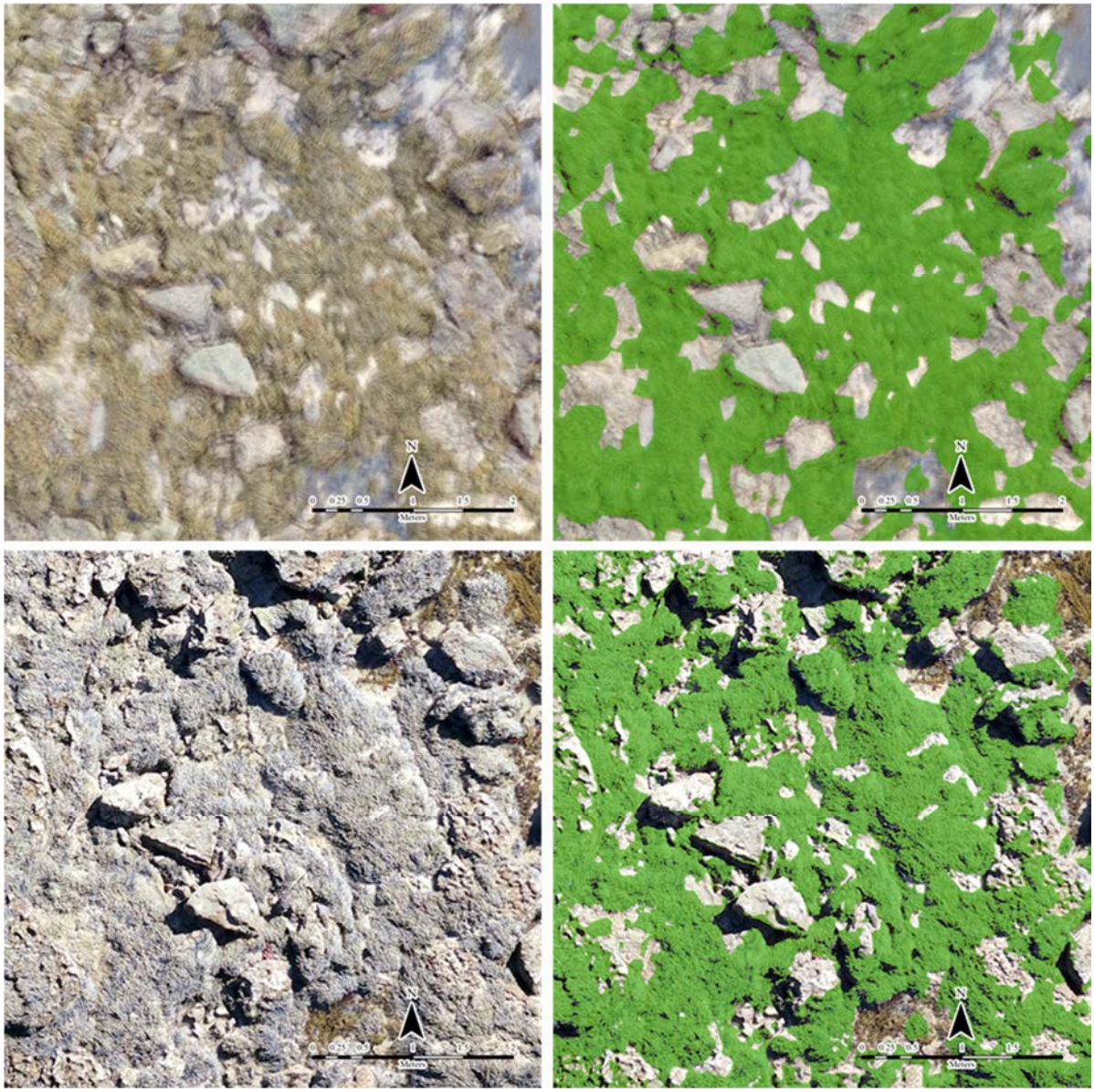

Figure 51. Classification of *H. banksii* (indicated in green) created from RGB imagery collected on April 21st 2018 (top) and March 28th 2019 (bottom). There is minor misclassification due to similar spectral and textural characteristics of other vegetation.

3.7.2 Intertidal Reef Monitoring Program & Control charts

Hormosira banksii cover was maintained above 42% (the LLAC) between 2005 and 2012. However in 2013 it dropped below, and was very close to exceeding the LCL. The latest surveys in 2018 and 2019 show an increase above the LLAC. There were no on ground surveys for 2018 or 2019 done at the reference site. To continue the time series for control charts % cover estimates were extracted from the UAV imagery from approximate quadrat positions provided by Parks Victoria for start and end of transects.

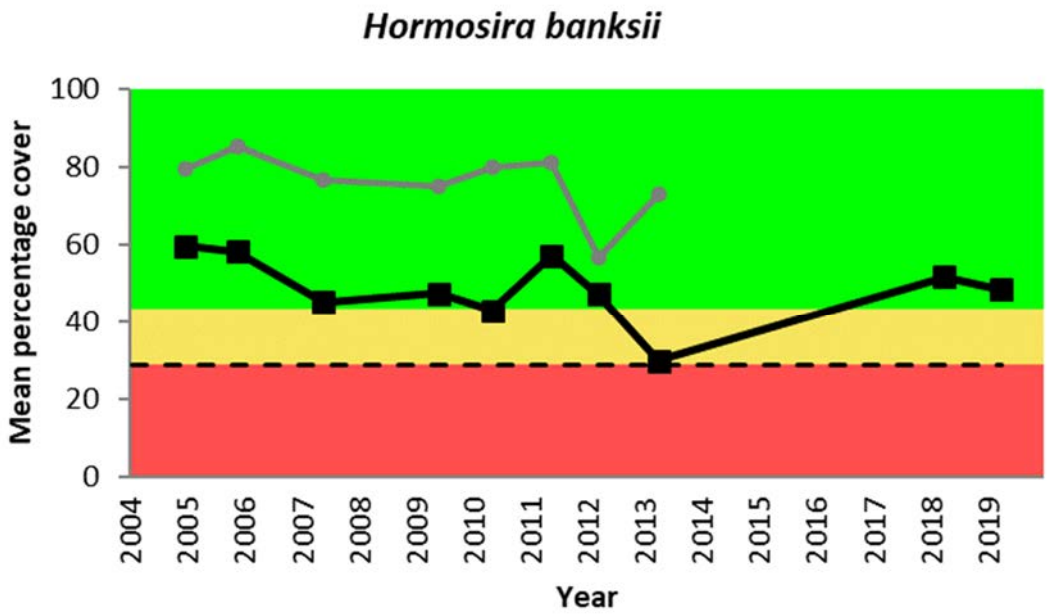

Figure 52. Control chart showing change in estimated percentage cover of *Hormosira banksii* within the Point Addis Marine National Park (black line) and reference sites (grey line). Observations prior to 2017 for these charts were sourced from historical IRMP surveys. The 2017 and 2018 observations replicated IRMP survey methods using virtual quadrats derived from UAV imagery. These charts have a lower limit of acceptable change (LLAC, yellow line-set as the minimum value inside the MPA from IRMP surveys in 2003, 2005 and 2006) and lower control limit (LCL, red line) based on the variation from surveys, which indicates the level when conditions are sufficiently poor that some management response is required.

4. Discussion

4.1 Subtidal Reefs (including shallow and deep reefs)

4.1.1 Benthic Communities

Subtidal demersal vegetation was observed using a range of data sources throughout this study. An Underwater Visual Census (UVC) approach was previously implemented as part of the Shallow Reef Monitoring Program (SRMP) across seven time-series since 2003 (Woods et al. 2014), allowing an understanding of trends through time. Whilst this study maintained a UVC aspect and completed surveys at the same sites, it implemented Reef Life Survey (RLS) methodology as opposed to SRMP methods. The main differences in this survey approach compared with previous SRMP methods is the replacement of *in situ* quadrat surveys with photo quadrats and a reduced survey effort from 200 m total transect distance in SRMP to 100 m at each site in RLS. However, it is noted that the survey area covered for invertebrates was the same for SRMP and RLS. Whilst a major advantage of using photoquadrats is that divers are not required to have high level algal taxonomic identification skills, it does pose limitations in terms of what data can be acquired. For example, in this study, we were only able to compare canopy-forming species to previous SRMP observations, as understory communities are often obscured. Since the inception of the SRMP program, RLS has become a common method for completing underwater visual census surveys of shallow subtidal reefs. Globally, the RLS technique has allowed approximately 2,000 sites to be surveyed using a standard set of survey methods. Adoption of such a common and wide-spread program now allows many opportunities for comparison of the condition of the Point Addis MNP with other areas globally. Locally it provides opportunities to increase survey effort across the network using the RLS approach. Continuation of reporting for timeseries analyses will; however, be dependent on the experience and quality of data provided by RLS divers.

While overall control charts showed that macroalgal indicators are in fair condition, the previously dominant species *Ecklonia radiata* has shown an alarming decline since 2012 (Figure 21). While some increases in other canopy-forming brown algae have occurred since then, in the 2018 survey canopy-forming algae has now fallen below the lower control limit. SRMP surveys previously revealed that coverage of *Ecklonia radiata* declined from a regional average of 29 % cover in 2012 to 6 % cover in 2013. There were bare stipes present in 2013 which indicated the loss was from some form of dieback disease (Woods et al. 2014). These were not identified in the photo quadrat analyses in the recent surveys. Coverage estimates for *Ecklonia* for these sites have indicated a further decline to a regional average of 0.75 % coverage in 2017 and complete absence in the 2018 RLS survey.

This project also implemented towed video surveys of subtidal reefs within the Point Addis MNP. This methodology allowed for both broad-scale forward facing video footage to be collected at the same time as highly detailed downward-facing still images. Oblique video in

this study was used to rapidly measure and model broad extents of Key Ecological Attributes such as canopy-forming macroalgae, in particular *Ecklonia radiata,* and rhodoliths beds (Figure 41, Figure 42, Figure 43 and Figure 44). Analyses of the oblique video imagery suggests that broad patterns of distribution for these groups has been fairly stable through time with no obvious changes in boundary of extents. For *Ecklonia* this suggests that habitat extent may be more resilient to change than those observed using RLS/SRMP methods. This may be due to RLS/SRMP sites in shallow water are more susceptible to heat stress. Whilst the oblique view poses challenges with extracting % cover estimates the down facing stills captured in 2017 and 2018 provide the opportunity to calculate cover estimates and monitor change through time for deeper components of the macroalgae assemblages observed.

Downward-facing still imagery collected using towed video was used to understand community structure throughout the park due to its ability to provide high taxonomic resolution and extensive spatial coverage across the MPA. As there is a reasonably uniform and gentle depth gradient throughout the park, clear boundaries of dominant vegetation were found with depth (Figure 40). Generally, this meant that there was a high prevalence of foliose brown algae in shallow areas less than 25 m depth, which then transitioned into red algae dominated areas, and further into high sessile invertebrate prevalence beyond 35 m depth (Figure 39). No significant differences in community structure were observed between 2017 and 2018 surveys.

Each of the three imaging methods implemented here played a different role in gaining an understanding of the distribution and change in benthic communities within the Point Addis MNP. Photo quadrats captured during underwater visual census helped to achieve the highest image clarity of all methods, however due to constraints of diving, the spatial extent of these surveys was limited. The UVC approach also had the least spatially explicit position information identified by a centroid of the site locality rather than individual referenced images. Towed video-derived downward facing stills achieved similar taxonomic resolution to UVC photoquadrats. This method can be extended to the entire park and had an advantage of precise geolocation provide by the USBL system. Towed video also allowed the capture of orders of magnitude more images than UVC and provides a cost-effective solution for sampling communities in deeper sections of the park. In the context of this study, however, UVC provided an important link to extend SRMP monitoring within the park and the ability to extend key time series in data collection but was restricted to canopy-forming species due to the use of photo quadrats. The oblique view provided by towed video also provided information on the broad extent of dominant habitats beyond typical safe diving depths, which proved useful for time series comparisons. This allowed comparison to oblique imagery captured in 2005 as part of the initial Coastal CRC works by University of Western Australia allowing the evaluation of temporal changes (Holmes et al. 2008). An added advantage of the towed video methodology is that multiple streams of data can be obtained at once, therefore dramatically increasing the efficiency of this

method. Classification of georeferenced towed video also proved to be an advantageous method for tracking the presence of key habitats of interest.

4.1.2 Large Mobile Fish (including sharks and rays)

Fish assemblages within and adjacent to the Point Addis MNP were observed using a range of data sources throughout this study. These fish assemblages have previously been monitored using SRMP UVC techniques only. As detailed above, this study also implemented UVC techniques but used the common Reef Life Survey methodology. Observations of fish were normalised to account for differences in area covered by SRMP and RLS techniques. Results showed the current status of all key mobile fish species to be healthy with all species analysed within the zone of good condition. A previously identified limitation of this method is the limited depth that it can monitored using diver approaches (Langlois et al. 2018). The importance of mesophotic reefs is now prevalent in the literature (Loya et al. 2016). In comparison with tropical mesophotic systems, little is known about temperate mesophotic ecosystems (Williams et al. 2019) and more data are needed. Moore et al. (2010) found species richness of a temperate fish assemblage increased with depth. They found that greatest species richness was present at depths between 20 and 50 m, generally inaccessible for UVC techniques. This depth range also coincides with the majority of available reef within the Point Addis MNP. Our study showed these trends to be especially prevalent in models created for carnivores and invertivores, where highest species richness was predicted to be found in the deeper, mesophotic zone and supported by our field observations.

This study allowed for the establishment of time series fish assemblage monitoring for the entire depth range of the Point Addis MNP, via the use of Baited Remote Underwater Videos (BRUVs). Whilst UVC techniques are known to sample a different set of species, including cryptic species, better than BRUVs (Colton & Swearer 2010, Lowry et al. 2012), in this study BRUVs increased species observed within the park by 48 % compared with UVC surveys simultaneously completed in this project. There are now three time-series of BRUV surveys within this MPA, and initial control charts indicate that the current status of all key mobile fish species are healthy with none of the species analysed in the ‘poor’ category (Figure 25). It should be noted that as these charts are based on only three surveys (using the lowest value from the reference sites as the LLAC), these surveys have helped establish a baseline for on-going monitoring rather than providing a true assessment of their current condition.

The inclusion of BRUVs in monitoring also allowed for spatially explicit models to be made for various diversity metrics and abundance of key groups and species throughout the park aided by the distribution of sample locations across environmental gradients observed (Figure 26, Figure 30 and Figure 31). Reaching the same density of field locations using UVC methods would not be feasible. Our approach, driven by a solid foundation understanding of the seabed structure provided by Sonar/LIDAR technologies allows for a spatially

balanced design across the environmental variability of the site. An advantage of distribution modelling approaches, such as those used in this study, is the ability to predict patterns in abundance and biodiversity beyond sampled locations, if relationships with environmental drivers can be inferred (Araújo & Guisan 2006, Sequeira et al. 2016). Distribution modelling can be relevant for a range of applications such as tracking invasive species and researching effects of climate change (Elith & Graham 2009). This study, for example, predicted hotspots of species richness and abundance across an area of over 100 km^2, including across the entire extent of the Point Addis Marine National Park. This knowledge can now be used by park authorities to target diversity assessments, as well as to identify sites of high biodiversity or public interest, previously not visited. As temporal sampling was considered in this study, park authorities can also gain an understanding of where changes may be occurring, and create more efficient sampling designs to track these changes. Furthermore, stakeholders are often interested in community-level metrics of assemblage patterns, such as an understanding of relationships between biodiversity patterns and the surrounding environment (Guisan & Thuiller 2005). Sequeira et al. (2016) suggested that efficient management tools should be focused on improving predictive ability of biodiversity distribution models, as opposed to studying and mapping each species individually. Our findings indicate that BRUVs provide sufficient information to reliably generate spatially explicit models of entire assemblages as well as functional groups and species, thereby maximizing understandings of dynamics within the assemblage and to test their relevance to known ecology.

4.1.3 Mobile Macroinvertebrates

***Jasus edwardsii* (Southern Rock Lobster)**

Fisheries independent surveys of *Jasus edwardsii* (Southern Rock Lobster) populations within and adjacent to the Point Addis Marine National Park show clear trends with respect to protection. Over 3.5 times the abundance and 4.5 times the number of legal rock lobsters were captured within the Park (Table 13). In accordance with other studies that have investigated the effect of protection on populations of *J. edwardsii* (Kelly et al. 2000, Shears & Babcock 2003, Barrett et al. 2009, Freeman et al. 2012, Young et al. 2016, Ierodiaconou et al. 2018), we found more and larger individuals inside the boundaries of the MPA. Specifically, male *J. edwardsii* were appreciably larger, and female *J. edwardsii* were found in considerably higher abundance inside of the MPA. This study showed abundance and biomass of *J. edwardsii* outside the MPA to increase closer to the MPA boundary, suggesting that the Point Addis MNP may be positively affecting the supply individuals to surrounding waters open to fishing.

Globally, spillover effects of biomass to waters adjacent to MPAs has been observed (McClanahan & Mangi 2000, Abesamis & Russ 2005, Goñi et al. 2008). Our results of higher abundance and biomass of lobster within the MPA, and known reproductive traits of *J. edwardsii*, suggest the potential for larval export of *J. edwardsii* from the MPA to contribute

to populations outside the study area. *Jasus edwardsii* have a complex early life cycle and can spend 12–24 months within oceanic waterbodies undergoing 11 larval stages before settling (Thomas et al. 2000, Linnane et al. 2013). Previous studies have suggested that Australian *J. edwardsii* populations are responsible for some trans-Tasman larval flow that contributes to and possibly maintains New Zealand populations (Chiswell et al. 2003, Morgan et al. 2013). Our study however, inexplicably observed that there were a lack of sub-legal lobster found in this survey (both inside and outside of the MPA). This could suggest a reduced supply of recruits to this population and could be monitored by repeating these surveys through time as well as by introducing juvenile specific sampling methods into future monitoring such as by using puerulus collectors. Our findings could also be due to the exclusion of pre-recruit lobster from traps by larger lobster (Miller 1990, Frusher & Hoenig 2001).

Jasus edwardsii are obligate crevice dwellers and are found on all rock types and geomorphological structures from the intertidal zone to 200 m deep, provided there is suitable shelter (MacDiarmid et al. 1991, Edmunds 1995, Booth 1997). They reside in 'dens' within crevices or under ledges formed by reefs and are important predators that forage on slow-moving benthic invertebrate prey such as bivalves, sea urchins and abalone (Jernakoff et al. 1987, Edmunds 1995). Although crevices and shelter are often associated with more complex reef habitat, we recognise that our methods did not measure differences in shelter availability directly. This study assumed that substratum complexity indices were related in to lobster shelter and foraging habitats and recognise that these analyses could be improved in the future through the inclusion of more direct geomorphological description, such as those of Harrington and Hovel (2016). In this study, we used different characteristics of the seafloor (e.g. slope, rugosity) as less labour-intensive proxies for favourable crevice habitat. We note that lobster crevice habitat can occur on non-complex substratum structures, but the indices used in this study provide a better indication of crevice habitat than no access to seafloor data, as indicated by the importance of standard deviation of depth (measure of structural complexity) in all models run across gender, abundance and biomass.

Overall, we found that the Point Addis Marine National Park has a substantial population density of *J. edwardsii* relative to the surrounding fished area which was expected after 16 years of protection. The results will act as an appropriate baseline for future studies documenting changes in this MNP assessing how the population responds to protection, recruitment and a changing climate through time. Continued sampling of this MPA into the future, along with other MPAs, will provide a more conclusive understanding of how *J. edwardsii* are responding to complete removal of fishing pressure within MPA boundaries across the state.

Other Key Macroinvertebrates

Point Addis MNP also provides refuge for a number of key macroinvertebrates such as the commercially-important *Haliotis laevigata* (Greenlip Abalone) and *Haliotis rubra* (Blacklip Abalone), as well as *Nectria* spp. (Seastars) and *Lunella undulata* (Turban Shell) (Woods et al. 2014). Control charts developed in this study found the *H. laevigata* and *Nectria* spp. in good abundance (Figure 20). Consistent declines over the last 15 years were observed in *H. rubra* and *L. undulata,* which are currently rated in poor and fair abundance respectively. While technically *L. undulata* has not crossed its lower control limit, as this is set at 0 %, this is not possible. In this study, a standardised approach was taken to choose LLAC for subitidal reef diver survey data. Given there was no data from before the area was declared a Marine National Park, the default was to set this as the minimum value inside the MPA from SRMP surveys in 2003, 2005 and 2006. However, for some species, due to either low values during this period or due to the degree of variability, the resultant Lower Control Limit (red zone) is then set as zero. This is problematic because being set at zero means it is impossible to cross this threshold. In future, Parks Victoria and partners should undergo a process to either eliminate such species as "indicators", or further refine the LLAC (yellow zone), to ensure a LCL of above zero.

Overall, macroinvertebrates were found to maintain fair abundance since 2006. Given that two of the four characteristic macroinvertebrates have shown substantial decline, it will be important to understand if there is any management action that could aid in the recovery of these species and the link between the decline in these species and the canopy-forming brown algae. One of the challenges in understanding macro invertebrate decline is the potential influence of changes in biotopes but also the geomorphic environment. Whilst somewhat anecdotal there was a string of pots fished within the MNP that were historically productive prior to protection but now appears to be substantially inundated with sediments. Similarly, changes in sediment transport may be impacting once suitable habitat for macroinvertebrates. No invasive or range-expanding/overabundant species such as *Centrostephanus rodgersii* or *Asterias amurensis*, were found during this survey.

4.2 Intertidal Reefs

4.2.1 *Hormosira banksii* dominated communities

Hormosira banksii cover was maintained above 42% (the LLAC) between 2005 and 2012. In 2013 coverage dropped below this threshold, and was very close to exceeding the LCL. In the latest surveys in 2018 and 2019 *Hormosira* has now increased back above the LLAC. The new approaches to intertidal reef community assessments provided in this report allow for the opportunity to move beyond spot count assessment to full platform census.

Use of unmanned aerial vehicles (UAVs) reveals the potential for high-resolution remote sensing to be implemented into current intertidal monitoring efforts through successful identification of dominant algal canopy cover and the potential to quantify geomorphological data across the entire platform. Numerous studies have observed

intertidal biota and assemblages from the ground (Underwood & Jernakoff 1981, Schiel 2004, O'Hara et al. 2010), providing detailed information on fine-scale influences and interactions of the intertidal biota. These include the importance of spatial scales and patches (e.g. (Archambault & Bourget 1996, Airoldi 2003)), interactions and competition between biota (e.g. (Dayton 1971, Borell et al. 2004)), and susceptibility to environmental and anthropogenic impacts (e.g. (Airoldi 1998, Jackson & McIlvenny 2011). The present study reveals ways to expand this knowledge to larger spatial scales, giving insight into entire platform extent of a habitat forming algae, *H. banksii.* The two most important findings include the quantification of dominant, habitat-forming macroalgae from the UAV imagery similar to on-ground measures, and the ability to capture fine (cm) scale geomorphological variables over the whole platform.

UAVs are becoming increasingly efficient to deploy in the field due to decreasing costs, increased performance and ease of use. Despite the benefits of cost savings in image acquisition, there are challenges in detecting objects by their spectral properties from aerial imagery. Data resolution, image clarity, flying height, timing of image capture, camera angle, and flight direction are just some of the considerations (Joyce et al. 2018). In intertidal environments, these considerations are further compounded by the need to consider tidal conditions, sun glint and shadows on imagery. We found that imagery obtained in bright sunlight in conjunction with low tides was better suited to object-based approaches. Excessive image blur in low light data capture, or moving water on the platform led to poor classifications. Bright sunny conditions decrease image blur in final orthomosaics, but are problematic as they increase the incidence of sun glint from standing water on the platform and deepen areas of shadow. Additionally, there is significant effort and cost involved in processing and automated interpretation of large sets of high resolution imagery (Joyce et al. 2018).

The addition of UAV surveys to existing intertidal monitoring programs provides benefits in terms of full-platform imagery and topographic coverage that can be achieved. This approach also allows the potential to better inform on ground monitoring programs to ensure representative observations are achieved that capture the environmental gradients that are observed. In this study, we used low cost UAV components that would be considered comparable to devices currently in vogue with recreational drone users. This poses enormous opportunities to increase temporal data capture to determine trends including seasonality through implementation of intertidal reef monitoring citizen science programs. Sea Search is one such program that relies on volunteers and community groups to observe intertidal reefs through quadrat surveys and benefits both the local community and scientific researchers through sharing of knowledge and creating partnerships between these groups (Koss et al. 2009). Studies have also shown that 'non-expert' volunteers are able to collect intertidal biota data within the same variation range as occurs between researchers (Cox et al. 2012). Already consumer multirotors such as DJIs phantom 4 are capable of autonomous flight and have been integrated seamlessly into photogrammetry

software such as Pix4D with specialist apps developed (PIX4DCapture) allowing for cloud based upload, data processing and storage. New laws regarding operation of UAVs and certification requirements are also making it easier for State organisations, such as Parks Victoria, to explore the application of these sensor platforms for monitoring programs. This includes the operation of UAVs up to 2 kg to be flown without a Civil Aviation Safety Authority (CASA) certification required by the operator, called the Excluded Category (CASR, 1998). This has already been adopted by citizen scientists as part of the Victorian Coastal Monitoring program, where community groups are mapping coastal erosion at 15 sites across the state every 4-6 weeks using UAVs. Combined with increased endurance through improvements in battery technology and miniaturisation of sensor technology, there is an opportunity for UAV technology become a part of sustained monitoring programs in the intertidal zone across the marine parks estate. Currently, Parks Victoria do not permit the operation of UAVs under the Excluded Category within their managed land, only operations conducted under a Remote Operators Certificate (ReOC) are permitted. The cost of an ReOC is likely untenable for most community groups, halting the potential of UAV Citizen Science in Parks Victoria managed land.

5. References

Abesamis RA, Russ GR (2005) Density-dependent spillover from a marine reserve: long-term evidence. Ecological applications 15:1798-1812

Airoldi L (1998) Roles of disturbance, sediment stress, and substratum retention on spatial dominance in algal turf. Ecology 79:2759-2770

Airoldi L (2003) The effects of sedimentation on rocky coast assemblages. Oceanography and Marine Biology, An Annual Review, Volume 41. CRC Press

Althaus F, Hill N, Ferrari R, Edwards L, Przeslawski R, Schönberg CH, Stuart-Smith R, Barrett N, Edgar G, Colquhoun J (2015) A standardised vocabulary for identifying benthic biota and substrata from underwater imagery: the CATAMI classification scheme. PloS one 10:e0141039

Araújo MB, Guisan A (2006) Five (or so) challenges for species distribution modelling. Journal of Biogeography 33:1677-1688

Archambault P, Bourget E (1996) Scales of coastal heterogeneity and benthic intertidal species richness, diversity and abundance. Marine Ecology Progress Series 136:111-121

Austin MP (1998) An ecological perspective on biodiversity investigations: examples from Australian eucalypt forests. Annals of the Missouri Botanical Garden:2-17

Barrett NS, Buxton CD, Edgar GJ (2009) Changes in invertebrate and macroalgal populations in Tasmanian marine reserves in the decade following protection. Journal of Experimental Marine Biology and Ecology 370:104-119

Barton J, Pope A, Howe S (2012) Marine Natural Values Study Vol 2: Marine Protected Areas of the Central Victoria Bioregion. Parks Victoria Technical Series No 76. Parks Victoria, Melbourne

Barton K (2016) Multi-model inference. R package version 1.15. 6.; 2016.

Bentley N, Breen PA, Kim SW, Starr PJ (2005) Can additional abundance indices improve harvest control rules for New Zealand rock lobster (Jasus edwardsii) fisheries? New Zealand Journal of Marine and Freshwater Research 39:629-644

Bjørnstad O (2009) ncf: spatial nonparametric covariance functions.–R package ver. 1.1-3.

Bolker BM, Brooks ME, Clark CJ, Geange SW, Poulsen JR, Stevens MHH, White J-SS (2009) Generalized linear mixed models: a practical guide for ecology and evolution. Trends in ecology & evolution 24:127-135

Booth JD (1997) Long-distance movements in Jasus spp. and their role in larval recruitment. Bulletin of Marine Science 61:111-128

Borell EM, Foggo A, Coleman RA (2004) Induced resistance in intertidal macroalgae modifies feeding behaviour of herbivorous snails. Oecologia 140:328-334

Cappo M, Speare P, De'ath G (2004) Comparison of baited remote underwater video stations (BRUVS) and prawn (shrimp) trawls for assessments of fish biodiversity in inter-reefal areas of the Great Barrier Reef Marine Park. Journal of Experimental Marine Biology and Ecology 302:123-152

Chiswell SM, Wilkin J, Booth JD, Stanton B (2003) Trans-Tasman Sea larval transport: Is Australia a source for New Zealand rock lobsters? Marine Ecology Progress Series 247:173-182

Colton MA, Swearer SE (2010) A comparison of two survey methods: differences between underwater visual census and baited remote underwater video. Marine Ecology Progress Series 400:19-36

Cox T, Philippoff J, Baumgartner E, Smith C (2012) Expert variability provides perspective on the strengths and weaknesses of citizen-driven intertidal monitoring program. Ecological Applications 22:1201-1212
Dayton PK (1971) Competition, disturbance, and community organization: the provision and subsequent utilization of space in a rocky intertidal community. Ecological Monographs 41:351-389
Devillers R, Pressey RL, Grech A, Kittinger JN, Edgar GJ, Ward T, Watson R (2015) Reinventing residual reserves in the sea: are we favouring ease of establishment over need for protection? Aquatic Conservation: Marine and Freshwater Ecosystems 25:480-504
Edmunds M (1995) The Ecology of the juvenile southern rock lobster, Jasus edwardsii (Hutton 1875)(Palinuridae). University of Tasmania,
Elith J, Graham CH (2009) Do they? How do they? WHY do they differ? On finding reasons for differing performances of species distribution models. Ecography 32:66-77
ESRI (2011) ArcGIS desktop: release 10. Environmental Systems Research Institute, CA
Faul F, Erdfelder E, Lang A-G, Buchner A (2007) G* Power 3: A flexible statistical power analysis program for the social, behavioral, and biomedical sciences. Behavior research methods 39:175-191
Freeman DJ, Macdiarmid AB, Taylor RB, Davidson RJ, Grace RV, Haggitt TR, Kelly S, Shears NT (2012) Trajectories of spiny lobster Jasus edwardsii recovery in New Zealand marine reserves: is settlement a driver? Environmental Conservation 39:295-304
Froese R, Pauly D (2010) FishBase. Fisheries Centre, University of British Columbia
Frusher S, Hoenig J (2001) Impact of lobster size on selectivity of traps for southern rock lobster (Jasus edwardsii). Canadian Journal of Fisheries and Aquatic Sciences 58:2482-2489
Galaiduk R, Radford BT, Wilson SK, Harvey ES (2017) Comparing two remote video survey methods for spatial predictions of the distribution and environmental niche suitability of demersal fishes. Scientific reports 7:17633
Goñi R, Adlerstein S, Alvarez-Berastegui D, Forcada A, Reñones O, Criquet G, Polti S, Cadiou G, Valle C, Lenfant P (2008) Spillover from six western Mediterranean marine protected areas: evidence from artisanal fisheries. Marine Ecology Progress Series 366:159-174
Guisan A, Thuiller W (2005) Predicting species distribution: offering more than simple habitat models. Ecology Letters 8:993-1009
Harrington AM, Hovel KA (2016) Patterns of shelter use and their effects on the relative survival of subadult California spiny lobster (Panulirus interruptus). Marine and Freshwater Research 67:1153-1162
Hart SP, Edmunds MJ (2005) Parks Victoria standard operating procedure: biological monitoring of intertidal reefs. Parks Victoria
Harvey ES, Newman SJ, McLean DL, Cappo M, Meeuwig JJ, Skepper CL (2012) Comparison of the relative efficiencies of stereo-BRUVs and traps for sampling tropical continental shelf demersal fishes. Fisheries Research 125:108-120
Hijmans RJ, van Etten J (2014) raster: Geographic data analysis and modeling. R package version 2
Holmes K, Van Niel K, Radford B, Kendrick G, Grove S (2008) Modelling distribution of marine benthos from hydroacoustics and underwater video. Continental Shelf Research 28:1800-1810

Ierodiaconou D, Laurenson L, Burq S, Reston M (2007) Marine benthic habitat mapping using Multibeam data, georeferencedvideo and image classification techniques in Victoria, Australia. Journal of Spatial Science 52:93-104

Ierodiaconou D, Monk J, Rattray A, Laurenson L, Versace V (2011) Comparison of automated classification techniques for predicting benthic biological communities using hydroacoustics and video observations. Continental Shelf Research 31:S28-S38

Ierodiaconou D, Young M, Miller A, Treml E, Swearer S, Sherman C, Murphy N, Strugnell J, Gorfine H (2018) Patterns of interaction between habitat and oceanographic variables affecting the connectivity and productivity of invertebrate fisheries. CC BY 3.0, Warrnambool

IMOS (2018) AVHRR L3S SST. Accessed September 28, 2018. http://rs-data1-mel.csiro.au/imos-srs/sst/ghrsst/L3S-1m/

Jackson A, McIlvenny J (2011) Coastal squeeze on rocky shores in northern Scotland and some possible ecological impacts. Journal of Experimental Marine Biology and Ecology 400:314-321

Jernakoff P, Phillips B, Maller R (1987) A quantitative study of nocturnal foraging distances of the western rock lobster Panulirus cygnus George. Journal of Experimental Marine Biology and Ecology 113:9-21

Joyce K, Duce S, Leahy S, Leon J, Maier S (2018) Principles and practice of acquiring drone-based image data in marine environments. Marine and Freshwater Research

Kelly S, Scott D, MacDiarmid A, Babcock R (2000) Spiny lobster, Jasus edwardsii, recovery in New Zealand marine reserves. Biological conservation 92:359-369

Keough MJ, Quinn GP (1998) Effects of periodic disturbances from trampling onrocky intertidal algal beds. Ecological Applications 8:141-161

Keough MJ, Ross DJ, Knott NA (2007) Ecological performance measures for Victorian Marine Protected Areas: Review of the existing biological sampling program. Parks Victoria

Keysers JH, Quadros ND, Collier PA (2013) Vertical datum transformations across the Australian littoral zone. Journal of Coastal Research 31:119-128

Koss R, Miller K, Wescott G, Bellgrove A, Boxshall A, McBurnie J, Bunce A, Gilmour P, Ierodiaconou D (2009) An evaluation of Sea Search as a citizen science programme in Marine Protected Areas. Pacific Conservation Biology 15:116-127

Langlois T, Harvey E, Fitzpatrick B, Meeuwig J, Shedrawi G, Watson D (2010) Cost-efficient sampling of fish assemblages: comparison of baited video stations and diver video transects. Aquatic Biology 9:155-168

Langlois T, Williams J, Monk J, Bouchet P, Currey L, Goetze J, Harasti D, Huveneers C, Ierodiaconou D, Malcolm H (2018) Marine sampling field manual for benthic stereo BRUVS (Baited Remote Underwater Videos). In: Field Manuals for Marine Sampling to Monitor Australian Waters.

Linnane A, McGarvey R, Gardner C, Walker TI, Matthews J, Green B, Punt AE (2013) Large-scale patterns in puerulus settlement and links to fishery recruitment in the southern rock lobster (Jasus edwardsii), across south-eastern Australia. ICES Journal of Marine Science 71:528-536

Lowry M, Folpp H, Gregson M, Suthers I (2012) Comparison of baited remote underwater video (BRUV) and underwater visual census (UVC) for assessment of artificial reefs in estuaries. Journal of Experimental Marine Biology and Ecology 416:243-253

Loya Y, Eyal G, Treibitz T, Lesser MP, Appeldoorn R (2016) Theme section on mesophotic coral ecosystems: advances in knowledge and future perspectives. Springer

MacDiarmid A, Hickey B, Maller R (1991) Daily movement patterns of the spiny lobster Jasus edwardsii (Hutton) on a shallow reef in northern New Zealand. Journal of Experimental Marine Biology and Ecology 147:185-205
McClanahan TR, Mangi S (2000) Spillover of exploitable fishes from a marine park and its effect on the adjacent fishery. Ecological applications 10:1792-1805
Miller RJ (1990) Effectiveness of crab and lobster traps. Canadian Journal of Fisheries and Aquatic Sciences 47:1228-1251
Montgomery DC (2007) Introduction to statistical quality control. John Wiley & Sons
Moore CH, Harvey ES, Van Niel K (2010) The application of predicted habitat models to investigate the spatial ecology of demersal fish assemblages. Marine Biology 157:2717-2729
Morgan EM, Green BS, Murphy NP, Strugnell JM (2013) Investigation of genetic structure between deep and shallow populations of the southern rock lobster, Jasus edwardsii in Tasmania, Australia. PloS one 8:e77978
Murfitt SL, Allan BM, Bellgrove A, Rattray A, Young MA, Ierodiaconou D (2017) Applications of unmanned aerial vehicles in intertidal reef monitoring. Scientific reports 7:10259
O'Hara TD, Addison PF, Gazzard R, Costa TL, Pocklington JB (2010) A rapid biodiversity assessment methodology tested on intertidal rocky shores. Aquatic Conservation: Marine and Freshwater Ecosystems 20:452-463
Povey A, Keough MJ (1991) Effects of trampling on plant and animal populations on rocky shores. Oikos:355-368
Power B, Boxshall A (2007) Marine National Park and Sanctuary Monitoring Plan 2007-2012. Parks Victoria Technical Series No 54. Parks Victoria, Melbourne
Punt AE (2003) The performance of a size-structured stock assessment method in the face of spatial heterogeneity in growth. Fisheries Research 65:391-409
Quadros N, Rigby J (2010) Construction of a high accuracy seamless, state-wide coastal DEM. FIG Coastal Zone Special Publication, Sydney
Schiel DR (2004) The structure and replenishment of rocky shore intertidal communities and biogeographic comparisons. Journal of Experimental Marine Biology and Ecology 300:309-342
Schiel DR, Taylor DI (1999) Effects of trampling on a rocky intertidal algal assemblage in southern New Zealand. Journal of experimental marine biology and ecology 235:213-235
Sequeira AM, Mellin C, Lozano-Montes HM, Vanderklift MA, Babcock RC, Haywood MD, Meeuwig JJ, Caley MJ (2016) Transferability of predictive models of coral reef fish species richness. Journal of Applied Ecology 53:64-72
Shears NT, Babcock RC (2003) Continuing trophic cascade effects after 25 years of no-take marine reserve protection. Marine ecology progress series 246:1-16
Spencer ML, Stoner AW, Ryer CH, Munk JE (2005) A towed camera sled for estimating abundance of juvenile flatfishes and habitat characteristics: Comparison with beam trawls and divers. Estuarine, Coastal and Shelf Science 64:497-503
Stuart-Smith RD, Bates AE, Lefcheck JS, Duffy JE, Baker SC, Thomson RJ, Stuart-Smith JF, Hill NA, Kininmonth SJ, Airoldi L, Becerro MA, Campbell SJ, Dawson TP, Navarrete SA, Soler GA, Strain EMA, Willis TJ, Edgar GJ (2013) Integrating abundance and functional traits reveals new global hotspots of fish diversity. Nature 501:539

Thomas C, Crear B, Hart P (2000) The effect of temperature on survival, growth, feeding and metabolic activity of the southern rock lobster, Jasus edwardsii. Aquaculture 185:73-84
Underwood A, Jernakoff P (1981) Effects of interactions between algae and grazing gastropods on the structure of a low-shore intertidal algal community. Oecologia 48:221-233
Valavanis VD, Pierce GJ, Zuur AF, Palialexis A, Saveliev A, Katara I, Wang J (2008) Modelling of essential fish habitat based on remote sensing, spatial analysis and GIS. Essential Fish Habitat Mapping in the Mediterranean. Springer
Victorian Environmental Assessment Council (2014) Marine Investigation - Final Report. Victorian Environmental Assessment Council, Melbourne
Walbridge S, Slocum N, Pobuda M, Wright DJ (2018) Unified geomorphological analysis workflows with benthic terrain modeler. Geosciences 8:94
Warnock B, Harvey ES, Newman SJ (2016) Remote drifted and diver operated stereo–video systems: A comparison from tropical and temperate reef fish assemblages. Journal of experimental marine biology and ecology 478:45-53
Williams J, Jordan A, Harasti D, Davies P, Ingleton T (2019) Taking a deeper look: Quantifying the differences in fish assemblages between shallow and mesophotic temperate rocky reefs. PloS one 14:e0206778
Winer BJ (1991) Statistical Principles in Experimental Design, Vol 1. McGraw-Hill, Sydney
Wood S (2015) Package 'mgcv'. R package version 1:29
Woods B, Edmunds M (2013) Victorian subtidal reef monitoring program: the reef biota at Merri Marine Sanctuary, February 2013. Parks Victoria Technical Series
Woods B, Edmunds M, Brown H (2014) Victorian Subtidal Reef Monitoring Program: The Reef Biota at Point Addis Marine National Park, June 2013. Parks Victoria Technical Series
Yee TW, Mitchell ND (1991) Generalized additive models in plant ecology. Journal of vegetation science 2:587-602
Young M, Ierodiaconou D, Womersley T (2015) Forests of the sea: Predictive habitat modelling to assess the abundance of canopy forming kelp forests on temperate reefs. Remote Sensing of Environment 170:178-187
Young MA, Ierodiaconou D, Edmunds M, Hulands L, Schimel ACG (2016) Accounting for habitat and seafloor structure characteristics on southern rock lobster (Jasus edwardsii) assessment in a small marine reserve. Marine Biology 163:141
Zavalas R, Ierodiaconou D, Ryan D, Rattray A, Monk J (2014) Habitat classification of temperate marine macroalgal communities using bathymetric LiDAR. Remote Sensing 6:2154-2175
Zevenbergen LW, Thorne CR (1987) Quantitative analysis of land surface topography. Earth surface processes and landforms 12:47-56

6. Appendix 1 - Relative Abundance of All Species Across Years

Appendix 1.1. Relative abundances (mean ± SE) of all fish species observed by stereo-BRUV for each year sampled (2013, 2017 and 2018).

Family	Species Name	Common Name	Functional Feeding Group	2013	2017	2018
Alopiidae	*Alopias vulpinus*	Common Thresher Shark	Carnivore	1 ± 0	0 ± 0	1 ± 0
Aplodactylidae	*Aplodactylus arctidens*	Marblefish	Herbivore	0 ± 0	0 ± 0	1 ± 0
Arripidae	*Arripis trutta*	Australian salmon	Carnivore	2 ± 0	0 ± 0	0 ± 0
Aulopidae	*Latropiscis purpurissatus*	Sergeant Baker	Carnivore	0 ± 0	1 ± 0	1 ± 0
Berycidae	*Centroberyx affinis*	Redfish	Carnivore	0 ± 0	0 ± 0	1 ± 0
	Centroberyx lineatus	Swallowtail	Carnivore	0 ± 0	7 ± 0	1 ± 0
Callionymidae	*Pseudocalliurichthys goodladi*	Longspine Dragonet	Invertivore	1.2 ± 0.13	0 ± 0	0 ± 0
Callorhinchidae	*Callorhinchus milii*	Elephantfish	Invertivore	0 ± 0	0 ± 0	1 ± 0
Carangidae	*Pseudocaranx* sp.	Trevally	Invertivore	3.67 ± 1.33	2.55 ± 0.69	2.15 ± 0.66
	Seriola lalandi	Yellowtail Kingfish	Carnivore	1 ± 0	1 ± 0	4.25 ± 2.29
	Trachurus sp.	Jack mackerel	Carnivore	19.71 ± 6.42	23.89 ± 4.32	47.85 ± 13.57
Carcharhinidae	*Carcharhinus brachyurus*	Bronze Whaler Shark	Carnivore	0 ± 0	0 ± 0	1 ± 0
Cheilodactylidae	*Cheilodactylus nigripes*	Magpie Perch	Invertivore	1.05 ± 0.05	1.25 ± 0.11	1.3 ± 0.1
	Cheilodactylus sp.	Morwong	Invertivore	0 ± 0	0 ± 0	1 ± 0
	Dactylophora nigricans	Dusky Morwong	Invertivore	1.25 ± 0.25	1 ± 0	1 ± 0
	Nemadactylus macropterus	Jackass Morwong	Invertivore	0 ± 0	1 ± 0	1.2 ± 0.2
	Nemadactylus valenciennesi	Blue Morwong	Invertivore	1 ± 0	1.25 ± 0.25	1.2 ± 0.13
Clupeidae	*Nematalosa vlaminghi*	Perth Herring	Planktivore	1 ± 0	0 ± 0	0 ± 0
Cyttidae	*Cyttus australis*	Silver Dory	Carnivore	1 ± 0	0 ± 0	0 ± 0
Dasyatidae	*Dasyatis* sp.	Common stingray	Invertivore	1 ± 0	1 ± 0	1 ± 0
Dinolestidae	*Dinolestes lewini*	Longfin Pike	Carnivore	1 ± 0	10.17 ± 3.59	11.44 ± 6.11
	Diodon nicthemerus	Globefish	Invertivore	1 ± 0	0 ± 0	0 ± 0
Enoplosidae	*Enoplosus armatus*	Old Wife	Invertivore	1 ± 0	1.55 ± 0.16	1.67 ± 0.14
Gempylidae	*Thyrsites atun*	Barracouta	Carnivore	1.6 ± 0.43	2 ± 0.38	1.22 ± 0.15
Gerreidae	*Parequula melbournensis*	Silverbelly	Invertivore	2.19 ± 0.41	1.3 ± 0.22	2.19 ± 0.48
Heterodontidae	*Heterodontus portusjacksoni*	Port Jackson Shark	Invertivore	1 ± 0	1.38 ± 0.26	1.27 ± 0.1
Hexanchidae	*Notorynchus cepedianus*	Broadnose Sevengill Shark	Carnivore	1 ± 0	1 ± 0	1 ± 0
Kyphosidae	*Girella zebra*	Zebrafish	Herbivore	1.5 ± 0.38	1.5 ± 0.34	2.78 ± 0.94
Labridae	*Achoerodus* sp.	Blue Groper	Invertivore	0 ± 0	1 ± 0	0 ± 0
	Eupetrichthys angustipes	Snakeskin Wrasse	Invertivore	0 ± 0	0 ± 0	1 ± 0

	Notolabrus fucicola	Purple Wrasse	Invertivore	1 ± 0	1 ± 0	0 ± 0
	Notolabrus tetricus	Bluethroat Wrasse	Invertivore	1.94 ± 0.14	3.6 ± 0.35	4.77 ± 0.33
	Pictilabrus laticlavius	Senator Wrasse	Invertivore	1.4 ± 0.13	1.27 ± 0.12	1.48 ± 0.12
	Pseudolabrus rubicundus	Rosy Wrasse	Invertivore	2.11 ± 0.27	1.36 ± 0.17	2.08 ± 0.3
Monacanthidae	*Acanthaluteres vittiger*	Toothbrush Leatherjacket	Herbivore	1 ± 0	2 ± 1	1.44 ± 0.24
	Eubalichthys gunnii	Gunns Leatherjacket	Herbivore	1 ± 0	1 ± 0	1 ± 0
	Eubalichthys mosaicus	Mosaic Leatherjacket	Herbivore	1.25 ± 0.25	1 ± 0	1 ± 0
	Meuschenia australis	Brownstriped Leatherjacket	Herbivore	0 ± 0	1 ± 0	0 ± 0
	Meuschenia flavolineata	Yellowstriped Leatherjacket	Herbivore	1.26 ± 0.1	1.39 ± 0.14	1.5 ± 0.14
	Meuschenia freycineti	Sixspine Leatherjacket	Herbivore	1.15 ± 0.09	1.81 ± 0.19	1.68 ± 0.15
	Meuschenia galii	Bluelined Leatherjacket	Herbivore	1.07 ± 0.07	1.11 ± 0.11	1 ± 0
	Meuschenia hippocrepis	Horseshoe Leatherjacket	Herbivore	2.87 ± 0.29	3.74 ± 0.54	5.14 ± 0.52
	Meuschenia scaber	Velvet Leatherjacket	Invertivore	1.35 ± 0.1	1.18 ± 0.12	1.82 ± 0.2
	Meuschenia venusta	Stars-and-stripes Leatherjacket	Herbivore	1 ± 0	1 ± 0	1.17 ± 0.17
	Nelusetta ayraud	Ocean Leatherjacket	Herbivore	1 ± 0	0 ± 0	0 ± 0
	Scobinichthys granulatus	Rough Leatherjacket	Herbivore	1.31 ± 0.12	1 ± 0	1 ± 0
	Thamnaconus degeni	Blue-finned Leatherjacket	Herbivore	2.91 ± 0.43	2.93 ± 0.54	2.94 ± 0.67
Moridae	*Lotella rhacina*	Largetooth Beardie	Carnivore	1 ± 0	0 ± 0	1 ± 0
	Pseudophycis sp.	Rock Cod	Invertivore	1.25 ± 0.25	1.78 ± 0.66	1 ± 0
Mullidae	*Upeneichthys vlamingii*	Bluespotted Goatfish	Invertivore	1.41 ± 0.11	1.32 ± 0.12	2.14 ± 0.33
Myliobatidae	*Myliobatis australis*	Southern Eagle Ray	Invertivore	0 ± 0	1 ± 0	1.16 ± 0.09
Neosebastidae	*Neosebastes scorpaenoides*	Common Gurnard Perch	Invertivore	1.64 ± 0.21	1.62 ± 0.24	1.18 ± 0.1
Odacidae	*Heteroscarus acroptilus*	Rainbow Cale	Herbivore	1 ± 0	1 ± 0	1 ± 0
	Olisthops cyanomelas	Herring Cale	Herbivore	1.22 ± 0.22	1 ± 0	1.45 ± 0.31
	Siphonognathus sp.	Weed Whiting	Herbivore	3 ± 0	0 ± 0	0 ± 0
Orectolobidae	*Orectolobus maculatus*	Spotted Wobbegong	Carnivore	1 ± 0	0 ± 0	1 ± 0
Ostraciidae	*Aracana aurita*	Shaws Cowfish	Invertivore	0 ± 0	1 ± 0	0 ± 0
	Aracana ornata	Ornate Boxfish	Invertivore	0 ± 0	1 ± 0	0 ± 0
Parascylliidae	*Parascyllium* sp.	Carpetshark	Carnivore	1 ± 0	1 ± 0	1 ± 0
Pempheridae	*Pempheris multiradiata*	Bigscale Bullseye	Invertivore	2.25 ± 0.86	1.5 ± 0.5	4.4 ± 1.69

Pentacerotidae	*Pentaceropsis recurvirostris*	Longsnout Boarfish	Invertivore	1 ± 0	1 ± 0	1 ± 0
Platycephalidae	*Platycephalus* sp.	Flathead	Carnivore	1.4 ± 0.24	1.8 ± 0.49	1.67 ± 0.49
Pomacentridae	*Parma* sp.	Scalyfin	Herbivore	1.09 ± 0.09	1 ± 0	1 ± 0
Pristiophoridae	*Pristiophorus cirratus*	Common Sawshark	Carnivore	0 ± 0	0 ± 0	1 ± 0
	Pristiophorus nudipinnis	Southern Sawshark	Carnivore	1 ± 0	1 ± 0	0 ± 0
Rajidae	*Dipturus whitleyi*	Melbourne Skate	Carnivore	1 ± 0	1 ± 0	1 ± 0
Rhinobatidae	*Trygonorrhina fasciata*	Eastern Fiddler Ray	Invertivore	1 ± 0	1 ± 0	1.29 ± 0.11
Scorpididae	*Atypichthys strigatus*	Australian Mado	Planktivore	2.5 ± 1.5	0 ± 0	1 ± 0
	Scorpis sp.	Sweep	Herbivore	1 ± 0	1.67 ± 0.42	2 ± 0.32
	Tilodon sexfasciatus	Moonlighter	Invertivore	1 ± 0	1 ± 0	1 ± 0
Scyliorhinidae	*Cephaloscyllium laticeps*	Draughtboard Shark	Carnivore	1.22 ± 0.15	1.22 ± 0.15	2.5 ± 0.5
Sebastidae	*Helicolenus percoides*	Reef Ocean Perch	Carnivore	2 ± 0	1 ± 0	1 ± 0
Serranidae	*Caesioperca* sp.	Butterfly Perch	Planktivore	7.48 ± 0.88	12.88 ± 2.38	13.17 ± 2.59
	Hypoplectrodes nigroruber	Banded Seaperch	Invertivore	0 ± 0	0 ± 0	1 ± 0
Sillaginidae	*Sillaginodes punctatus*	King George Whiting	Invertivore	1.67 ± 0.67	0 ± 0	0 ± 0
Sparidae	*Chrysophrys auratus*	Snapper	Invertivore	5.31 ± 0.51	12.87 ± 1.4	10.95 ± 1.06
Sphyraenidae	*Sphyraena novaehollandiae*	Snook	Carnivore	1 ± 0	1 ± 0	0 ± 0
Tetraodontidae	*Contusus brevicaudus*	Prickly Toadfish	Invertivore	1 ± 0	1.5 ± 0.5	1 ± 0
	Tetractenos glaber	Smooth Toadfish	Invertivore	0 ± 0	1 ± 0	0 ± 0
Trachichthyidae	*Paratrachichthys macleayi*	Sandpaper Fish	Planktivore	0 ± 0	1 ± 0	0 ± 0
Triakidae	*Galeorhinus galeus*	School Shark	Carnivore	0 ± 0	1 ± 0	0 ± 0
	Mustelus antarcticus	Gummy Shark	Carnivore	1.15 ± 0.1	1 ± 0	1.21 ± 0.12
Urolophidae	*Urolophus* sp.	Stingaree	Invertivore	1 ± 0	1 ± 0	2 ± 0

Appendix 1.2. Relative abundances (mean ± SE) of all fish species observed in method 1 of Reef Life Surveys, for each year sampled (2017 and 2018).

Species Name	Common Name	2017	2018
Acanthaluteres vittiger	Toothbrush leatherjacket	1 ± 0	1.67 ± 0.67
Aetapcus maculatus	Warty prowfish	1 ± 0	0 ± 0
Aplodactylus arctidens	Marblefish	1 ± 0	1 ± 0
Atypichthys strigatus	Mado sweep	2 ± 0	1 ± 0
Cheilodactylus nigripes	Magpie perch	1.7 ± 0.23	1.18 ± 0.12
Cheilodactylus spectabilis	Banded morwong	1.33 ± 0.33	1 ± 0
Dactylophora nigricans	Dusky morwong	1 ± 0	1.25 ± 0.25
Dinolestes lewini	Long-fin pike	6 ± 1.35	30 ± 0
Dotalabrus aurantiacus	Castelnaus wrasse	1.5 ± 0.5	1 ± 0
Enoplosus armatus	Old wife	1.5 ± 0.38	4 ± 0
Girella zebra	Zebra fish	2.33 ± 0.61	11.25 ± 5.36
Meuschenia flavolineata	Yellow-stripe leatherjacket	2.6 ± 0.43	2.65 ± 0.51
Meuschenia galii	Blue-lined leatherjacket	1.12 ± 0.12	1.33 ± 0.33
Meuschenia hippocrepis	Horseshoe leatherjacket	3.44 ± 0.53	3.95 ± 0.75
Meuschenia scaber	Velvet leatherjacket	1 ± 0	0 ± 0
Meuschenia venusta	Stars-and-stripes leatherjacket	2 ± 0	0 ± 0
Meuschenia venusta	Stars and Stripes Leatherjacket	2 ± 0	0 ± 0
Nesogobius maccullochi	Girdled goby	3 ± 0	0 ± 0
Notolabrus tetricus	Blue-throat wrasse	10.69 ± 0.93	8.42 ± 0.81
Odax acroptilus	Rainbow cale	1 ± 0	0 ± 0
Olisthops cyanomelas	Herring cale	1.73 ± 0.25	1.73 ± 0.6
Orectolobus maculatus	Spotted wobbegong	1 ± 0	0 ± 0
Pagrus auratus	Snapper	1.57 ± 0.3	1.12 ± 0.12
Parascyllium variolatum	Varied catshark	1.33 ± 0.33	0 ± 0
Parma victoriae	Victorian scalyfin	2.84 ± 0.28	2.31 ± 0.28
Pempheris multiradiata	Common bullseye	4 ± 0	26.33 ± 14.45
Pictilabrus laticlavius	Senator wrasse	2.36 ± 0.31	2.22 ± 0.29
Pseudocaranx georgianus	Silver trevally	1.75 ± 0.48	0 ± 0
Scobinichthys granulatus	Rough leatherjacket	1.67 ± 0.33	1 ± 0
Scorpis aequipinnis	Sea sweep	4.79 ± 1.68	3.88 ± 1.33
Scorpis lineolata	Silver sweep	1 ± 0	0 ± 0
Siphonognathus beddomei	Pencil weed whiting	1.5 ± 0.29	1.5 ± 0.5
Sphyraena novaehollandiae	Snook	1 ± 0	0 ± 0
Upeneichthys vlamingii	Southern goatfish	1.33 ± 0.33	1 ± 0

Appendix 1.3. Relative abundances (mean ± SE) of all macroinvertebrate and cryptic fish species observed in method 2 of Reef Life Surveys, for each year sampled (2017 and 2018).

Species Name	Common Name	2017	2018
Acanthistius ocellatus	Eastern wirrah	1 ± 0	0 ± 0
Astralium tentoriformis	Turban shell	1 ± 0	1 ± 0
Cabestana spengleri	Triton shell	2.5 ± 1.19	1.5 ± 0.5
Chironemus maculosus	Silver Spot	1 ± 0	0 ± 0
Chironemus maculosus		1 ± 0	0 ± 0
Comanthus tasmaniae	Tasmanian feather star	1.5 ± 0.5	0 ± 0
Comanthus trichoptera	Orange feather star	2.85 ± 0.55	3.38 ± 0.56
Conus anemone	Anemone cone	1 ± 0	0 ± 0
Dicathais orbita	Dog whelk	2.33 ± 0.64	1.69 ± 0.31
Doriopsilla aurea	a nudibranch	1 ± 0	0 ± 0
Echinaster arcystatus	Pale mosaic seastar	1 ± 0	0 ± 0
Fromia polypora	Many-spotted seastar	1 ± 0	1.5 ± 0.5
Haliotis laevigata (legal)	Greenlip abalone legal	3.57 ± 1.43	4 ± 1.46
Haliotis rubra (legal)	Blacklip abalone legal	1.38 ± 0.26	2 ± 0.58
Haliotis scalaris	Grooved abalone	1 ± 0	4 ± 0
Heliocidaris erythrogramma	Purple urchin	1 ± 0	1.45 ± 0.21
Hermit crab unidentified	Hermit crab	1 ± 0	0 ± 0
Heteroclinus kuiteri	Weedfish	1 ± 0	0 ± 0
Holopneustes purpurascens	Short-spine urchin	1 ± 0	2 ± 0
Jasus edwardsii (legal)	Southern rock lobster legal	1.25 ± 0.16	1.44 ± 0.29
Nectria macrobrachia	Large-plated seastar	2.8 ± 0.34	3.92 ± 0.57
Nectria multispina	Multi-spined seastar	1.33 ± 0.16	1.88 ± 0.36
Nectria ocellata	Ocellate seastar	1.8 ± 0.37	1 ± 0
Paguristes frontalis	Southern hermit crab	1.33 ± 0.33	1 ± 0
Parascyllium variolatum	Varied catshark	1.17 ± 0.17	1 ± 0
Pempheris multiradiata	Common bullseye	3 ± 0	17.33 ± 16.33
Pentagonaster dubeni	Fire-brick star	1.14 ± 0.14	0 ± 0
Petricia vernicina	Velvet star	1 ± 0	1.5 ± 0.29
Phasianotrochus eximius	Giant kelp shell	2.25 ± 0.95	1.5 ± 0.22
Plagusia chabrus	Red bait crab	1 ± 0	1.5 ± 0.5
Plectaster decanus	Mosaic seastar	1 ± 0	1.33 ± 0.33
Pleuroploca australasia	Tulip shell	1 ± 0	1.33 ± 0.33
Pseudonepanthia troughtoni	Troughtons seastar	1.83 ± 0.28	2.13 ± 0.36
Scorpaena papillosa	Southern rock cod	1 ± 0	1 ± 0
Scutus antipodes	Elephant snail	1 ± 0	0 ± 0
Lunella undulata	Turban shell	1 ± 0	2 ± 0.58

7. Appendix 2 - Power Analysis (Progressively Unbalanced t-test)

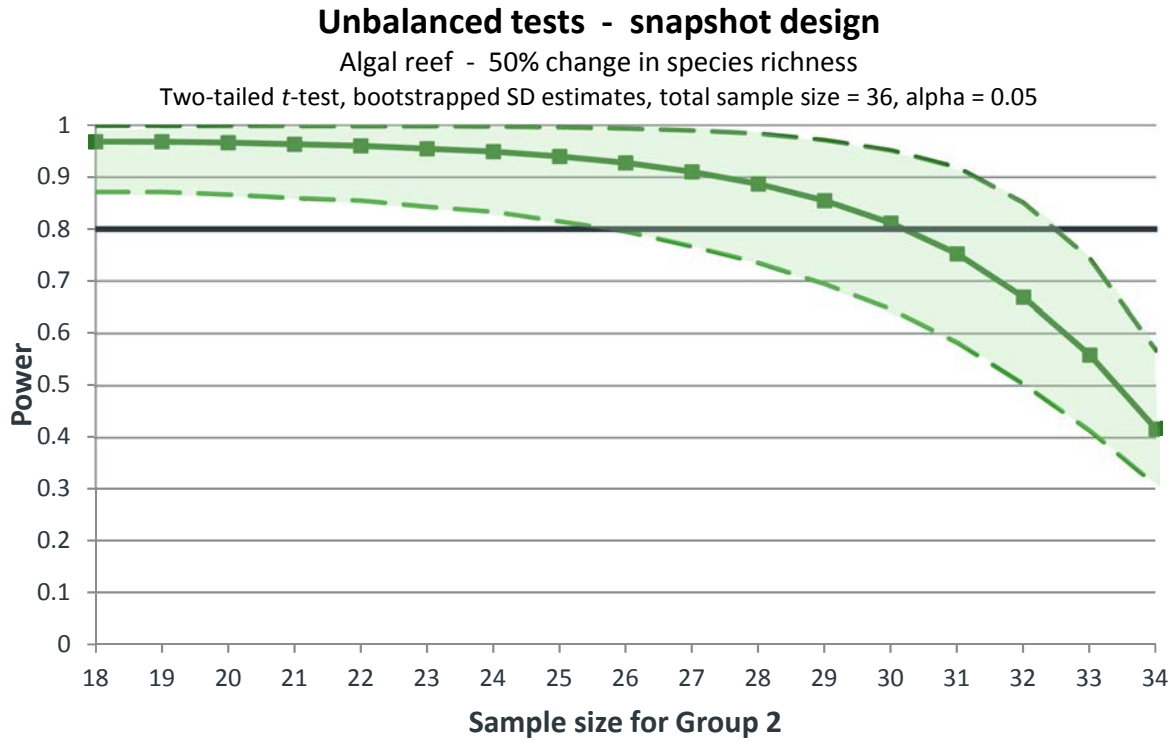

Appendix 2.1. Results of a progressively unbalanced t-test completed in GPower (Faul et al. 2007) to test out of 36 deployments how many samples need to be collected inside the MPA to have enough power to detect change in total fish species richness on infralittoral (algal) reef. A statistical power of 0.8 was considered sufficient and is represented here by a thick black line.

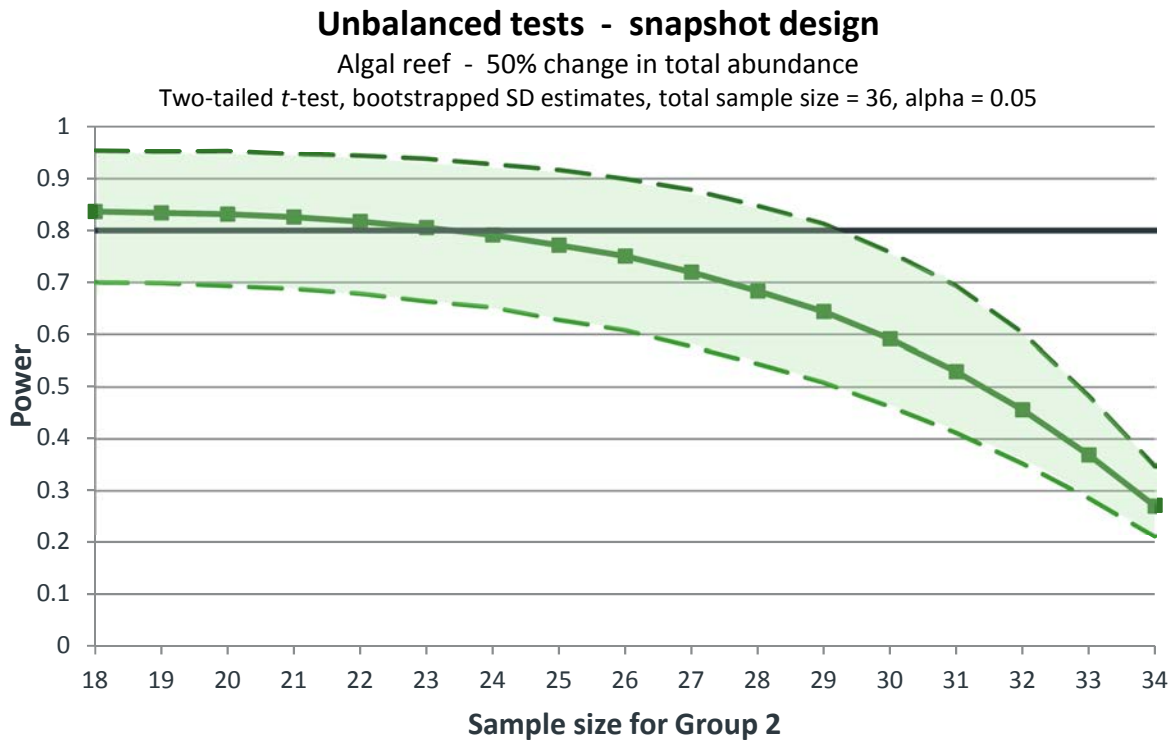

Appendix 2.2. Results of a progressively unbalanced t-test completed in GPower (Faul et al. 2007) to test out of 36 deployments how many samples need to be collected inside the MPA to have enough power to detect change in total fish abundance on infralittoral (algal) reef. A statistical power of 0.8 was considered sufficient and is represented here by a thick black line.